

**Effects of Multiple Phases and Ionic Constituents on Gas/Particle
Partitioning in Atmospheric and Other Aerosols**

Garnet Bailey Erdakos

B.S. Illinois State University, 1997

M.S. Oregon Graduate Institute of Science and Technology, 1998

A dissertation presented to the faculty of the
OGI School of Science & Engineering
at Oregon Health & Science University
in partial fulfillment of the
requirements for the degree of
Doctor of Philosophy
in
Environmental Science and Engineering

August 2004

The dissertation “Effects of Multiple Phases and Ionic Constituents on Gas/Particle Partitioning in Atmospheric and Other Aerosols” by Garnet Bailey Erdakos has been examined and approved by the following Examination Committee:

James F. Pankow, Thesis Advisor
Professor

James J. Huntzicker
Professor

Richard L. Johnson
Associate Professor

Dr. William E. Asher
University of Washington

ACKNOWLEDGEMENTS

The time I have spent at OGI has been extremely rewarding and I owe thanks to many people for making it so. Most of all, I would like to thank my advisor, Jim Pankow, for taking me under his wing. Jim has spent an extraordinary amount of time providing me with an excellent and thorough education; he has been an excellent mentor and role model. I am indebted to him for the support and opportunities he has provided. I would also like to thank my thesis committee: Jim Huntzicker, for his support and encouragement; Rick Johnson, for joining my committee with such short notice; and Bill Asher, for his unique sense of humor, helping me overcome my allergic reaction to Visual Basic, and for all of the time he spent helping me through research struggles.

My time at OGI would not have been so rewarding without the support of friends who have shared in many good times and always listened to my research and personal woes. I would like to thank Annika Fain: for being a wonderful friend, who got me out dancing and supported me through the toughest times; Ameer Tavakoli: who has been there from my first days at OGI, for providing many laughs and delicious chocolates; Kelley Barsanti: for commiserating over research and life, and for being my rock-climbing heroine; Jenny Kanter, Shannon Huss, and Joy Misra: for all the great talks and soul-searching; Oleg Lytchanyi, for salsa dancing and making my coffee habit affordable; Anna Farrenkopf: for being a great mentor and friend, and for all the big hugs; and last but not at all least, Russ Hodgins: for the late-night programming challenges, and especially for bringing Roxi (the sweetest pit-bull on the planet) into my life.

Finally, I would like to thank my family: my mom, Susan, for teaching me to believe in myself; my dad, Gary, for always letting me be exactly who I am; my older brother, Marc, for leading the way; my sister-in-law, Maria, for making me laugh and adding spice to our family; and my step-mom, Mary, for all the long talks, support, and advice. I owe my life to each of them for their patience and love.

TABLE OF CONTENTS

Acknowledgements	iii
Table of Contents	iv
List of Tables	vii
List of Figures	ix
Notation	xiii
Abstract	xviii
CHAPTER 1. INTRODUCTION	1
1.1 Overview	1
1.2 Format of Dissertation	4
1.3 References	4
CHAPTER 2. PHASE SEPARATION IN LIQUID PARTICULATE MATTER CONTAINING BOTH POLAR AND LOW-POLARITY ORGANIC COMPOUNDS	7
2.1 Abstract	7
2.2 Introduction	8
2.3 PM Composition Cases	9
2.4 Methods	10
2.4.1 The pseudo-diffusion phase stability method	10
2.4.1.1 Basic considerations	10
2.4.1.2 Implementation	11
2.4.2 Errors incurred by assuming a single PM phase	13
2.5 Results and Discussion	13
2.5.1 Phase stability in RH-dependent PM from the ozone oxidation	

of four monoterpenes and cyclohexene (without and with added LP mix	13
2.5.2 Errors incurred by assuming a single PM phase in RH- dependent PM with added LP mix	14
2.6 Conclusions	15
2.7 Acknowledgement	15
2.8 References	15
 CHAPTER 3. IONIC-UNIFAC.1: A METHOD FOR PREDICTING ACTIVITY COEFFICIENTS OF NEUTRAL COMPOUNDS IN LIQUID PARTICULATE MATTER CONTAINING ORGANIC COMPOUNDS, DISSOLVED INORGANIC SALTS AND WATER	
	28
3.1 Abstract	28
3.2 Introduction	29
3.3 Method	30
3.4 LLE Data	32
3.4.1 General	32
3.4.2 Calculating activity coefficients from LLE data	33
3.5 Optimization of Ionic-UNIFAC.1	35
3.6 Fit Characteristics of Ionic-UNIFAC.1	36
3.7 Validation of Ionic-UNIFAC.1	37
3.8 Final Set of Optimized Ionic-UNIFAC.1 Parameters	37
3.9 Implications for Atmospheric Applications	38
3.10 Conclusions	38
3.11 Acknowledgement	39
3.12 References	39
 CHAPTER 4. THE PREDICTED EFFECTS OF DISSOLVED INORGANIC SALTS ON THE FORMATION OF LIQUID PARTICULATE MATTER CONTAINING ORGANIC COMPOUNDS AND	

WATER	59
4.1 Abstract	59
4.2 Introduction	60
4.3 Aerosol Systems Studied	61
4.4 Thermodynamic Modeling Approach	62
4.4.1 Gas-particle partitioning numerics	62
4.4.2 Input p_L^o values	64
4.4.3 Estimating ζ with Ionic-UNIFAC.1	65
4.5 Modeling Results	67
4.5.1 Total aerosol yields	67
4.5.2 Concentrations of organic species and water	68
4.5.3 Comparison between model predictions and experimental results	69
4.6 Conclusions	70
4.7 Acknowledgement	70
4.8 References	70
CHAPTER 5. SUMMARY	90
5.1 General	90
5.2 Implications	91
APPENDIX 1	93
APPENDIX 2	94
APPENDIX 3	96
APPENDIX 4	98

LIST OF TABLES

Table 2.1	Distribution of compounds in the low-polarity (LP) mix used to amend model RH-dependent PM compositions for phase stability tests	18
Table 2.2	Distribution of compounds in previously modeled water-organic PM compositions for the ozone oxidation of four monoterpenes and cyclohexene	19
Table 2.3	Errors in predicted TPM ($\mu\text{g m}^{-3}$) assuming single-phase PM in selected two-phase PM cases derived by amending the PM composition from the ozone oxidation of cyclohexene at RH = 50% as reported by Seinfeld et al. (2001) for experiment 05/19/99b with the low-polarity (LP) mix of compounds	21
Table 3.1	Group volume (R_k) and surface area (Q_k) parameters used for Ionic-UNIFAC.1	43
Table 3.2	Basis set liquid-liquid equilibrium (LLE) datasets, their components, temperatures, and the number of systems	44
Table 3.3	Test set liquid-liquid equilibrium (LLE) datasets, their components, temperatures, and the number of systems	45
Table 3.4a	Group-group interaction parameters obtained by Ionic-UNIFAC.1 optimization using the basis set (Table 3.2)	46
Table 3.4b	Group-group interaction parameters obtained by Ionic-UNIFAC.1 optimization using the basis set (Table 3.2)	47

Table 3.5	Average standard errors of solvent compounds in the test set (Table 3.3)	48
Table 3.6a	Group-group interaction parameters obtained by Ionic-UNIFAC.1 optimization using the basis set (Table 3.2) and the test set (Table 3.3)	49
Table 3.6b	Group-group interaction parameters obtained by Ionic-UNIFAC.1 optimization using the basis set (Table 3.2) and the test set (Table 3.3)	50
Table 3.7	PM-phase activity coefficients of water and four α -pinene/O ₃ oxidation products at RH = 50% and $T = 306$ K	51
Table 4.1	Comparison of estimated sub-cooled p_L° values of pinonic acid and norpinonic acid using the UNIFAC- p_L° and SPARC methods	73
Table 4.2a	Products of the ozone oxidation of α -pinene and their physico- chemical properties	74
Table 4.2b	Products of the ozone oxidation of cyclohexene and their physico- chemical properties	75
Table 4.3	Average percent changes in predicted total mass concentrations M_t from conditions of wet homogeneous nucleation to aqueous salt seed in the α -pinene/O ₃ and cyclohexene/O ₃ systems	76
Table 4.4	Measured and predicted change in aerosol yield Y from conditions of wet nucleation to aqueous salt seed at RH = 50% and $T = 301$ K	77
Table 4.5	Measured and predicted aerosol yields with aqueous salt seed at RH = 50% and $T = 301$ K	78
Table 4.6	Measured and predicted growth factors for mixed (NH ₄) ₂ SO ₄ - organic aerosol PM at RH = 85%	79

LIST OF FIGURES

Figure 2.1	Illustration of the initial hypothetical forced phase separation used in the pseudo-diffusion method for testing phase stability22
Figure 2.2	Predicted two-phase distribution of components in the PM formed by amending the modeled PM composition (Table 2.2) for the α -pinene/O ₃ case so that 10% of the total organic carbon (OC) in the resulting PM was from the low-polarity (LP) mix (Table 2.1)23
Figure 2.3	Predicted two-phase distribution of components in the PM formed by amending the modeled PM composition (Table 2.2) for the β -pinene/O ₃ case so that 10% of the total organic carbon (OC) in the resulting PM was from the low-polarity (LP) mix (Table 2.1)24
Figure 2.4	Predicted two-phase distribution of components in the PM formed by amending the modeled PM composition (Table 2.2) for the sabinene/O ₃ case so that 10% of the total organic carbon (OC) in the resulting PM was from the low-polarity (LP) mix (Table 2.1)25
Figure 2.5	Predicted two-phase distribution of components in the PM formed by amending the modeled PM composition (Table 2.2) for the Δ^3 -carene/O ₃ case so that 10% of the total organic carbon (OC) in the resulting PM was from the low-polarity (LP)	

	mix (Table 2.1)	26
Figure 2.6	Predicted two-phase distribution of components in the PM formed by amending the modeled PM composition (Table 2.2) for the cyclohexene/O ₃ case so that 10% of the total organic carbon (OC) in the resulting PM was from the low-polarity (LP) mix (Table 2.1)	27
Figure 3.1	Comparison of back-calculated aqueous- and organic-phase activities of all solvent compounds in the basis and test set LLE systems listed in Tables 3.2 and 3.3	52
Figure 3.2	The logarithm of the standard error of each predicted activity coefficient $\zeta_n^{\varphi,\text{pred}}$ of each solvent n in each phase φ of each system p in the basis set (Table 3.2) as a function of a	53
Figure 3.3	The logarithm of the standard error of each predicted activity coefficient $\zeta_n^{\varphi,\text{pred}}$ of each solvent n in each phase φ of each system p in the basis set (Table 3.2) as a function of I	54
Figure 3.4	The logarithm of the standard error of each predicted activity coefficient $\zeta_n^{\varphi,\text{pred}}$ of each solvent n in each phase φ of each system p in the test set (Table 3.3) as a function of a	55
Figure 3.5	The logarithm of the standard error of each predicted activity coefficient $\zeta_n^{\varphi,\text{pred}}$ of each solvent n in each phase φ of each system p in the test set (Table 3.3) as a function of I	56
Figure 3.6	The logarithm of the standard error of each predicted activity	

	coefficient $\zeta_n^{\phi,\text{pred}}$ of each solvent n in each phase ϕ of each system p in the basis and test sets (Table 3.2 and 3.3) as a function of a	57
Figure 3.7	The logarithm of the standard error of each predicted activity coefficient $\zeta_n^{\phi,\text{pred}}$ of each solvent n in each phase ϕ of each system p in the basis and test sets (Table 3.2 and 3.3) as a function of I	58
Figure 4.1	Predicted total mass concentrations M_t , including organic species and water, at $T = 306$ K in the α -pinene/ O_3 system without and with 2 mol kg^{-1} dissolved inorganic salt from RH = 45% to RH = 60%	80
Figure 4.2	Predicted total mass concentrations M_t , including organic species and water, at $T = 298$ K in the cyclohexene/ O_3 system without and with 2 mol kg^{-1} dissolved inorganic salt from RH = 45% to RH = 60%	81
Figure 4.3	Predicted total mass concentrations M_t , including organic species and water, at $T = 306$ K in the α -pinene/ O_3 system without and with 1 and 2 mol kg^{-1} dissolved inorganic salt from RH = 45% to RH = 60%	82
Figure 4.4	Predicted total mass concentrations M_t , including organic species and water, at $T = 298$ K in the cyclohexene/ O_3 system without and with 1 and 2 mol kg^{-1} dissolved inorganic salt from RH = 45% to RH = 60%	83
Figure 4.5	Predicted mass concentrations of organic species at $T = 306$ K	

	in the α -pinene/O ₃ system without and with 2 mol kg ⁻¹ dissolved inorganic salt84
Figure 4.6	Predicted mass concentrations of water at $T = 306$ K in the α -pinene/O ₃ system without and with 2 mol kg ⁻¹ dissolved inorganic salt85
Figure 4.7	Predicted mass concentrations of organic species at $T = 298$ K in the cyclohexene/O ₃ system without and with 2 mol kg ⁻¹ dissolved inorganic salt86
Figure 4.8	Predicted mass concentrations of water at $T = 298$ K in the cyclohexene/O ₃ system without and with 2 mol kg ⁻¹ dissolved inorganic salt87
Figure 4.9	Predicted activity coefficients of the major oxidation products in the α -pinene/O ₃ system at $T = 306$ K without and with 2 mol kg ⁻¹ dissolved inorganic salt88
Figure 4.10	Predicted activity coefficients of the major oxidation products in the cyclohexene/O ₃ system at $T = 298$ K without and with 2 mol kg ⁻¹ dissolved inorganic salt89

NOTATION

a	activity
a_i^k	activity of component i in phase k
a_{ij} (J mol ⁻¹)	molecule-molecule interaction parameter
a_ε	dielectric constant correlation coefficient
A (cm ²)	interfacial area
A_i (ng m ⁻³)	gas-phase concentration
A_{mo} (K ⁻¹)	group-group interaction parameter
A_ρ	density correlation coefficient
b_ε	dielectric constant correlation coefficient
B_ρ	density correlation coefficient
c (g cm ⁻³)	concentration
Δc (g cm ⁻³)	concentration difference
c_i^k (g cm ⁻³)	concentration of i in phase k
$c_{i,bulk}^k$ (g cm ⁻³)	bulk concentration of i in phase k
$c_{i,int}^k$	interfacial concentration of i in phase k
c_ε	dielectric constant correlation coefficient
C	combinatorial
\bar{C}_i	mean oxidation state of carbon in molecule i
\bar{C}_{PM}	mean oxidation state of carbon in a PM phase
d_ε	dielectric constant correlation coefficient
D (cm ² s ⁻¹)	diffusion coefficient
f	mass fraction of absorbing phase in total particulate matter
f_n	parameterization function
F (ng m ⁻³)	particle-phase concentration

$F_{\text{non-vol}}$ (ng m^{-3})	mass concentration of the non-volatile component of total particulate matter
G	gas
G (J)	free energy
G_f	hygroscopic growth factor
GCM	group contribution method
HC	hydrocarbon
ΔHC ($\mu\text{g m}^{-3}$)	amount of reacted hydrocarbon
i	component index
I (mol kg^{-1})	ionic strength
j	component index
k	phase index (Chapter 2); functional group index (Chapter 3 and 4)
$K_{p,i}$ ($\text{m}^3 \mu\text{g}^{-1}$)	partition constant
LLE	liquid-liquid equilibrium
LP	low-polarity
m	functional group index
m_i (g)	mass
m_j (mol kg^{-1})	molality of ion j
M_o ($\mu\text{g m}^{-3}$)	organic mass concentration
M_t ($\mu\text{g m}^{-3}$)	total mass concentration
M_w ($\mu\text{g m}^{-3}$)	water mass concentration
MW_n (g mol^{-1})	molecular weight of solvent n
MW_{om} (g mol^{-1})	number average molecular weight of organic matter
MW_s (g mol^{-1})	molecular weight of solution phase
n	solvent compound index
$n_{C,i}$	number of carbon atoms in compound i
n_i^k (mols)	number of moles of component i in phase k
n_T^k (mols)	total number of moles in phase k
n_ρ	density correlation coefficient
N	number of components
N_p	number of solvent compounds in system p

N_S	number of experimental systems
N_ζ	number of ζ values
o	organic
o	functional group index
OC	organic carbon
OPM	organic particulate matter
p	system index
p_L° (Torr)	pure compound vapor pressure (sub-cooled if necessary)
P	particle
PM	particulate matter
q_i	surface area of component i
Q_k	surface area parameter of functional group k
r_i	volume of component i
R	residual
R	ideal gas constant
R_k	volume parameter of functional group k
RH	relative humidity
SOA	secondary organic aerosol
SPARC	Scalable processor architecture Performs Automated Reasoning in Chemistry
Δt (s)	time step
T (K)	temperature
T_i (ng m ⁻³)	total gas + particle mass concentration
T_c (K)	critical temperature
TPM (μg m ⁻³)	total particulate matter
u_{ij} (J mol ⁻¹)	interaction energy between constituents i and j
U_{mo} (J mol ⁻¹)	interaction energy between constituents m and o
UNIFAC	UNIQUAC Functional Activity Coefficients
UNIQUAC	UNIversal QUAsi-Chemical
v^k (cm ³)	volume of phase k
\bar{v}^k (cm ³ mol ⁻¹)	molar volume of phase k

v_T (cm ³)	total volume
V (m ³ mol ⁻¹)	molar volume
V_n (m ³ mol ⁻¹)	molar volume of solvent n
VLE	vapor-liquid equilibrium
VOC	volatile organic compound
w	water
x	x -direction in Cartesian coordinate system
X	mole fraction
X'_n	salt-free mole fraction of solvent n
Y	aerosol yield
Y_o	organic aerosol yield
Y_w	water aerosol yield
Y_t	total aerosol yield

Greek Symbols

α_i	mass stoichiometric factor
δ (cm)	hypothetical diffusion length
δ^k (cm)	hypothetical diffusion length in phase k
ε	numerical tolerance
ε_n	dielectric constant of solvent n
ε_s	dielectric constant of a solution phase
ζ	activity coefficient
ζ_i^k	activity coefficient of component i in phase k
$\zeta_{i,bulk}^k$	bulk-phase activity coefficient of component i in phase k
$\zeta_n^{\phi, \text{expt}}$	activity coefficient of solvent n in phase ϕ calculated from experimental data
$\zeta_n^{\phi, \text{pred}}$	predicted activity coefficient of solvent n in phase ϕ
Z_k	residual activity coefficient of group k
Z_k^n	residual activity coefficient of group k in a reference solution of components n

θ_i	surface area fraction of component i
Θ_m	surface area fraction of group m
μ (J mol ⁻¹)	chemical potential
μ° (J mol ⁻¹)	standard state chemical potential
μ_i^k (J mol ⁻¹)	chemical potential of component i in phase k
v_k^i	number of groups of type k in component i
ρ_i (g cm ⁻³)	density of component i
ρ_n (kg m ⁻³)	density of solvent n
ρ_s (kg m ⁻³)	density of a solution phase
σ_{FIT}	standard error of fit
$\sigma_{\text{FIT,signed}}$	signed standard error of fit
$\sigma_{n,p}^\phi$	standard error for solvent n in phase ϕ of system p
$\bar{\sigma}_a$	average standard error in an activity grouping
$\bar{\sigma}_n$	average standard error for solvent n
τ	molecular interaction term
φ	phase index
Φ_i	volume fraction of component i
Ψ	group interaction term

ABSTRACT

Effects of Multiple Phases and Ionic Constituents on Gas/Particle Partitioning in
Atmospheric and Other Aerosols

Garnet Bailey Erdakos

Ph.D., OGI School of Science & Engineering
at Oregon Health & Science University

August 2004

Thesis Advisor: James F. Pankow

The overall composition and concentration of atmospheric particulate matter (PM) influences the effects of PM on visibility, cloud formation, and human health. Aerosol PM in the ambient atmosphere may be comprised of a mixture of non-polar and relatively polar organic compounds, inorganic salts, and water. When significant amounts of water, non-polar compounds related to primary anthropogenic emissions and/or plant wax debris, and organic species are present in an aerosol system, the aerosol PM may be more stable as two liquid phases than as one homogeneous liquid phase. When phase separation to two liquid phases can occur, with one phase relatively more polar and the other relatively less polar, it can be expected that the increased stability of the system that is accomplished will generally lead to higher total PM (TPM, $\mu\text{g m}^{-3}$) concentrations than would otherwise be the case. On the other hand, the additional presence of PM-phase dissolved inorganic salts has been observed to decrease the organic portion of TPM. A modeling method was developed for use in predicting the stability of multiple liquid phases in atmospheric PM. The method utilizes a pseudo-diffusion process that simulates the multicomponent inter-phasic movement of constituents

between adjacent PM phases. It can be used as a stand-alone application, and can also be incorporated in overall gas/particle (G/P) partitioning models of aerosol PM formation. The well-known UNIFAC (UNIQUAC Functional-group Activity Coefficients) method was used to calculate the necessary activity coefficient (ζ) values of all diffusing constituents. UNIFAC applies only to mixtures of non-electrolytes. In order to predict the effects of dissolved inorganic salts on the formation of aerosol PM, a UNIFAC-based method (Ionic-UNIFAC.1) was developed for calculating activity coefficients of neutral compounds in general PM comprised of a mixture of organic compounds, dissolved inorganic salts, and water, with total salt concentrations as much as 2 mol kg^{-1} . The ζ values are considered to be determined by a combination of short- and long-range interactions. The expression utilized for ζ involves both a Debye-Hückel term and conventional UNIFAC terms. This method was then implemented in a G/P partitioning model to predict the formation of general PM and changes in PM concentrations and compositions relative to cases in which no salt was present.

It was predicted that the combined presence of low-polarity compounds together with higher polarity compounds can lead to phase separation to two phases, even in the absence of water in the PM. The assumption of a single PM phase when in fact the PM is more stable as two phases will lead to errors in the predicted TPM value; the examples considered here gave errors in the range -3.9% to -21.8%. The relative error in ζ values predicted with Ionic-UNIFAC.1 was found to be independent of the ionic strength (I). On average, the relative error tended to decrease with increasing activity (a) over the range $-2 < \log a < 0.5$, and did not exceed 20% for the data fitted. Average errors in predicted aerosol yields and hygroscopic growth factors in general aerosol systems with dissolved salt concentrations $\approx 2 \text{ mol kg}^{-1}$ were $\sim 20\%$, which is within the expected range of error for Ionic-UNIFAC.1. Excellent agreement was obtained between predicted and measured decreases in aerosol yield in the α -pinene/ O_3 system at RH = 50% with aqueous $(\text{NH}_4)_2\text{SO}_4$ and CaCl_2 seed: 45% vs. 44%, and 21% vs. 24%, respectively.

The methods developed here can be used as tools to predict concentrations and compositions of aerosol PM, and can be applied within three-dimensional air-shed models to assist in air quality management.

CHAPTER 1

INTRODUCTION

1.1 Overview

Aerosol particulate matter (PM) in the ambient atmosphere can contribute to visibility degradation and global climate change and can have adverse environmental and human health effects. The effects of atmospheric PM are largely determined by its composition and concentration as well as particle size. Fine PM, or PM with an aerodynamic diameter $\leq 2.5 \mu\text{m}$, has been implicated as a major contributor to the effects mentioned above. PM in this size range can form by direct emission as primary PM, or by secondary processes. Secondary aerosol PM can form by condensation of the oxidation products of reacted volatile organic compounds (VOCs). These products can form PM by homogeneous nucleation and by condensation onto preexisting particles.

Secondary organic aerosol (SOA) has been identified in the atmosphere and has been characterized in smog chamber studies. Pankow (1994a,b) introduced a model of absorptive gas/particle (G/P) partitioning that describes theoretically the formation of organic PM (OPM) that forms in SOA systems. Pankow et al. (2001) successfully implemented that model to predict the formation of OPM in several monoterpene/O₃ systems and the cyclohexene/O₃ system. Their results agreed well with observed data. Seinfeld et al. (2001) extended the work of Pankow et al. (2001) to include the effects of relative humidity (RH) on the formation of OPM. Their predictions showed a greater uptake of water in the cyclohexene/O₃ system, in which the oxidation products were generally of higher polarity than those in the monoterpene/O₃ systems. In both of these studies, the UNIFAC (Fredenslund et al., 1975) group contribution method (GCM) was used to calculate necessary activity coefficients.

The UNIFAC (*UNIQUAC* Functional-group Activity Coefficients) method was developed to estimate activity coefficients of compounds in nonelectrolyte mixtures to

assist in the design of chemical separation processes. Parameters for UNIFAC were therefore optimized using primarily data for mixtures of nonionizing short-chained organic species and water. As a GCM, UNIFAC does not account for structural characteristics such as the presence of multiple oxygenated functional groups in a single molecule. This feature may be problematic for atmospheric applications, as many condensable organic species in the atmosphere are multi-functional oxygenated compounds. However, the method has been used with success, as exemplified by the Pankow et al. (2001) study, and there are currently no other sufficient methods available for calculating activity coefficients in organic/water mixtures.

Atmospheric PM is not limited in composition to organic compounds and water. Indeed, inorganic species can comprise a large fraction of total PM (TPM) mass in the ambient atmosphere (Seinfeld and Pandis, 1998). It has been observed in chamber experiments that the mass fraction of PM contributed by organic compounds and water can be significantly reduced by the presence of dissolved inorganic salts (Cocker et al., 2001). Furthermore, while multiple PM phases may form in OPM when both non-polar and relatively polar organic species are present, it is also likely that multiple phases will form when both organic and inorganic species are present. The presence of multiple PM phases in either OPM or general mixed organic/inorganic PM will influence the composition and concentration of TPM.

Prior to the work presented in this dissertation, no models were available to predict the formation of multi-phasic PM or PM composed of a general mixture of organic species, water, and inorganic salts. However, other researchers have made steps toward such predictions. Pun et al. (2002) developed an initial approach that modeled the formation of organic/water PM by assuming the *a priori* existence of two liquid phases: one comprised primarily of water, the water-soluble organic compounds, and possibly inorganic ions; and the other phase containing only the lower-polarity organic compounds. This model places a non-thermodynamic *phase lock* on the system because it does not allow all species to move among all compartments. Griffin et al. (2003) propose a model that largely relaxes that phase lock by allowing all modeled organic compounds to partition from the gas phase to both the higher polarity (“hydrophilic”) and lower polarity (“hydrophobic”) phases. In the cases considered by Griffin et al. (2003),

however, water was still confined to the “hydrophilic” phase. While this assumption will be justified in many important cases, the general case nevertheless requires allowing all constituents to exist in both liquid phases. A new general modeling tool is presented in Chapter 2 of this dissertation. This tool can be used for examining when a given liquid PM composition can achieve a more stable state by undergoing phase separation into two liquid phases, with all constituents allowed in both liquid phases. It may be incorporated in overall gas/particle G/P partitioning models of PM formation as described by Pankow (2003).

A method for predicting activity coefficients in a general PM mixture composed of organic species, dissolved inorganic salts, and water is necessary to model the overall G/P equilibrium of such mixtures (Pankow, 2003). A number of activity coefficient methods are available for limiting cases of general mixed PM. They include several “extended-UNIQUAC” (UNIversal QUAsi-Chemical) and “extended-UNIFAC” methods, which were primarily developed to assist in the design of chemical separation processes (e.g., Sander et al., 1986; Cardoso and O’Connell, 1987; Macedo et al., 1990; Kikic et al., 1991; Li et al., 1994; Achard et al. 1994; Yan et al., 1999). Consequently, the scope of those models does not encompass some important atmospheric PM conditions and chemical compositions. More recently, Clegg et al. (2001) and Ming and Russell (2002) introduced activity coefficient parameterizations that were developed intently for organic/inorganic salt/water mixtures relevant to atmospheric PM. The approach of Clegg et al. (2001) assumes ion-water, ion-organic, and organic-water interactions to be independent of each other, but in doing so allows the user to select among different existing models for each type of interaction. This model is applicable to only mixtures in which organic compound concentrations are low. Ming and Russell (2002) present a similar approach using a combined “Pitzer-UNIFAC” model. Their distinct treatment of chemical groups in multi-functional oxygenated organic compounds (e.g., diacids and hydroxy-acids) is a significant advancement beyond previous “extended-UNIFAC” models. However, the optimization of ion-organic interaction parameters was limited to NaCl-containing mixtures. A new method for predicting activity coefficients in general organic/ inorganic salt/water mixtures with salt concentrations $\leq 2 \text{ mol kg}^{-1}$ is presented in Chapter 3 of this dissertation.

Chapter 4 of this dissertation covers implementation of the new activity coefficient prediction method within a G/P equilibrium model for two atmospherically relevant aerosol systems: 1) the α -pinene/O₃ system; and 2) the cyclohexene/O₃ system. These two systems have been well-characterized and successfully modeled in the absence of dissolved salts (Pankow et al., 2001; Seinfeld et al., 2001; Erdakos and Pankow, 2003). Moreover, the α -pinene/O₃ system was investigated experimentally by Cocker et al. (2001) in the presence of dissolved inorganic salts. Effects of dissolved inorganic salts on the formation of OPM are predicted over a range of RH values. Four individual salts (NaCl; (NH₄)₂SO₄; Na₂SO₄; and CaCl₂) are investigated. Changes in: 1) aerosol yields; 2) PM composition; and 3) individual oxidation product activity coefficients are quantified. There is reasonable agreement between predicted results and the experimental observations of Cocker et al. (2001) for the α -pinene/O₃ system containing dissolved inorganic salt.

In summary, the objectives of the research presented in this dissertation are to advance the understanding of the effects of (1) multiple phases and (2) ionic constituents on atmospheric (and other) aerosol PM formation. A new model for testing the stability of multiple phases in aerosol PM and a new method for estimating activity coefficients in general organic/inorganic salt/water PM mixtures were developed to achieve those objectives. The results of this work are a significant contribution toward better representation and understanding of complex aerosols that exist in the atmosphere and in other general aerosol systems.

1.2 Format of Dissertation

Where noted, chapters of this dissertation are reproductions of manuscripts that have either been published in a scientific journal or have been submitted for publication in such. References to each manuscript are given as footnotes at the beginning of each chapter.

1.3 References

Achard, C., Dussap, C.G., Gros, J.B., 1994. Representation of vapour-liquid equilibria in water-alcohol-electrolyte mixtures with a modified UNIFAC group-contribution method. *Fluid Phase Equilibria* 98, 71-89.

- Cardoso, M.J.E. De M., O'Connell, J.P., 1987. Activity coefficients in mixed solvent electrolyte solutions. *Fluid Phase Equilibria* 33, 315-326.
- Clegg, S.L., Seinfeld, J.H., Brimblecombe, P., 2001. Thermodynamic modelling of aqueous aerosols containing electrolytes and dissolved organic compounds. *Journal of Aerosol Science* 32, 713-738.
- Cocker, D. R. III; Clegg, S. L.; Flagan, R. C.; Seinfeld, J. H., 2001. The effect of water on gas-particle partitioning of secondary organic aerosol. Part I: α -pinene/ozone system. *Atmospheric Environment* 35, 6049-6072.
- Erdakos, G.B., Pankow, J.F., 2003. Gas/Particle Partitioning of Neutral and Ionizing Compounds to Single- and Multi-Phase Aerosol Particles. 2. Phase Separation in Liquid Particulate Matter Containing Both Polar and Low-Polarity Organic Compounds. *Atmospheric Environment* 38, 1005-1013.
- Fredenslund, A., Jones, R.L., Prausnitz, J.M., 1975. Group-contribution estimation of activity coefficients in nonideal liquid mixtures. *American Institute of Chemical Engineers Journal* 21, 1086-1099.
- Griffin, R.J., Nguyen, K., Dabdub, D., Seinfeld, J.H., 2003. A coupled hydrophobic-hydrophilic model for predicting secondary organic aerosol formation. *Journal of Atmospheric Chemistry* 44, 171-190.
- Kikic, I., Fermeglia, M., Rasmussen, P., 1991. UNIFAC prediction of vapor-liquid equilibria in mixed solvent-salt systems. *Chemical Engineering Science* 46, 2775-2780.
- Li, J., Polka, H-M., Gmehling, J., 1994. A g^E model for single and mixed solvent electrolyte systems. 1. Model and results for strong electrolytes. *Fluid Phase Equilibria* 94, 89-114.
- Macedo, E.A., Skovborg, P., Rasmussen, P., 1990. Calculation of phase equilibria for solutions of strong electrolytes in solvent-water mixtures. *Chemical Engineering Science* 45, 875-882.
- Ming, Y., Russell, L.M., 2002. Thermodynamic equilibrium of organic-electrolyte mixtures in aerosol particles. *American Institute of Chemical Engineers Journal* 48, 1331-1348.
- Pankow, J.F., 1994a. An absorption model of gas/particle partitioning of organic compounds in the atmosphere. *Atmospheric Environment* 28, 185-188.
- Pankow, J.F., 1994b. An absorption model of the gas/aerosol partitioning involved in the formation of secondary organic aerosol. *Atmospheric Environment* 28, 189-193.

- Pankow, J.F., 2003. Gas/particle partitioning of neutral and ionizing compounds to single and multi-phase particles. 1. Unified modeling framework. *Atmospheric Environment* 37, 3323-3333.
- Pankow, J.F., Seinfeld, J.H., Asher, W.E., Erdakos, G.B., 2001. Modeling the formation of secondary organic aerosol: 1. The application of theoretical principles to measurements obtained in the α -pinene-, β -pinene-, sabinene-, Δ^3 -carene-, and cyclohexene-ozone systems. *Environmental Science and Technology* 35, 1164-1172.
- Pun, B.K., Griffin, R.J., Seigneur, C., and Seinfeld, J.H., 2002: Secondary organic aerosol: 2. Thermodynamic model for gas/particle partitioning of molecular constituents. *Journal of Geophysical Research* 107, AAC4/1-AAC4/15.
- Sander, B., Fredenslund, A., Rasmussen, P., 1986. Calculation of vapour-liquid equilibria in mixed solvent/salt systems using an extended UNIQUAC equation. *Chemical Engineering Science* 41, 1171-1183.
- Seinfeld, J.H., Pandis, S.N., 1998. *Atmospheric Chemistry and Physics: from air pollution to climate change*, John Wiley & Sons, New York.
- Seinfeld, J.H., Erdakos, G.B., Asher, W.E., Pankow, J.F., 2001. Modeling the formation of secondary organic aerosols: 2. The predicted effects of relative humidity on aerosol formation in the α -pinene-, β -pinene-, sabinene-, Δ^3 -carene-, and cyclohexene-ozone systems. *Environmental Science and Technology* 35, 1806-1817.
- Yan, W., Topphoff, M., Rose, C., Gmehling, J., 1999. Prediction of vapor-liquid equilibria in mixed-solvent electrolyte systems using the group contribution concept. *Fluid Phase Equilibria* 162, 97-113.

CHAPTER 2

PHASE SEPARATION IN LIQUID PARTICULATE MATTER CONTAINING BOTH POLAR AND LOW-POLARITY ORGANIC COMPOUNDS¹

2.1 Abstract

A modeling method is developed for use in predicting the stability of multiple liquid phases in atmospheric particulate matter (PM). The method utilizes a pseudo-diffusion process that simulates the multicomponent inter-phasic movement of constituents between adjacent PM phases. It can be used as a stand-alone application, and can also be incorporated in overall gas/particle (G/P) partitioning models of aerosol PM formation. Previously-studied (Seinfeld et al., 2001) relative-humidity (RH) dependent PM compositions resulting from the ozone oxidation of five different volatile organic compounds (VOCs) were verified as being stable as single phases. A number of additional cases were considered in which RH-dependent secondary PM compositions were amended with a mix of low-polarity (LP) organic compounds. It was determined that, depending on the mass fraction of added LP-mix, the PM can be more stable as a two-phase system. Phase separation to two phases can occur even in the absence of water in the PM. Assuming a single liquid PM phase when two are actually present will generally lead to an underprediction of total PM (TPM). For the cases considered here, the calculated errors in predicted TPM levels were found to range from -3.9% to -21.8%; conditions can be envisioned that would lead to even larger errors.

¹ Erdakos, G.B., Pankow, J.F., 2003. Gas/particle partitioning of neutral and ionizing compounds to single- and multi-phase aerosol particles. 2. Phase separation in liquid particulate matter containing both polar and low-polarity compounds. *Atmospheric Environment* 38, 1005-1013.

2.2 Introduction

The concentration of organic particulate matter (OPM, $\mu\text{g m}^{-3}$) in the atmosphere is determined in large part by absorptive partitioning between the gas and PM phases (Pankow, 1994a,b). When the PM is composed largely of the secondary, polar oxidation products of volatile organic compounds (VOCs), modeling the PM formation process has involved the assumption that only one liquid PM phase is present (e.g., Pankow 1994a,b; Odum et al., 1996; Pankow et al., 2001; Seinfeld et al., 2001; Seinfeld and Pankow, 2003). However, when significant amounts of water and/or non-polar compounds related to primary anthropogenic emissions and/or plant wax debris are also present, the aerosol PM may be more stable as two liquid phases than as one homogeneous liquid phase. When phase separation to two liquid phases can occur, with one phase relatively more polar and the other relatively less polar, it can be expected that the increased stability of the system that is accomplished will generally lead to higher total PM (TPM, $\mu\text{g m}^{-3}$) concentrations than would otherwise be the case. It is therefore of considerable interest to have a modeling tool that allows the prediction of which types of aerosol system compositions will lead to such phase separation, and which will not.

Pun et al. (2002) developed an initial approach that modeled the formation of organic/water PM by assuming the *a priori* existence of two liquid phases: one comprised primarily of water, the water-soluble organic compounds, and possibly inorganic ions; and the other phase containing only the lower-polarity organic compounds. This model places a non-thermodynamic *phase lock* on the system because it does not allow all species to move among all compartments. Griffin et al. (2003) propose a model that largely relaxes that phase lock by allowing all modeled organic compounds to partition from the gas phase to both the higher polarity (“hydrophilic”) and lower polarity (“hydrophobic”) phases. In the cases considered by Griffin et al. (2003), however, water was still confined to the “hydrophilic” phase. While this assumption will be justified in many important cases, the general case nevertheless requires allowing all constituents to exist in both liquid phases. The purpose of the current work is to describe a general modeling tool that can be used for examining when a given liquid PM composition can achieve a more stable state by undergoing phase separation into two liquid phases, with all constituents allowed in both liquid phases. This tool may be used

in stand-alone considerations of the phase stability of specific PM compositions, and also incorporated in overall gas/particle (G/P) partitioning models of PM formation as described by Pankow (2003).

In prior work, we developed a mathematical framework for modeling the condensation of VOC oxidation products to form secondary OPM (Pankow, 1994b; Pankow *et al.*, 2001). More recently, Seinfeld *et al.* (2001) considered how initially-dry OPM will absorb water as the relative humidity (RH) increases from RH = 0% to near 100%. A primary conclusion of that work was that when the oxidation products that condense to form the OPM are relatively polar, then the OPM can absorb significant amounts of water as RH rises above ~50%. For all of those calculations: 1) it was assumed that the modeled PM phase was thermodynamically stable and would not tend to separate into two phases at any of the RH values considered; and 2) that assumption was examined by verifying that for each component the chemical activity a was less than unity in each single-phase PM case of interest. However, the requirement that $a_i < 1$ for each component i in a liquid mixture is only a *necessary* condition for the stability as a single liquid phase, and not a *sufficient* condition (Seinfeld *et al.*, 2001). It is necessary because when $a_i = 1$, pure liquid i becomes stable at equilibrium; it is not sufficient because it does not rule out the possibility that the liquid could undergo phase separation after which a_i is equal in the two phases as well as less than 1. In this study, a modeling tool is developed and utilized to examine phase stability in PM for a variety of organic and water-organic systems; the overall thermodynamic gas-particle (G/P) equilibrium was also calculated for each PM case considered.

2.3. PM Composition Cases

The cases considered included the RH-dependent secondary PM compositions discussed by Seinfeld *et al.* (2001) for the ozone oxidation of α -pinene, β -pinene, sabinene, Δ^3 -carene, and cyclohexene, as well as hypothetical PM compositions derived from those cases by adding relevant amounts of non-polar, lipid compounds such as long-chain hydrocarbons from primary emissions and aerosolized plant wax debris.

Lipid compounds can comprise 10-30% of the total organic carbon (OC) in ambient atmospheric aerosols (Simoneit and Mazurek, 1982; Simoneit, 1986,1989;

Rogge et al., 1993; Fraser et al., 1997,1998; Didyk et al., 2000; Kendall et al., 2001). These compounds include $\sim C_{10}$ - C_{40+} aliphatic hydrocarbons, alcohols, and acids (Simoneit and Mazurek, 1982; Simoneit, 1986; Rogge et al., 1993). The distribution of the low-polarity (LP) mix of compounds added to the secondary PM cases considered here (Table 2.1) was based on the data of Simoneit and Mazurek (1982) for series of n -alkanes, n -fatty acids, and n -fatty alcohols in aerosol samples collected at two urban Los Angeles area sites. The identities and proportions of the compounds in the LP mix were based on: 1) the fraction of the total lipid concentration comprised by each series; and 2) the number of dominant compounds in each series. The monoterpene/ozone and cyclohexene/ozone PM cases discussed above were then amended by adding lipid compounds so that 10% of the total OC in each resulting composition was from the LP mix.

2.4 Methods

2.4.1 The pseudo-diffusion phase stability method

2.4.1.1 Basic considerations

In a multi-phase system composed of N different compounds, the criterion for equilibrium in the overall system is an equality of the chemical potential μ of each compound i among all phases $\alpha, \beta, \dots, \omega$:

$$\mu_i^\alpha = \mu_i^\beta = \dots = \mu_i^\omega \quad (2.1)$$

where $\omega \leq N$. Taking the standard state for each compound i in all the phases to be pure liquid i at the temperature of interest leads directly to

$$a_i^\alpha = a_i^\beta = \dots = a_i^\omega \quad (2.2)$$

or

$$\zeta_i^\alpha X_i^\alpha = \zeta_i^\beta X_i^\beta = \dots = \zeta_i^\omega X_i^\omega \quad (2.3)$$

where ζ is the activity coefficient, and X is the mole fraction.

Consider a closed system composed of two liquid compounds A and B that are not miscible over all proportions (*e.g.*, pinonic acid and water at ambient temperature (Cruz and Pandis, 2000)), and for which a system composition of $X_A = X_B$ is within the composition region where two liquid phases are thermodynamically stable, *i.e.*, within

the miscibility gap. If equi-molar amounts of A and B are placed in contact with one another, diffusive transport of A into the initially-pure B, and of B into the initially-pure A will eventually bring the two phases into saturation equilibrium with one another such that Eq. (2.3) is satisfied. The same type of diffusion process can be envisioned to take place when a single liquid phase containing many components is *hypothetically* separated into two phases (α = more polar; β = less polar) that are most probably not at equilibrium with one another. Multicomponent interdiffusion over time will then move such a system either back to a single phase, or to two new liquid phases at equilibrium. In the latter case, the overall free energy of the two-phase system will be lower than that of the initial single-phase system. Separation to three liquid phases would not be common in atmospheric aerosols, and so was not considered here.

2.4.1.2. *Implementation*

The initial total volume v_T of PM in each case is a fixed value calculated as that occupied by some specific volume of air (e.g., 1 m³). The two separate phase volumes (v^α and v^β) are assumed to be adjacent rectangular compartments. The hypothetical liquid/liquid interfacial area A (cm²) is then calculated as $(v_T)^{2/3}$. In an initial phase-separated system, there will be concentration gradients in both of the adjacent phases. Fick's First Law of diffusion (flux = $-D(dc/dx)$) gives the flux (g cm⁻² s⁻¹) of each component across the area A according to a compound-independent diffusion coefficient D (approximated in this study as 10⁻⁵ cm² s⁻¹ for all compounds), and a hypothetical mass concentration gradient dc/dx assumed to exist orthogonal to A . This use of Fick's First Law provides that the flux for each i is properly scaled according to the size and direction of the inter-phase chemical-potential for i . The goal of each diffusion simulation is to find the final equilibrium state, and not to reproduce the actual time course of any real interdiffusion process.

Fick's First Law may be discretized according to

$$\text{flux} = -D \frac{\Delta c}{\delta} \quad (2.4)$$

where Δc is a concentration difference (g cm⁻³) over a hypothetical diffusion length δ (cm), and the x -direction is measured positively from the α to the β phase. The δ values

are scaled according to $\delta^\alpha = (v^\alpha)^{1/3}$ and $\delta^\beta = (v^\beta)^{1/3}$. For each component i at each time step, the model utilizes two bulk ($c_{i,\text{bulk}}^\alpha$ and $c_{i,\text{bulk}}^\beta$) concentrations and two interfacial ($c_{i,\text{int}}^\alpha$ and $c_{i,\text{int}}^\beta$) concentrations (Figure 2.1). The hypothetical discrete concentration gradients $\Delta c / \delta$ are thus computed as $(c_{i,\text{int}}^\alpha - c_{i,\text{bulk}}^\alpha) / \delta^\alpha$ and $(c_{i,\text{bulk}}^\beta - c_{i,\text{int}}^\beta) / \delta^\beta$. The $c_{i,\text{int}}^\alpha$ and $c_{i,\text{int}}^\beta$ values are calculated for each time step as the concentrations that i would assume in the α and β phases for equilibrium with $c_{i,\text{bulk}}^\beta$ and $c_{i,\text{bulk}}^\alpha$, respectively. The calculations of $c_{i,\text{int}}^\alpha$ and $c_{i,\text{int}}^\beta$ are based on the assumption of equilibrium directly at the interface so that from Eq. (2.3)

$$X_{i,\text{int}}^\alpha = \frac{\zeta_{i,\text{bulk}}^\beta X_{i,\text{bulk}}^\beta}{\zeta_{i,\text{bulk}}^\alpha} \quad \text{and} \quad X_{i,\text{int}}^\beta = \frac{\zeta_{i,\text{bulk}}^\alpha X_{i,\text{bulk}}^\alpha}{\zeta_{i,\text{bulk}}^\beta} \quad (2.5)$$

(see Appendix 1). The time-step dependent ζ values are computed using the time-step dependent bulk-phase compositions. In this work, UNIFAC (Fredenslund et al., 1977,1994) was used to determine the needed ζ values.

For every i at every time step, the two computed flux values will share the same sign, and so will tend to move i in the same direction. For example, if $c_{i,\text{int}}^\alpha > c_{i,\text{bulk}}^\alpha$, then most likely $c_{i,\text{bulk}}^\beta > c_{i,\text{int}}^\beta$, Δc will be positive and the flux will be negative in both phases, and movement of i will be in the $-x$ -direction (from the β phase to the α phase). In this work, the value with the largest magnitude was used to compute the mass moved from one bulk phase to the other according to:

$$\Delta m_i = \text{flux}_i A \Delta t \quad (2.6)$$

The time step Δt (s) is scaled according to $\Delta t = sA/D$, where the additional scaling factor s can be used as necessary to maintain numerical stability. Each simulation is continued until the system either returns to a single phase, or finds a two-phase system at equilibrium with all $a_i^\alpha / a_i^\beta = 1 \pm \varepsilon$. In this work, the tolerance ε was set at 10^{-2} .

2.4.2 Errors incurred by assuming a single PM phase

When it occurs, phase separation in PM will lead to a lower free energy level in the PM (see Appendix 2). Consequently, as noted above, in a corresponding G/P distribution problem of this type, the amount of PM predicted to be present will be different and generally larger when two phases form as compared to that calculated when a single homogeneous PM phase is assumed. Errors incurred by assuming a single PM phase were calculated in selected cases as follows. For each case, after completion of the phase separation calculations, equilibrium values of the gas-phase concentrations A_i (ng m^{-3}) were first calculated. Then, a specific TPM value was assumed, and the particle-associated concentrations F_i (ng m^{-3}) and the total G+P concentrations $= A_i + F_i = T_i$ (ng m^{-3}) were calculated by means of the unified modeling framework presented by Pankow (2003) (especially Eqs.(39,40)). Lastly, the G/P equilibrium and associated TPM for each vector of T_i values were calculated assuming a *single* PM phase using the approach of Pankow et al. (2001); the difference between that TPM and the true, two-phase TPM constitutes the error associated with assuming a single PM phase.

2.5 Results and Discussion

2.5.1 Phase stability in RH-dependent PM from the ozone oxidation of four monoterpenes and cyclohexene (without and with added LP mix)

All of the RH-dependent (0 to 90%) PM compositions predicted by Seinfeld et al. (2001) for the ozone oxidation of five parent VOCs (α -pinene, β -pinene, sabinene, Δ^3 -carene, and cyclohexene) were verified as being stable as single phases. (The PM compositions at RH = 50% are given in Table 2.2.) Conversely, after amending the RH-dependent α -pinene, β -pinene, sabinene, and cyclohexene PM compositions by adding LP compounds so that 10% of the total OC in each resulting composition was from the LP mix, two phases were predicted to be stable in every case. For the LP-mix amended Δ^3 -carene PM compositions, the PM was stable as one phase at $\text{RH} \leq 15\%$, but as two phases at $\text{RH} > 15\%$. When the Δ^3 -carene PM compositions were amended so that 35% of the total OC was from the LP mix, then two phases were found over the entire RH range.

Figures. 2.2-2.6 provide the calculated two-phase compositions at RH = 50% for LP-mix amended PM derived from the five parent VOCs of interest. The results for all of the monoterpene cases are generally similar, though the total mass percentage of the β (less polar) phase for the Δ^3 -carene case is approximately half that in the other monoterpene cases. Also, the total mass fraction of the water in the PM for the Δ^3 -carene case is less than that for the other monoterpene cases. This is a consequence of the fact that the oxidation products in the Δ^3 -carene case are generally less polar than the oxidation products in the other monoterpene cases.

The polarity difference between the α and β phases is greatest for the LP-mix amended PM from the ozone oxidation of cyclohexene. Indeed, in the cyclohexene case as compared to the monoterpene-derived cases, in the α phase the mass percentage of the LP material is significantly lower and that of water is significantly higher. We note here that the polarity of an organic compound i composed of carbon, hydrogen, and oxygen can be related in rough terms to the mean oxidation state of the carbon in the molecule (\bar{C}_i) (Seinfeld et al., 2001). We here define the mean oxidation state of the carbon in the PM as

$$\bar{C}_{\text{PM}} = \frac{\sum_i n_{C,i} X_i \bar{C}_i}{\sum_i n_{C,i} X_i} \quad (2.7)$$

where $n_{C,i}$ is the number of carbon atoms in compound i .

The above observations are therefore consistent with the fact that the organic PM predicted by Seinfeld et al. (2001) to have formed at RH = 0% in cases involving the ozone oxidation of Δ^3 -carene, α -pinene, β -pinene, sabinene, and cyclohexene have been calculated here to have \bar{C}_{PM} values of approximately -0.87, -0.84, -0.81, -0.76, and 0.11, respectively (ascending order).

2.5.2 Errors incurred by assuming a single PM phase in RH-dependent PM with added LP mix

Several two-phase PM cases were examined to determine the error that would result in predicting TPM by having incorrectly assumed a single PM phase. The five

cases considered (Table 2.3) were based on an initial PM composition of Seinfeld et al. (2001) for the ozone oxidation of cyclohexene with equilibration to RH = 50% (Table 2.2), and then amended so that a particular percentage of the OC in the PM was from the LP mix (Table 2.1). In all cases, the incorrect assumption of a single-phase PM composition results in predicted TPM values that are lower than those of the true two-phase PM compositions. And, as expected, the error increases as the fractional contribution of the LP mix becomes similar to the fractional contribution from the higher polarity oxidation products.

2.6 Conclusions

Phase stability in atmospheric PM systems can be tested using the pseudo-diffusion method developed in this work. In such PM, the combined presence of low-polarity compounds together with higher polarity compounds from the oxidation of parent VOCs can clearly lead to phase separation to two phases. This can occur even in the absence of water in the PM. The assumption of a single PM phase when in fact the PM is more stable as two phases will lead to errors in the predicted TPM value; the examples considered here gave errors in the range -3.9% to -21.8%. It is also concluded that, all other factors remaining equal, the error in the predicted TPM value will tend to maximize as the fractional mass contribution from higher polarity compounds and low polarity compounds become similar.

2.7 Acknowledgement

This work was supported by the Electric Power Research Institute (EPRI) research grant EP-P4650/C2267, Thermodynamics of Atmospheric Organic Aerosols.

2.8 References

Cruz, N.C., Pandis, S.N., 2000. Deliquescence and hygroscopic growth of mixed inorganic-organic atmospheric aerosol. *Environmental Science and Technology* 34, 4313—4319.

- Didyk, B.M., Simoneit, B.R.T., Pezoa, L.A., Riveros, M.L., Flores, A.A., 2000. Urban aerosol particles of Santiago, Chile: organic content and molecular characterization. *Atmospheric Environment* 34, 1167-1179.
- Fraser, M.P., Cass, G.R., Simoneit, B.R.T., Rasmussen, R.A., 1997. Air quality model evaluation data for organics: 4. C₁ to C₃₆ non-aromatic hydrocarbons. *Environmental Science and Technology* 31, 2356-2367.
- Fraser, M.P., Cass, G.R., Simoneit, B.R.T., Rasmussen, R.A., 1998. Air quality model evaluation data for organics: 5. C₆ to C₂₂ nonpolar and semipolar aromatic compounds. *Environmental Science and Technology* 32, 1760-1770.
- Fredenslund, A., Gmehling, J., Rasmussen, P., 1977. *Vapor-Liquid Equilibria Using UNIFAC: A Group-Contribution Method*, Elsevier Scientific Publishing, New York.
- Fredenslund, A., Sorensen, J.M., 1994. *Group Contribution Estimation Methods. Models for Thermodynamic and Phase Equilibria Calculations*; Sandler, S. I. (Ed.), Marcel Dekker Inc., New York.
- Griffin, R.J., Nguyen, K., Dabdub, D., Seinfeld, J.H., 2003. A coupled hydrophobic-hydrophilic model for predicting secondary organic aerosol formation. *Journal of Atmospheric Chemistry* 44, 171-190.
- Hilal, S.H., Carreira, L.A., Karickhoff, S.W., 1994. *Estimation of chemical reactivity parameters and physical properties of organic molecules using SPARC*. In: Murray, P.P.a.J.S. (Ed.), *Quantitative Treatments of Solute/Solvent Interactions*. Elsevier, Amsterdam.
- Kendall, M., Hamilton, R.S., Watt, J., Williams, I.D., 2001. Characterisation of selected speciated organic compounds associated with particulate matter in London. *Atmospheric Environment* 35, 2483-2495.
- Odum, J.R., Hoffmann, T., Bowman, F., Collins, D., Flagan, R.C., Seinfeld, J.H., 1996. Gas/particle partitioning and secondary organic aerosol yields. *Environmental Science and Technology* 30, 2580-2585.
- Pankow, J.F., 1994a. An absorption model of gas/particle partitioning of organic compounds in the atmosphere. *Atmospheric Environment* 28, 185-188.
- Pankow, J.F., 1994b. An absorption model of the gas/aerosol partitioning involved in the formation of secondary organic aerosol. *Atmospheric Environment* 28, 189-193.
- Pankow, J.F., 2003. Gas/particle partitioning of neutral and ionizing compounds to single and multi-phase particles. 1. Unified modeling framework. *Atmospheric Environment* 37, 3323-3333.

- Pankow, J.F., Seinfeld, J.H., Asher, W.E., Erdakos, G.B., 2001. Modeling the formation of secondary organic aerosol: 1. The application of theoretical principles to measurements obtained in the α -pinene-, β -pinene-, sabinene-, Δ^3 -carene-, and cyclohexene-ozone systems. *Environmental Science and Technology* 35, 1164-1172.
- Pun, B.K., Griffin, R.J., Seigneur, C., and Seinfeld, J.H., 2002: Secondary organic aerosol: 2. Thermodynamic model for gas/particle partitioning of molecular constituents. *Journal of Geophysical Research* 107, AAC4/1-AAC4/15.
- Rogge, W.F., Mazurek, M.A., Hildemann, L.M., Cass, G.R., Simoneit, B.R.T., 1993. Quantification of urban organic aerosols at a molecular level: Identification, abundance and seasonal variation. *Atmospheric Environment* 27A, 1309-1330.
- Seinfeld, J.H., Erdakos, G.B., Asher, W.E., Pankow, J.F., 2001. Modeling the formation of secondary organic aerosols: 2. The predicted effects of relative humidity on aerosol formation in the α -pinene-, β -pinene-, sabinene-, Δ^3 -carene-, and cyclohexene-ozone systems. *Environmental Science and Technology* 35, 1806-1817.
- Simoneit, B.R.T., 1986. Characterization of organic constituents in aerosols in relation to their origin and transport: A review. *International Journal of Environmental Analytical Chemistry* 23, 207-237.
- Simoneit, B.R.T., 1989. Organic matter of the troposphere: V. Application of molecular marker analysis to biogenic emissions into the troposphere for source reconciliations. *Journal of Atmospheric Chemistry* 8, 251-275.
- Simoneit, B.R.T., Mazurek, M.A., 1982. Organic matter of the troposphere: II. Natural background of biogenic lipid matter in aerosols over the rural western United States. *Atmospheric Environment* 16, 2139-2159.
- Zhang, Y., Seigneur, C., Seinfeld, J.H., Jacobson, M., Clegg, S.L., Binkowski, F.S., 2000. A comparative review of inorganic aerosol thermodynamic equilibrium modules: similarities, differences, and their likely causes. *Atmospheric Environment* 34, 117-137.

Table 2.1

Distribution of compounds in the low-polarity (LP) mix used to amend model RH-dependent PM compositions for phase stability tests

low-polarity compound	molecular formula	compound type	mass percent
nonacosane	C ₂₉ H ₆₀	<i>n</i> -alkane	17.00
palmitic acid	C ₁₆ H ₃₂ O ₂	<i>n</i> -acid	12.45
octacosanoic acid	C ₂₈ H ₅₆ O ₂	<i>n</i> -acid	2.55
1-dodecanol	C ₁₂ H ₂₆ O	<i>n</i> -alcohol	11.56
1-octadecanol	C ₁₈ H ₃₈ O	<i>n</i> -alcohol	13.60
1-hexacosanol	C ₂₆ H ₅₄ O	<i>n</i> -alcohol	20.40
1-octacosanol	C ₂₈ H ₅₈ O	<i>n</i> -alcohol	10.88
1-triacontanol	C ₃₀ H ₆₂ O	<i>n</i> -alcohol	11.56

Table 2.2
Distribution of compounds in previously modeled water-organic PM compositions
for the ozone oxidation of four monoterpenes and cyclohexene

parent VOC ^a	compound	% of M_{OP+W}
α -pinene	pinic acid	26.1
	norpinonic acid and isomers	25.6
	pinonic acid	21.1
	hydroxy pinonic acid	15.8
	X (pinonic acid)	6.0
	hydroxy pinonaldehydes	1.3
	norpinic acid	0.3
	pinonaldehyde	0.008
	norpinonaldehyde	0.0003
	water	3.8
	total	100.0
β -pinene	norpinonic acid and isomers	52.2
	pinic acid	27.3
	hydroxy norpinonic acids	5.6
	pinonic acid	5.1
	hydroxy pinonic acid	3.4
	norpinic acid	1.7
	X (pinonic acid)	1.2
	hydroxy pina ketone	0.006
	water	3.6
	total	100.0
sabinene	norsabinonic acid and isomers	37.8
	pinic acid	28.2
	sabinic acid	24.2
	S ₁₀ (1-(2-isopropyl)-3-(1-oxo-2-hydroxy-ethyl)-cyclopropyl-ethanoic acid)	3.3
	norsabinic acid	2.3
	X (norsabinonic acid)	0.2
	sabina ketone	0.2
	hydroxy sabina ketone	0.02
	S ₅ (2-(2-isopropyl)-2-formyl-cyclopropyl-methanoic acid)	0.0001
	water	3.7
		total

^a The distribution of compounds in each case is that predicted by Seinfeld et al. (2001) for the ozone oxidation of the parent volatile organic compound (VOC) at RH = 50%. The five cases considered from that earlier work are the following: 1) α -pinene/O₃ experiment 06/17/98a; 2) β -pinene/O₃ experiment 06/11/98b; 3) sabinene/O₃ experiment 06/15/98a; 4) Δ^3 -carene/O₃ experiment 06/15/98b; and 5) cyclohexene/O₃ experiment 05/19/99b.

Table 2.2 (*continued*)

Distribution of compounds in previously modeled water-organic PM compositions for the ozone oxidation of four monoterpenes and cyclohexene

parent VOC ^a	compound	% of M_{OP+W}	
Δ^3 -carene	X (3-caronic acid)	51.7	
	3-caric acid	19.4	
	pinic acid	13.0	
	hydroxy 3-caronic acid	12.6	
	3-caronic acid	0.2	
	nor-3-caronic acid and isomers	0.03	
	C ₄ (2-hydroxy-4-oxo-butanoic acid)	0.005	
	hydroxy caronaldehydes	0.003	
	caronaldehyde	0.00002	
	C ₅ (2,6-dimethyl-4-heptanone)	0.000002	
	water	3.0	
		total	100.0
	cyclohexene	2-hydroxy-glutaric acid	19.8
glutaric acid		15.7	
2-hydroxy-adipic acid		11.2	
6-oxo-hexanoic acid		10.7	
adipic acid		9.0	
5-oxo-pentanoic acid		6.5	
4-oxo-butanoic acid		5.6	
malonic acid		5.6	
oxalic acid		2.5	
adipaldehyde		2.5	
succinic acid		0.9	
glutaraldehyde		0.4	
1,4-butanediol		0.2	
4-hydroxy-butyraldehyde		0.2	
2-hydroxy-pentanoic acid		0.1	
water		8.9	
	total	100.0	

^a The distribution of compounds in each case is that predicted by Seinfeld et al. (2001) for the ozone oxidation of the parent volatile organic compound (VOC) at RH = 50%. The five cases considered from that earlier work are the following: 1) α -pinene/O₃ experiment 06/17/98a; 2) β -pinene/O₃ experiment 06/11/98b; 3) sabinene/O₃ experiment 06/15/98a; 4) Δ^3 -carene/O₃ experiment 06/15/98b; and 5) cyclohexene/O₃ experiment 05/19/99b.

Table 2.3

Errors in predicted TPM ($\mu\text{g m}^{-3}$) assuming single-phase PM in selected two-phase PM cases derived by amending the PM composition from the ozone oxidation of cyclohexene at RH = 50% as reported by Seinfeld et al. (2001) for experiment 05/19/99b with the low-polarity (LP) mix of compounds.

Case:	1	2	3	4	5
% OC from LP mix	10	10	30	30	40
TPM ($\mu\text{g m}^{-3}$) two phases (true)	50.0	30.0	50.0	30.0	30.0
TPM ($\mu\text{g m}^{-3}$) assuming one phase	48.1	28.8	43.1	25.4	23.4
error (%)	-3.9	-4.1	-13.9	-15.4	-21.8

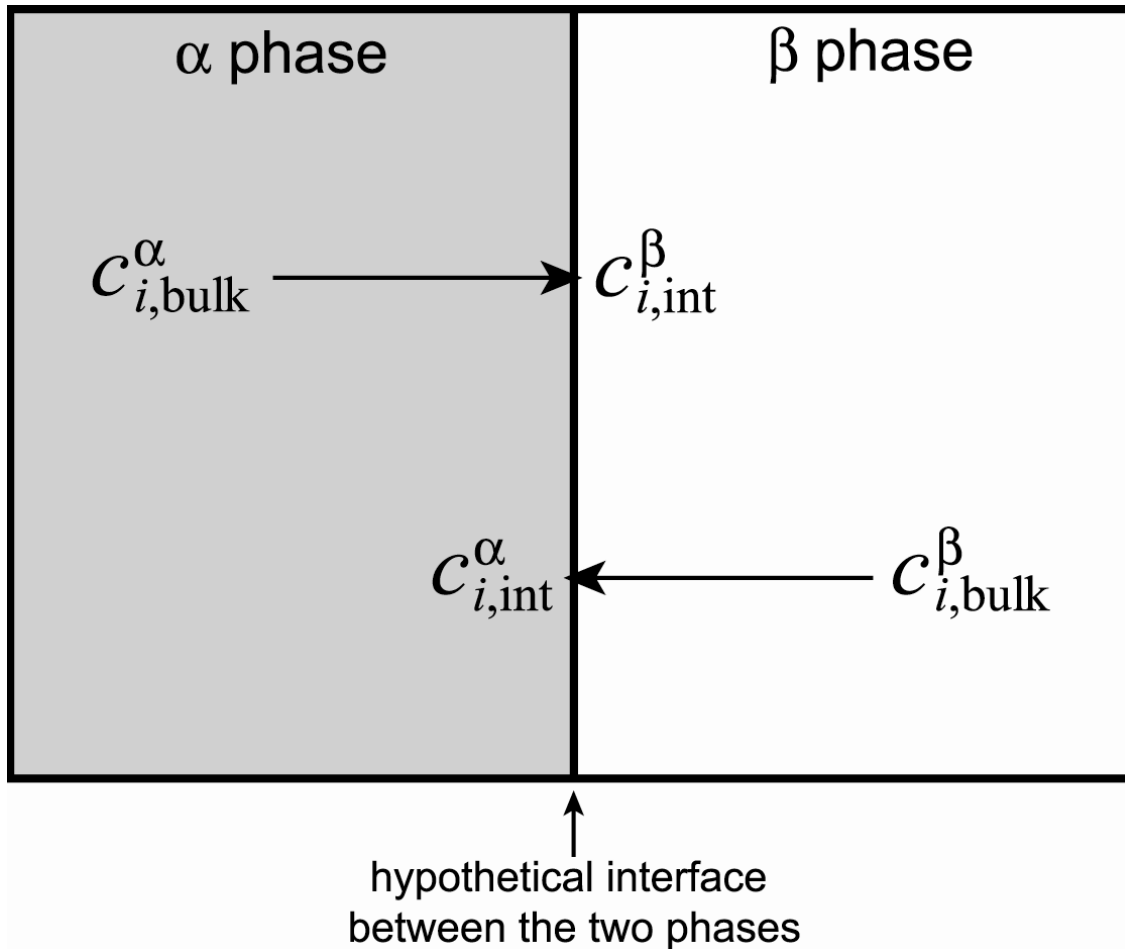


Figure 2.1. Illustration of the initial hypothetical forced phase separation used in the pseudo-diffusion method for testing phase stability. The positive x -direction is measured going from the α to the β phase. The two bulk concentration values $c_{i,bulk}^{\alpha}$ and $c_{i,bulk}^{\beta}$ were used to calculate the interface concentrations in the respective opposite phases, $c_{i,int}^{\beta}$ and $c_{i,int}^{\alpha}$.

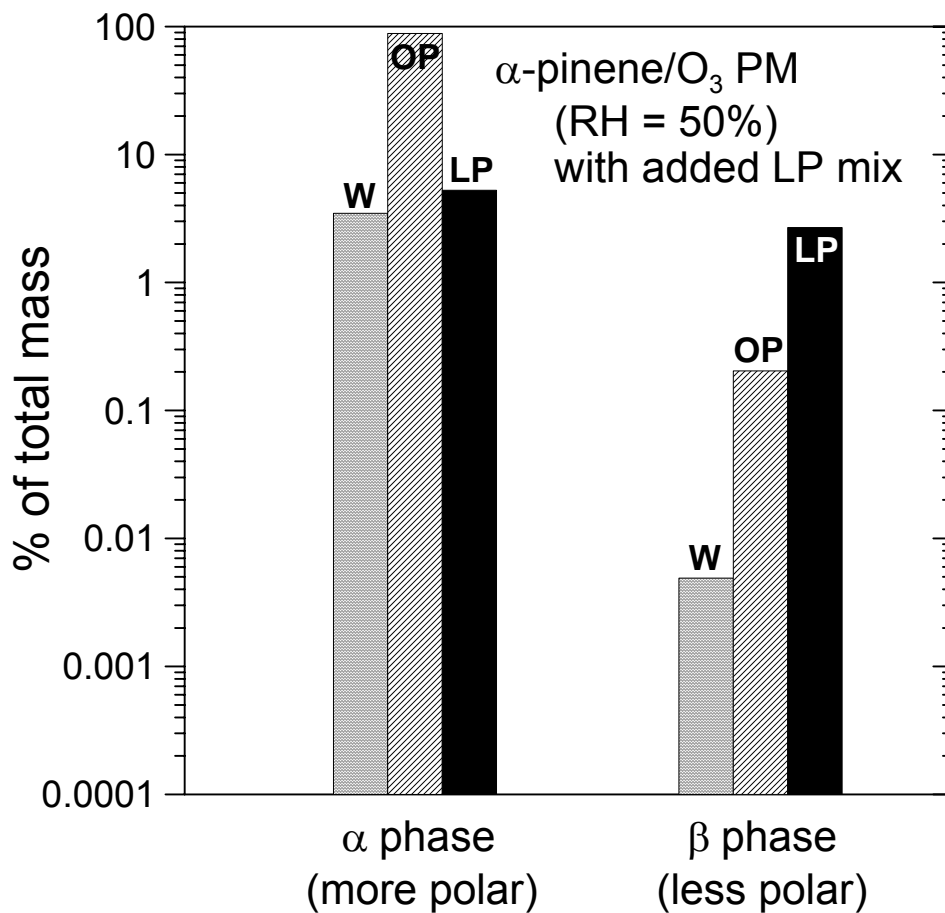


Figure 2.2. Predicted two-phase distribution of components in the PM formed by amending the modeled PM composition (Table 2.2) for the α -pinene/O₃ case so that 10% of the total organic carbon (OC) in the resulting PM was from the low-polarity (LP) mix (Table 2.1). The mass percentages of the α -pinene/O₃ oxidation products (OP), water (W), and LP mix compounds sum to 100% over the two phases (α -more polar, and β -less polar).

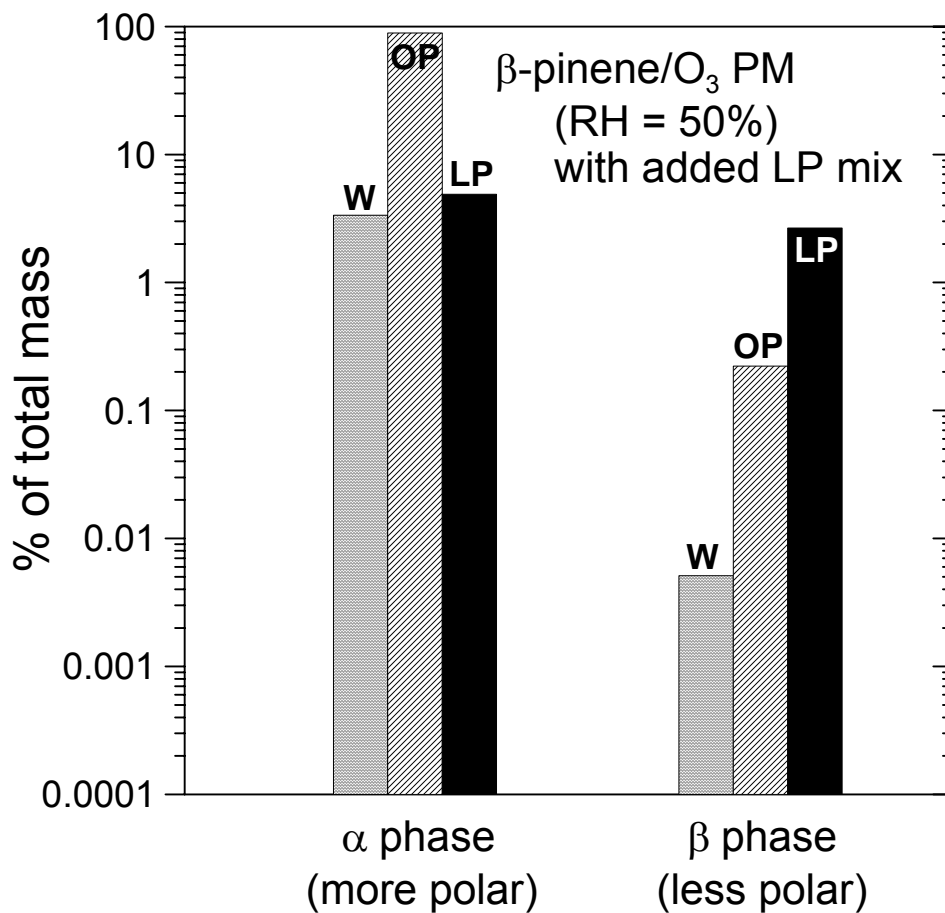


Figure 2.3. Predicted two-phase distribution of components in the PM formed by amending the modeled PM composition (Table 2.2) for the β -pinene/O₃ case so that 10% of the total organic carbon (OC) in the resulting PM was from the low-polarity (LP) mix (Table 2.1). The mass percentages of the β -pinene/O₃ oxidation products (OP), water (W), and LP mix compounds sum to 100% over the two phases (α -more polar, and β -less polar).

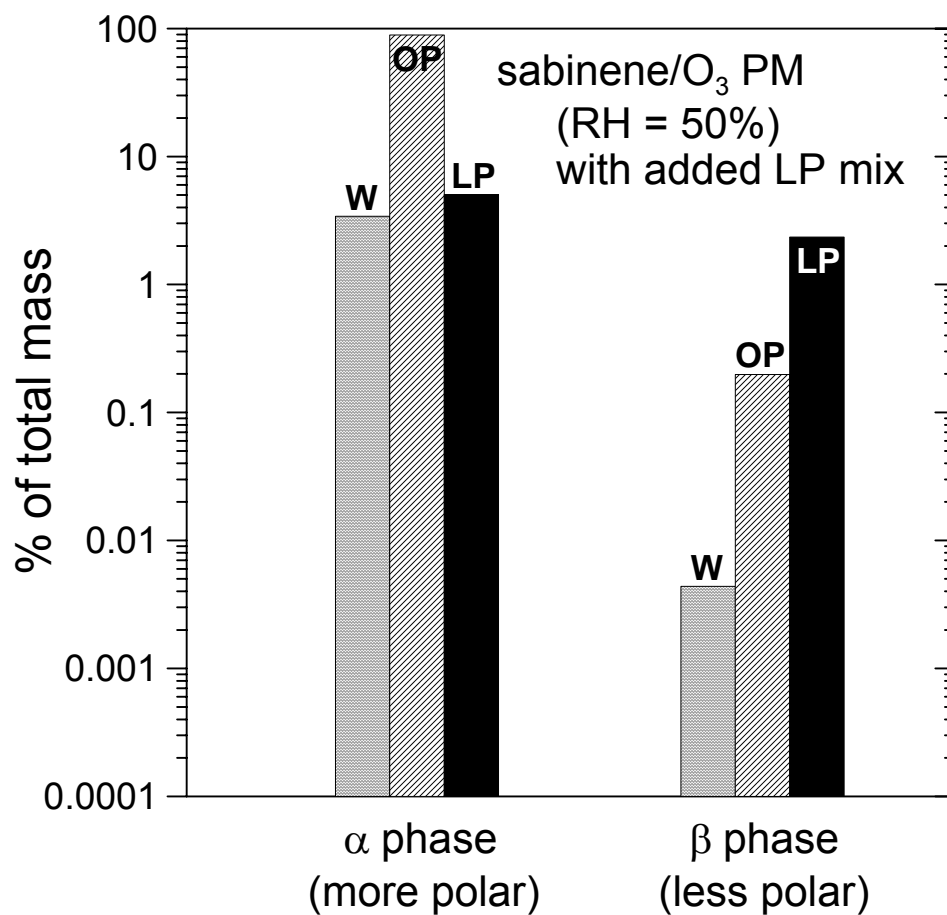


Figure 2.4. Predicted two-phase distribution of components in the PM formed by amending the modeled PM composition (Table 2.2) for the sabinene/O₃ case so that 10% of the total organic carbon (OC) in the resulting PM was from the low-polarity (LP) mix (Table 2.1). The mass percentages of the sabinene/O₃ oxidation products (OP), water (W), and LP mix compounds sum to 100% over the two phases (α -more polar, and β -less polar).

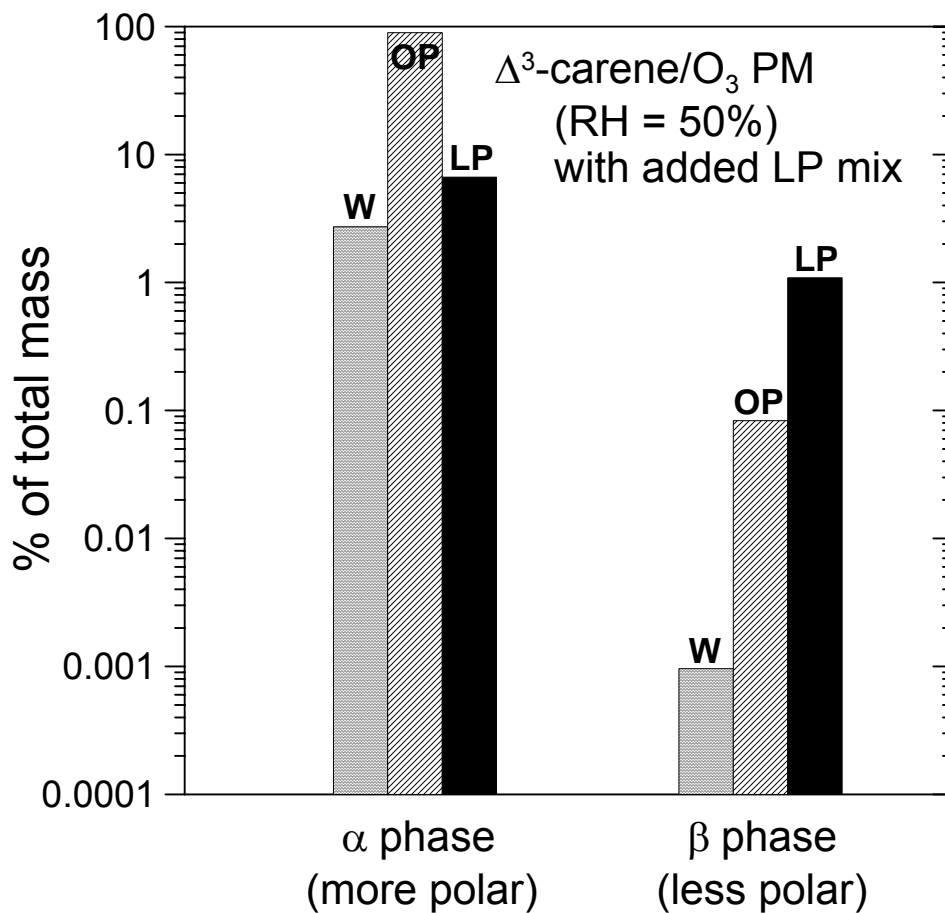


Figure 2.5. Predicted two-phase distribution of components in the PM formed by amending the modeled PM composition (Table 2.2) for the Δ^3 -carene/O₃ case so that 10% of the total organic carbon (OC) in the resulting PM was from the low-polarity (LP) mix (Table 2.1). The mass percentages of the Δ^3 -carene/O₃ oxidation products (OP), water (W), and LP mix compounds sum to 100% over the two phases (α -more polar, and β -less polar).

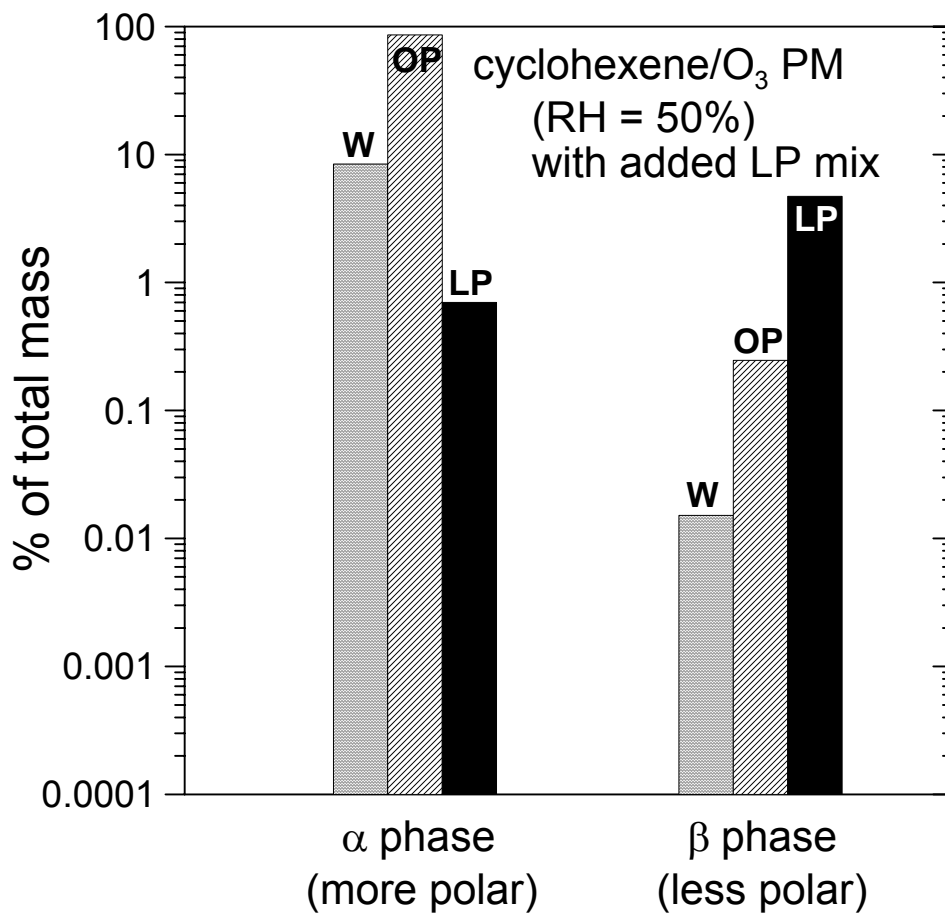


Figure 2.6. Predicted two-phase distribution of components in the PM formed by amending the modeled PM composition (Table 2.2) for the cyclohexene/O₃ case so that 10% of the total organic carbon (OC) in the resulting PM was from the low-polarity (LP) mix (Table 2.1). The mass percentages of the cyclohexene/O₃ oxidation products (OP), water (W), and LP mix compounds sum to 100% over the two phases (α -more polar, and β -less polar).

CHAPTER 3
IONIC-UNIFAC.1: A METHOD FOR PREDICTING ACTIVITY
COEFFICIENTS OF NEUTRAL COMPOUNDS IN LIQUID
PARTICULATE MATTER CONTAINING ORGANIC COMPOUNDS,
DISSOLVED INORGANIC SALTS, AND WATER¹

3.1 Abstract

Ionic-UNIFAC.1 is developed as a group contribution method for estimating activity coefficient (ζ) values of neutral organic compounds in liquid aerosol particles composed of organic compounds, dissolved inorganic salts, and water. The ζ values are considered to be determined by a combination of short- and long-range interactions. The expression utilized for ζ involves both a Debye-Hückel term and conventional UNIFAC terms. The UNIFAC terms are computed using group-group interaction parameters. Organic-organic interaction parameters are assumed to be the same as given by UNIFAC-LLE as described by Magnussen *et al.* [1981, Ind. Eng. Chem. Process Design Develop., **20**, 331-339]. Organic-ion interaction parameters and anion-cation interaction parameters were estimated based on 1026 organic-compound ζ values obtained using available liquid-liquid equilibrium (LLE) data for a range of organic/inorganic salt/water mixtures at 293-308 K and UNIQUAC fits similar to those described by Fredenslund *et al.*, [1977, Elsevier Scientific Publishing, New York]. The mixture compositions range from primarily organic solutions to primarily aqueous solutions with maximum salt concentrations of $\sim 2 \text{ mol kg}^{-1}$. The groups represented in the organic compounds include

¹ Erdakos, G.B., Asher, W.E., Seinfeld, J.H., Pankow, J.F., 2004. Gas/particle partitioning of neutral and ionizing compounds to single- and multi-phase aerosol particles. 3. Ionic-UNIFAC.1: A method for predicting activity coefficients of neutral compounds in liquid particulate matter containing organic compounds, water, and dissolved inorganic salts. Submitted to Atmospheric Environment.

CH_3- , $-\text{CH}_2-$, $-\overset{|}{\text{C}}\text{H}-$, $-\overset{|}{\text{C}}-$, $-\text{OH}$, $-\text{CH}_2\text{CO}-$, and $-\text{COOH}$ (*i.e.*, single bonded carbon with three, two, one, and zero hydrogens respectively, hydroxyl, $-\text{CH}_2$ -carbonyl, and carboxyl, respectively). These groups are characteristic of compounds found in atmospheric PM. The inorganic salts represented in the mixture data include NaCl , NaNO_3 , Na_2SO_4 , $(\text{NH}_4)_2\text{SO}_4$, and CaCl_2 so that the cations considered included Na^+ , NH_4^+ , and Ca^{2+} , and the anions considered included Cl^- , NO_3^- , and SO_4^{2-} . An optimization fitting using 762 of the ζ values yielded initial estimates of the desired interaction parameters. The remaining 264 ζ values were used as a test set to evaluate the quality of the fit. The method was found to predict the UNIQUAC-estimated activity coefficients for both the fitting and test datasets with an average maximum error of 20%. In an application of the method, activity coefficients were predicted in a hypothetical aerosol PM phase containing four α -pinene/ O_3 oxidation products without and with 2 mol kg^{-1} dissolved $(\text{NH}_4)_2\text{SO}_4$ at $\text{RH} = 50\%$ and $T = 306 \text{ K}$. In the absence vs. presence of the dissolved salt, the ζ values for hydroxy pinonic acid and water were predicted to be 0.67 vs. 0.22 and 1.66 vs. 0.50, respectively. These results reflect the “salting in” effects of $(\text{NH}_4)_2\text{SO}_4$ for hydroxy pinonic acid and water, respectively. For pinic acid on the other hand, in the absence vs. presence of the dissolved salt the ζ values were predicted to be 1.13 vs. 8.76, respectively. These results indicate the important role played by dissolved salts in affecting the thermodynamics of atmospheric PM.

3.2 Introduction

As discussed by Pankow (1994a, 1994b, 2003), when the formation of atmospheric particulate matter (PM) can be described by absorptive gas/particle (G/P) partitioning, a method is needed for estimating the liquid-phase activity coefficient (ζ) values of all partitioning species in the PM phase of interest. The “UNIFAC” group contribution method of Fredenslund *et al.* (1975, 1977, 1994) has proven useful for calculating activity coefficients in organic PM (OPM) (Jang *et al.*, 1997; Pankow *et al.*, 2001), and in PM composed of organic compounds and water (Seinfeld *et al.*, 2001; Pun *et al.*, 2002; Griffin *et al.*, 2003; Erdakos and Pankow, 2004). When considering inorganic PM, one may choose from several successful models (see Zhang, 2000).

Studies of the activity coefficients of organic compounds in phases that also contain inorganic salts and water include those of Sander *et al.* (1986), Cardoso and O'Connell (1987), Macedo *et al.* (1990), Kikic *et al.* (1991), Li *et al.* (1994), Achard *et al.* (1994), Yan *et al.* (1999), Clegg *et al.* (2001), and Ming and Russell (2002). However, the predictive methods discussed in those studies pertain only to limiting types of liquid compositions found in atmospheric PM. For example, the activity coefficient parameterizations of Clegg *et al.* (2001) apply only to mixtures in which the organic compound concentrations are low. Similarly, while the Ming and Russell (2002) study provides for the distinct treatment of relevant multi-functional oxygenated organic compounds (*e.g.*, diacids and hydroxy-acids), and is a significant advancement beyond previous "extended-UNIFAC" studies, its "Pitzer-UNIFAC" optimization of ion-organic interaction parameters was carried out with only solutions of the single salt NaCl.

This work uses published liquid-liquid equilibrium (LLE) data for a wide range of organic/inorganic salt/water mixtures to obtain optimized parameter values that can be used to predict liquid-phase activity coefficient values for neutral organic compounds in mixtures containing maximum overall salt levels of $\sim 2 \text{ mol kg}^{-1}$. The LLE data selected for the optimization were obtained from partitioning studies carried out at ambient temperatures (293-308 K) using: 1) organic compounds composed of atmospherically-relevant organic functional groups. *i.e.*, CH_3- , $-\text{CH}_2-$, $-\overset{|}{\text{C}}\text{H}-$, $-\overset{|}{\text{C}}-$, $-\text{OH}$, $-\text{CH}_2\text{CO}-$, and $-\text{COOH}$ (single bonded carbon with three, two, one, and zero hydrogens respectively, hydroxyl, $-\text{CH}_2$ -carbonyl, and carboxylic acid groups, respectively); 2) several atmospherically-relevant inorganic salts (NaCl, NaNO_3 , Na_2SO_4 , $(\text{NH}_4)_2\text{SO}_4$, and CaCl_2); and 3) water.

3.3 Method

Every species in a solution contributes to the solvation properties of the liquid phase, regardless of its concentration. This includes the dissolved ions, though in this work we reserve "solvent compound" as a term to be used to refer specifically to neutral compounds. The expression used here to represent the activity coefficient of solvent compound n in a liquid phase of interest is that proposed by Kikic *et al.* (1991)

$$\ln \zeta_n = \ln \zeta_n^{\text{D-H}} + \ln \zeta_n^{\text{C}} + \ln \zeta_n^{\text{R}} \quad (3.1)$$

where $\ln \zeta_n^{\text{D-H}}$ is a Debye-Hückel term that accounts for the long-range electrostatic effects of ions on ζ_n . The terms $\ln \zeta_n^{\text{C}}$ and $\ln \zeta_n^{\text{R}}$ are the combinatorial (C) and residual (R) portions of the original UNIFAC equation, and account for short-range interactions between component n and all other solution species (including ions).

The form of $\ln \zeta_n^{\text{D-H}}$ used here is that derived by Macedo *et al.* (1990), namely

$$\ln \zeta_n^{\text{D-H}} = \frac{2AMW_n \rho_s}{b^3 \rho_n} \left[1 + b\sqrt{I} - \frac{1}{1 + b\sqrt{I}} - 2 \ln(1 + b\sqrt{I}) \right] \quad (3.2)$$

where: $A = 1.327757 \times 10^5 \rho_s^{1/2} / (\epsilon_s T)^{3/2}$; $b = 6.359696 \rho_s^{1/2} / (\epsilon_s T)^{1/2}$; I (mol kg^{-1}) = ionic strength of the mixture of interest defined as usual (e.g., see Pankow, 1991); MW_n (g mol^{-1}) = molecular weight of n ; ρ_n (kg m^{-3}) = density of pure n as a liquid; ρ_s (kg m^{-3}) = density of the salt-free solution phase; ϵ_s (dimensionless) = dielectric constant of the solution; T (K) = temperature. The methods used for calculating pure solvent and solvent mixture ρ values and ϵ_s are given in Appendices 3 and 4, respectively.

The combinatorial term of the UNIFAC equation is given by Fredenslund *et al.* (1975):

$$\ln \zeta_n^{\text{C}} = \ln \frac{\Phi_n}{X_n} + 5q_n \frac{\theta_n}{\Phi_n} + l_n - \frac{\Phi_n}{X_n} \sum_i X_i l_i \quad (3.3)$$

where: $l_n = 5(r_n - q_n) - (r_n - 1)$; $\theta_n = q_n X_n / \sum_i q_i X_i$; $\Phi_n = r_n X_n / \sum_i r_i X_i$; and X_i = mole fraction of i . The summations in these equations are taken over all mixture components i (i.e., all ions and solvent compounds). The parameters q_i and r_i represent the surface area and volume, respectively, of component i . They are calculated from the surface area (Q_k) and volume (R_k) parameters (see Table 3.1) of the individual functional groups k that comprise i according to: $q_i = \sum_k v_k^i Q_k$ and $r_i = \sum_k v_k^i R_k$, where v_k^i is the number of groups of type k in i .

The residual term of the UNIFAC equation is given by Fredenslund *et al.* (1975):

$$\ln \zeta_n^{\text{R}} = \sum_k v_k^n [\ln Z_k - \ln Z_k^n] \quad (3.4)$$

where Z_k (zeta) is the residual activity coefficient of functional group k and Z_k^n is the residual activity coefficient of group k in a reference solution containing only molecules of type n . Both Z_k and Z_k^n are given by Fredenslund *et al.* (1975):

$$\ln Z_k = Q_k [1 - \ln(\sum_m \Theta_m \Psi_{mk}) - \sum_m (\Theta_m \Psi_{mk} / \sum_o \Theta_o \Psi_{om})] \quad (3.5)$$

where the summations are carried out over all functional groups m and o in the mixture, and $\Theta_m = Q_m X_m / \sum_o Q_o X_o$ is the area fraction of group m in the mixture. The interaction term Ψ_{mo} is given by Fredenslund *et al.* (1975):

$$\Psi_{mo} = \exp\left[-\frac{U_{mo} - U_{oo}}{RT}\right] = \exp(-A_{mo}/T) \quad (3.6)$$

where: U_{mo} (J mol⁻¹) = measure of the energy of interaction between groups m and o in the mixture; R (J mol⁻¹ K⁻¹) = the ideal gas constant; A_{mo} (K⁻¹) = group-group interaction parameter; and $A_{mm} \equiv 0$ because the standard state chosen for i is pure component in which $\zeta \equiv 1$. For each distinct pair of functional groups, there are two m - o group-group interaction parameters, A_{mo} and A_{om} , where $A_{mo} \neq A_{om}$. The group-group interaction parameters can be estimated by an optimized fitting of the method to experimental data.

3.4 LLE Data

3.4.1 General

Optimization of the method parameters was carried out using experimental datasets found in the literature. The LLE data selected for method optimization and validation was limited to data for mixtures in which the salt concentration in each phase was ≤ 2.0 mol kg⁻¹ because of the limited applicability of the Debye-Hückel parameterization. Each dataset was obtained from an LLE experiment series in which increasing amounts of an organic compound were added to an initial aqueous solution containing a particular amount of a salt of interest (and in some cases a second organic compound) to yield a series of two-phase systems at equilibrium. For each such system, the compositions of each of two phases were determined. The mole fraction (X) values for all of the components in each phase were computed here based on that data. The primarily aqueous phase is referred to here as the α phase; the other is referred to as the β

phase. In most of the cases, the β phase was mostly organic in composition; for a few $X_{\text{water}} > X_{\text{organic}}$. The datasets from each literature reference utilized were distributed between the optimization basis set (with a total of 15 datasets, Table 3.2,) and a method validation set (with a total of 8 datasets, Table 3.3). To achieve good rigor in the testing process, the validation set was designed to include datasets for system types that do not exist in the basis set. Also, some of the system types in the validation set have analogs in the basis set, though at other temperatures.

3.4.2 Calculating activity coefficients from LLE data

The activity coefficients needed for development of ζ prediction methods can be calculated directly from vapor-liquid equilibrium (VLE) data, but not from LLE data. It is possible, however, to estimate ζ values from LLE data. This is done by first choosing a preliminary fitting parameterization that can be used to estimate the needed ζ values.

Then, for each component in an LLE system, consider that $\mu_n^\alpha = \mu_n^\beta$ where μ_n^α and μ_n^β are the chemical potentials of n in the α and β phases, respectively. If a_n (activity of n) $\equiv \zeta_n X_n$, taking the standard state for n in both phases to be pure liquid n at the T of interest leads to

$$\zeta_n^\alpha X_n^\alpha = \zeta_n^\beta X_n^\beta \quad (3.7)$$

so that it is possible to obtain values for the parameters of the preliminary fitting by minimizing

$$F_{\text{MIN},\zeta} = \sum_n \sum_p \left(\ln(f_n^\alpha X_n^\alpha) - \ln(f_n^\beta X_n^\beta) \right)_p^2 \quad (3.8)$$

where p is an index that refers to a given LLE system. (An analogous LLE-based optimization process was used in the initial development of UNIFAC for solutions that only contain non-electrolytes.)

In this work, the expression used for f_n involves the original UNIQUAC terms of Abrams and Prausnitz (1975) plus the Debye-Hückel term in Eq. (3.2). UNIQUAC, as the simpler molecular-level analog of UNIFAC, utilizes combinatorial and residual terms between entire solution constituents rather than between the groups making up those

constituents. For this work, the combinatorial term of the UNIQUAC model is identical to that of UNIFAC (Eq. (3.3)), and we write the residual UNIQUAC term as

$$\ln \zeta_n^R = q_n [1 - \ln(\sum_i \theta_i \tau_{in}) - \sum_i (\theta_i \tau_{in} / \sum_j \theta_j \tau_{ji})] \quad (3.9)$$

where the summations are taken over all constituents i and j including ions. The interaction term τ_{ij} is given by

$$\tau_{ij} = \exp\left(-\frac{u_{ij} - u_{jj}}{RT}\right) = \exp(-a_{ij} / RT) \quad (3.10)$$

where: u_{ij} (J mol^{-1}) = interaction energy between constituents i and j ; a_{ij} (J mol^{-1}) = molecule-molecule interaction parameter, and $a_{ii} \equiv 0$. Pairs of molecule-molecule interaction parameters (a_{ij} and a_{ji} , where $a_{ij} \neq a_{ji}$) are optimized by minimization of Eq. (3.8) and then used with the expression for f_n to back-calculate estimates of the ζ values for use in minimization of (3.11) as given below in the acquisition of the parameters of Ionic-UNIFAC.1.

Eq. (3.8) was minimized separately for each dataset reported for the LLE systems used in this work. These individual minimizations allowed a higher degree of accuracy in the estimated activity coefficients than would have been achieved by an overall minimization for all datasets. Indeed, the intent here was not to obtain a single overall set of UNIQUAC parameters for organic/inorganic salt/water systems, but rather to obtain the most accurate set of activity coefficients for subsequent minimization of the governing equation for Ionic-UNIFAC.1. The individual minimizations of Eq.(3.8) were accomplished using the nonlinear optimization routines LOADNLP and OPTIMIZE from SOLVER.DLL (Frontline Systems, Boulder, Colorado). The central-differencing method in LOADNLP was selected to calculate derivatives. At the start of each minimization, initial values of all interaction parameters were set equal to zero. The optimization process proceeded iteratively until the objective function changed by less than 10^{-9} . Each optimization resulted in a set of molecule-molecule interaction parameters that were then used to back-calculate activity coefficients of the solvent compounds in the corresponding LLE dataset.

Figure 3.1 shows the agreement between aqueous and organic phase activities of each solvent n in the $N_S = 193$ experimental LLE systems of the basis and test sets

(Tables 3.2 and 3.3). On average, agreement between the activities in the two phases is excellent; an arithmetic average of 1.00 was calculated for 513 activity ratios (a_n^{α}/a_n^{β}). The total number of solvent activity coefficient values (= 1026) provided by the datasets in Tables 3.2 and 3.3 is given by

$$N_{\zeta} = 2 \sum_{p=1}^{N_s} N_p \quad (3.11)$$

where the factor 2 originates in the fact that in each LLE system there were two phases, and N_p is the number of solvent compounds in the LLE system referred to by the index p .

3.5 Optimization of Ionic-UNIFAC.1

The activity coefficient values obtained from the LLE experimental data were used to optimize the group-group interaction parameters in Ionic-UNIFAC.1 by minimizing the objective function

$$F_{\text{MIN}} = \sum_n \sum_{\varphi} \sum_{p=1}^{N_s} (\ln \zeta_n^{\varphi, \text{pred}} - \ln \zeta_n^{\varphi, \text{expt}})^2 \quad (3.12)$$

where: φ = the phase index (= α or β); $\zeta_n^{\varphi, \text{pred}}$ = predicted activity coefficient (by Ionic-UNIFAC.1) for n in phase φ for LLE system p ; and $\zeta_n^{\varphi, \text{expt}}$ = corresponding UNIQUAC-calculated activity coefficient based on the experimental data. Minimization of the objective function occurred as with Eq. (3.8) except that: 1) an upper limit of 3000 K was imposed (as in Fredenslund *et al.* (1975)) upon all optimized values of A_{mo} ($m \neq o$) to maintain computational stability; 2) only ion-solvent and ion-ion group-group interaction parameters were optimized; 3) the values of the group-group interaction parameters for solvent groups were taken to be the same as in UNIFAC-LLE (Magnussen *et al.*, 1981), which were optimized by fitting the original UNIFAC equation to a large amount of salt-free binary and ternary LLE systems in the temperature range 20–30 °C (Magnussen *et al.*, 1981; Gupte and Danner, 1987). Use of those UNIFAC-LLE parameters in the present work preserves the accuracy of predicted activity coefficients when the current model is applied to systems in which no salt is present.

3.6 Fit Characteristics of Ionic-UNIFAC.1

The solvent activity coefficients in the basis set of experimental LLE systems in Table 3.2 were used to optimize an initial set of Ionic-UNIFAC.1 parameters. Those parameters are listed in Tables 3.4a and 3.4b. The quality of this optimization is examined here by considering differences between the activity coefficients used in the fit and the corresponding activity coefficients predicted by Ionic-UNIFAC.1 with the fit parameters (Tables 3.4a and 3.4b).

The standard error of the Ionic-UNIFAC.1 fit was calculated as

$$\sigma_{\text{FIT}} = \frac{1}{N_{\zeta}} \sum_n \sum_{\varphi} \sum_{p=1}^{N_s} \left| \log \zeta_n^{\varphi, \text{pred}} - \log \zeta_n^{\varphi, \text{expt}} \right|_p \quad (3.13)$$

For the total of 762 basis set $\zeta_n^{\varphi, \text{pred}}$ values, the standard error was $\sigma_{\text{FIT}} = 0.09$. This means that the $\zeta_n^{\varphi, \text{expt}}$ values are predicted to within a factor of 1.2 ($= 10^{0.09}$). An overall understanding of the direction and magnitude of the bias in a ζ -prediction method can be examined using the signed standard error

$$\sigma_{\text{FIT, signed}} = \frac{1}{N_{\zeta}} \sum_n \sum_{\varphi} \sum_{p=1}^{N_s} \left(\log \zeta_n^{\varphi, \text{pred}} - \log \zeta_n^{\varphi, \text{expt}} \right)_p \quad (3.14)$$

Since $\sigma_{\text{FIT, signed}} = 0.0006$, the method shows no bias for the basis set.

The standard error for each $\zeta_n^{\varphi, \text{pred}}$ was calculated as

$$\sigma_{n,p}^{\varphi} = \left| \log \zeta_n^{\varphi, \text{pred}} - \log \zeta_n^{\varphi, \text{expt}} \right|_p \quad (3.15)$$

$\log \sigma_{n,p}^{\varphi}$ is plotted in Figure 3.2 as a function of the logarithm of the corresponding solvent activity, $\log a$, and in Figure 3.3 as a function of the logarithm of the ionic strength, $\log I$ for all $\log \zeta_n^{\varphi, \text{pred}}$ values. The $\sigma_{n,p}^{\varphi}$ values were then sorted in order of increasing a into five different groups: $\log a < -1.5$; $-1.5 \leq \log a < -1$; $-1 \leq \log a < -0.5$; $-0.5 \leq \log a < 0$; and $0 \leq \log a < 0.5$. Average standard errors for a given activity group ($\bar{\sigma}_a$) were calculated based on the $\sigma_{n,p}^{\varphi}$ values in that group. For that series of groups, the $\bar{\sigma}_a = 0.31, 0.18, 0.11, 0.03, \text{ and } 0.06$, respectively. Figure 3.2 illustrates this tendency of $\bar{\sigma}_a$ to decrease as a approaches unity within the range considered here. Figure 3.3 shows no correlation between $\log \sigma_{n,p}^{\varphi}$ and $\log I$.

3.7 Validation of Ionic-UNIFAC.1

The accuracy of Ionic-UNIFAC.1 was tested by using the initial group-group interaction parameters in Tables 3.4a and 3.4b to predict activity coefficients of solvent compounds in the test set mixtures listed in Table 3.3. The overall standard error calculated from Eq. (3.13) for 264 values of $\zeta_n^{\phi,\text{pred}}$ was $\sigma_{\text{FIT}} = 0.11$, so that the test set $\zeta_n^{\phi,\text{expt}}$ values were predicted to within a factor of 1.3. The $\log \sigma_{n,p}^{\phi}$ values are plotted in Figure 3.4 vs. $\log a$, and in Figure 3.5 vs. $\log I$. The $\sigma_{n,p}^{\phi}$ values were then sorted again in order of increasing a into five different groups: $\log a < -1.5$; $-1.5 \leq \log a < -1$; $-1 \leq \log a < -0.5$; $-0.5 \leq \log a < 0$; and $0 \leq \log a < 0.5$. For those groups, $\bar{\sigma}_a = 0.005$, 0.13, 0.11, 0.03, and 0.07, respectively. For the group with the lowest values of a , the test set value of $\bar{\sigma}_a$ is significantly less than the corresponding basis set value. The remaining values demonstrate the same tendency observed in the method optimization, namely the tendency of $\bar{\sigma}_a$ to decrease as $a \rightarrow 1$. Again, no correlation is observed between $\log \sigma_{n,p}^{\phi}$ and $\log I$.

Values of the average standard error ($\bar{\sigma}_n$) for each solvent n were calculated based on the $\sigma_{n,p}^{\phi}$ values for the test set and are given in Table 3.5. The largest $\bar{\sigma}_n$ (= 0.19) is observed for *t*-butanol. The poor performance of Ionic-UNIFAC.1 in predicting *t*-butanol activity coefficients is elucidated by a comparison of the basis and test datasets containing *t*-butanol (Tables 3.2 and 3.3), which indicates that $\zeta_n^{\phi,\text{expt}}$ values at temperatures outside those of the basis set are not predicted well by the method.

3.8 Final Set of Optimized Ionic-UNIFAC.1 Parameters

The optimization and test characteristics presented above indicate that Ionic-UNIFAC.1 predicts the $\zeta_n^{\phi,\text{expt}}$ values obtained here with reasonable accuracy. In order to fully develop Ionic-UNIFAC.1 using all of the LLE data used in this study, the basis set systems listed in Table 3.2 were combined with the test set systems listed in Table 3.3 to create a new and more complete basis set containing all 1026 $\zeta_n^{\phi,\text{expt}}$ values. A new set of group-group interaction parameters were then obtained by using this basis set in the

minimization of Eq. (3.12). The standard error of the optimization was then $\sigma_{\text{FIT}} = 0.09$ (a factor of 1.2 error), and $\sigma_{\text{FIT,signed}} = -0.002$, which again indicates no bias in the optimized method. Figures 3.6 and 3.7 show the $\log \sigma_{n,p}^{\phi}$ values for each of the 1026 new basis set $\zeta_n^{\phi,\text{pred}}$ values vs. $\log a$ and $\log I$, respectively. The final set of parameters in Tables 3.6a and 3.6b should be used when implementing Ionic-UNIFAC.1.

3.9 Implications for Atmospheric Applications

Ionic-UNIFAC.1 can be implemented to predict activity coefficients of atmospherically relevant compounds that can be represented by functional groups for which interaction parameters have been fitted. As an example, we use the method here to predict activity coefficients in PM without and with dissolved inorganic salts. We consider a PM phase at $T = 306$ K that is comprised of four major α -pinene/ O_3 oxidation products (norpinonic acid, pinonic acid, pinic acid, and hydroxy pinonic acid), $(\text{NH}_4)_2\text{SO}_4$, and water. (The organic/water composition (Table 3.7) of the PM phase is that discussed in a system considered by Seinfeld et al. (2001) at RH = 50%.) Ionic-UNIFAC.1 provides all of the pairs of interaction parameters needed to model this system, except for the pair OH- NH_4^+ ; the calculations carried out here assumed that the values for the pair OH- Na^+ could also be used for OH- NH_4^+ .

In the absence of dissolved salt, the predicted ζ values are close to unity (Table 3.7). The addition of 2 mol kg^{-1} of dissolved $(\text{NH}_4)_2\text{SO}_4$ causes some of the ζ values to increase by as much as a factor of eight (Table 3.7). The presence of $(\text{NH}_4)_2\text{SO}_4$ is predicted to decrease the ζ value for hydroxy pinonic acid by 67%; this result is likely due to the presence of an -OH group on this compound.

3.10 Conclusions

Ionic-UNIFAC.1 can be used with the parameter values in Table 3.6 to predict activity coefficient (ζ) values of neutral species in liquid particulate matter (PM) comprised of organic compounds, dissolved inorganic salts, and water at total salt levels as high as 2 mol kg^{-1} . Preliminary applications of Ionic-UNIFAC.1 to hypothetical liquid PM compositions provide estimates of the significant thermodynamic errors that can

result when neglecting the effects of such levels of dissolved salts on organic-compound ζ values. The relative error in ζ values predicted with this method is independent of the ionic strength (I). On average, the relative error tends to decrease with increasing activity (a) over the range $-2 < \log a < 0.5$, and does not exceed 20% for the data fitted here. As with any other semi-empirical method, predictions based on Ionic-UNIFAC.1 will be most accurate for systems that are similar to those in the method basis set. While some important constituents are absent (e.g., NH_4HSO_4 and the aldehyde ($-\text{CHO}$) functional group), the basis set used here pertains to ambient temperatures and involves salts and organic compound groups typically found in atmospheric PM.

3.11 Acknowledgement

This work was supported by the Electric Power Research Institute (EPRI) research grant EP-P4650/C2267, Thermodynamics of Atmospheric Organic Aerosols.

3.12 References

- Abrams, D.S., Prausnitz, J.M., 1975. Statistical thermodynamics of liquid mixtures: A new expression for the excess Gibbs energy of partly or completely miscible systems. *American Institute of Chemical Engineers Journal* 21, 116-128.
- Achard, C., Dussap, C.G., Gros, J.B., 1994. Representation of vapour-liquid equilibria in water-alcohol-electrolyte mixtures with a modified UNIFAC group-contribution method. *Fluid Phase Equilibria* 98, 71-89.
- Aznar, M., Araújo, R.N., Romanato, J.F., Santos, G.R., d'Ávila, S.G., 2000. Salt effects on liquid-liquid equilibrium in water + ethanol + alcohol + salt systems. *Journal of Chemical and Engineering Data* 45, 1055-1059.
- Cardoso, M.J.E. De M., O'Connell, J.P., 1987. Activity coefficients in mixed solvent electrolyte solutions. *Fluid Phase Equilibria* 33, 315-326.
- Clegg, S.L., Seinfeld, J.H., Brimblecombe, P., 2001. Thermodynamic modelling of aqueous aerosols containing electrolytes and dissolved organic compounds. *Journal of Aerosol Science* 32, 713-738.
- De Santis, R., Marrelli, L., Muscetta, P.N., 1976. Influence of temperature on the liquid-liquid equilibrium of the water-*n*-butyl alcohol-sodium chloride system. *Journal of Chemical and Engineering Data* 21, 324-327.

- Fredenslund, A., Jones, R.L., Prausnitz, J.M., 1975. Group-contribution estimation of activity coefficients in nonideal liquid mixtures. *American Institute of Chemical Engineers Journal* 21, 1086-1099.
- Fredenslund, A., Gmehling, J., Rasmussen, P., 1977. *Vapor-Liquid Equilibria Using UNIFAC: A Group-Contribution Method*, Elsevier Scientific Publishing, New York.
- Fredenslund, A., Sorensen, J.M., 1994. *Group Contribution Estimation Methods*. In: Sandler, S. I. (Ed.), *Models for Thermodynamic and Phase Equilibria Calculations*. Marcel Dekker Inc., New York.
- Gomis, V., Ruiz, F., Asensi, J.C., Saquete, M.D., 1996. Liquid-liquid-solid equilibria for the ternary systems butanols + water + sodium chloride or + potassium chloride. *Journal of Chemical and Engineering Data* 41, 188-191.
- Gomis, V., Ruiz, F., Boluda, N., Saquete, M.D., 1999. Liquid-liquid-solid equilibria for ternary systems water + sodium chloride + pentanols. *Journal of Chemical and Engineering Data* 44, 918-920.
- Govindarajan, M., Sabarathinam, P., 1995. Salt effect on liquid-liquid equilibrium of the methyl isobutyl ketone-acetic acid-water system at 35 °C. *Fluid Phase Equilibria* 108, 269-292.
- Govindarajan, M., Sabarathinam, P., 1997. Effect of some inorganic salts on the ternary liquid-liquid equilibria of the water + 4-methyl-2-pentanone + propanoic or butanoic acid at 35 °C. *Journal of Chemical and Engineering Data* 42, 402-408.
- Griffin, R.J., Nguyen, K., Dabdub, D., Seinfeld, J.H., 2003. A coupled hydrophobic-hydrophilic model for predicting secondary organic aerosol formation. *Journal of Atmospheric Chemistry* 44, 171-190.
- Gupte, P.A., Danner, R.P., 1987. Prediction of liquid-liquid equilibria with UNIFAC: A critical evaluation. *Industrial and Engineering Chemistry Research* 26, 2036-2042.
- Hasted, J.B., 1973. *Dielectric Properties*. In: Franks, F. (Ed.), *Water: A Comprehensive Treatise* Vol. 2. Plenum Press, New York.
- Jang, M.; Kamens, R.M.; Leach, K.B.; Strommen, M.R., 1997. A thermodynamic approach using group contribution methods to model the partitioning of semivolatile organic compounds on atmospheric particulate matter. *Environmental Science and Technology* 31, 2805-2811.
- Kikic, I., Fermeglia, M., Rasmussen, P., 1991. UNIFAC prediction of vapor-liquid equilibria in mixed solvent-salt systems. *Chemical Engineering Science* 46, 2775-2780.

- Li, J., Polka, H.-M., Gmehling, J., 1994. A g^E model for single and mixed solvent electrolyte systems. 1. Model and results for strong electrolytes. *Fluid Phase Equilibria* 94, 89-114.
- Lynn, S., Schiozer, A.L., Jaecksch, W.L., Cos, R., Prausnitz, J.M., 1996. Recovery of anhydrous Na_2SO_4 from SO_2 -scrubbing liquor by extractive crystallization: Liquid-liquid equilibria for aqueous solutions of sodium carbonate, sulfate, and/or sulfite plus acetone, 2-propanol, or *tert*-butyl alcohol. *Industrial and Engineering Chemistry Research* 35, 4236-4245.
- Macedo, E.A., Skovborg, P., Rasmussen, P., 1990. Calculation of phase equilibria for solutions of strong electrolytes in solvent-water mixtures. *Chemical Engineering Science* 45, 875-882.
- Magnussen, T., Rasmussen, P., Fredenslund, A., 1981. UNIFAC parameter table for prediction of liquid-liquid equilibria. *Industrial and Engineering Chemistry Process Design and Development* 20, 331-339.
- Mar Olaya, M., Garcia, A.N., Marcilla, A., 1996. Liquid-liquid-solid equilibria for the quaternary system water + acetone + 1-butanol + sodium chloride at 25 °C. *Journal of Chemical and Engineering Data* 41, 910-917.
- Ming, Y., Russell, L.M., 2002. Thermodynamic equilibrium of organic-electrolyte mixtures in aerosol particles. *American Institute of Chemical Engineers Journal* 48, 1331-1348.
- Pankow, J.F., 1991. *Aquatic Chemistry Concepts*. Lewis Publishers, Chelsea, Michigan.
- Pankow, J.F., 1994a. An absorption model of gas/particle partitioning of organic compounds in the atmosphere. *Atmospheric Environment* 28, 185-188.
- Pankow, J.F., 1994b. An absorption model of the gas/aerosol partitioning involved in the formation of secondary organic aerosol. *Atmospheric Environment* 28, 189-193.
- Pankow, J.F., 2003. Gas/particle partitioning of neutral and ionizing compounds to single and multi-phase particles. 1. Unified modeling framework. *Atmospheric Environment* 37, 3323-3333.
- Pankow, J.F., Seinfeld, J.H., Asher, W.E., Erdakos, G.B., 2001. Modeling the formation of secondary organic aerosol: 1. The application of theoretical principles to measurements obtained in the α -pinene-, β -pinene-, sabinene-, Δ^3 -carene-, and cyclohexene-ozone systems. *Environmental Science and Technology* 35, 1164-1172.

- Pun, B.K., Griffin, R.J., Seigneur, C., and Seinfeld, J.H., 2002: Secondary organic aerosol: 2. Thermodynamic model for gas/particle partitioning of molecular constituents. *Journal of Geophysical Research* 107, AAC4/1-AAC4/15.
- Sander, B., Fredenslund, A., Rasmussen, P., 1986. Calculation of vapour-liquid equilibria in mixed solvent/salt systems using an extended UNIQUAC equation. *Chemical Engineering Science* 41, 1171-1183.
- Seinfeld, J.H., Erdakos, G.B., Asher, W.E., Pankow, J.F., 2001. Modeling the formation of secondary organic aerosols: 2. The predicted effects of relative humidity on aerosol formation in the α -pinene-, β -pinene-, sabinene-, Δ^3 -carene-, and cyclohexene-ozone systems. *Environmental Science and Technology* 35, 1806-1817.
- Wohlfarth, C., 1995. *Temperature Dependence of the Permittivity (Dielectric Constant) of Liquids*. In: Lide, D.R. (Editor-in-Chief), *CRC Handbook of Chemistry and Physics*. CRC Press, Boca Raton.
- Yan, W., Toppoff, M., Rose, C., Gmehling, J., 1999. Prediction of vapor-liquid equilibria in mixed-solvent electrolyte systems using the group contribution concept. *Fluid Phase Equilibria* 162, 97-113.
- Yaws, C.L., 1999. *Chemical Properties Handbook: Physical, Thermodynamic, Environmental, Transport, Safety, and Health Related Properties for Organic and Inorganic Chemicals*, McGraw-Hill, New York.
- Zhang, Y., Seigneur, C., Seinfeld, J.H., Jacobson, M., Clegg, S.L., Binkowski, F.S., 2000. A comparative review of inorganic aerosol thermodynamic equilibrium modules: similarities, differences, and their likely causes. *Atmospheric Environment* 34, 117-137.
- Zurita, J.L., Gramajo de Doz, M.B., Bonatti, C.M., Sólamo, H.N., 1998. Effect of addition of calcium chloride on the liquid-liquid equilibria of the water + propionic acid + 1-butanol system at 303.15 K. *Journal of Chemical and Engineering Data* 43, 1039-1042.

Table 3.1. Group volume (R_k) and surface area (Q_k) parameters used in Ionic-UNIFAC.1.^a

Main Group	Subgroup	R_k	Q_k
CH ₂	CH ₃	0.9011	0.848
	CH ₂	0.6744	0.540
	CH	0.4469	0.228
	C	0.2195	0.000
OH	OH	1.0000	1.200
H ₂ O	H ₂ O	0.9200	1.400
CH ₂ CO	CH ₃ CO	1.6724	1.488
	CH ₂ CO	1.4457	1.180
COOH	COOH	1.3013	1.224
Na ⁺	Na ⁺	3.0	3.0
NH ₄ ⁺	NH ₄ ⁺	3.0	3.0
Ca ²⁺	Ca ²⁺	1.0	1.0
Cl ⁻	Cl ⁻	0.9861	0.9917
NO ₃ ⁻	NO ₃ ⁻	1.64	1.60
SO ₄ ²⁻	SO ₄ ²⁻	2.8560	2.015

^a Solvent group parameters are taken from Fredenslund *et al.*, 1977; Na⁺, Ca²⁺, Cl⁻, and NO₃⁻ parameters are taken from Kikic *et al.* (1991); NH₄⁺ parameters are taken to be the same as those for Na⁺; and SO₄²⁻ parameters are taken from Achard *et al.* (1994).

Table 3.2. Basis set liquid-liquid equilibrium (LLE) datasets, their components, temperatures, and the number of systems.

Components	T (K)	No. of solvents	No. of systems ^a	Reference ^b
NaCl; Water; 1-Butanol	293; 313	2	27	A
NaCl; Water; 2-Butanol	298	2	3	B
NaCl; Water; 1-Pentanol	298	2	3	C
NaCl; Water; 2-Pentanol	298	2	3	C
NaCl; Water; 2-Methyl-2-butanol	298	2	3	C
NaCl; Water; Acetone; 1-Butanol	298	3	9	D
NaCl; Water; MIBK ^c ; Acetic acid	308	3	6	E
NaNO ₃ ; Water; MIBK; Acetic acid	308	3	7	E
NaNO ₃ ; Water; MIBK; Propanoic acid	308	3	15	F
Na ₂ SO ₄ ; Water; <i>t</i> -Butanol	308	2	9	G
Na ₂ SO ₄ ; Water; MIBK; Acetic acid	308	3	5	E
Na ₂ SO ₄ ; Water; MIBK; Propanoic acid	308	3	17	F
(NH ₄) ₂ SO ₄ ; Water; MIBK; Acetic acid	308	3	6	E
(NH ₄) ₂ SO ₄ ; Water; MIBK; Propanoic acid	308	3	9	F
CaCl ₂ ; Water; 1-Butanol; Propanoic acid	303	3	21	G

^a Each LLE system contains two distinct compositions: one aqueous phase (α phase) composition and one organic phase (β phase) composition.

^b A: De Santis *et al.* (1976); B: Gomis *et al.* (1996); C: Gomis *et al.* (1999); D: Mar Olaya *et al.* (1996);

E: Govindarajan and Sabarathinam (1995); E: Govindarajan and Sabarathinam (1997); F: Lynn *et al.* (1996); G: Zurita *et al.* (1998).

^c MIBK: methyl isobutyl ketone (i.e., 4-methyl-2-pentanone).

Table 3.3. Test set liquid-liquid equilibrium (LLE) datasets, their components, temperatures, and the number of systems.

Components	T (K)	No. of solvents	No. of systems ^a	Reference ^b
NaCl; Water; 1-Butanol	303	2	7	A
NaCl; Water; 3-Pentanol	298	2	3	C
NaCl; Water; 2-Methyl-1-butanol	298	2	3	C
NaCl; Water; MIBK ^c ; Propanoic acid	308	3	7	E
NaNO ₃ ; Water; MIBK; Butanoic acid	308	3	8	E
Na ₂ SO ₄ ; Water; <i>t</i> -Butanol	296-299; 301	2	5	F
Na ₂ SO ₄ ; Water; MIBK; Butanoic acid	308	3	9	E
(NH ₄) ₂ SO ₄ ; Water; MIBK; Butanoic acid	308	3	8	E

^a Each LLE system contains two distinct compositions: one aqueous phase (α phase) composition and one organic phase (β phase) composition.

^b A: De Santis *et al.* (1976); C: Gomis *et al.* (1999); E: Govindarajan and Sabarathinam (1997); F: Lynn *et al.* (1996).

^c MIBK: methyl isobutyl ketone (i.e., 4-methyl-2-pentanone).

Table 3.4a. Group-group interaction parameters obtained by Ionic-UNIFAC.1 optimization using the basis set (Table 3.2).

	CH ₂	OH	H ₂ O	CH ₂ CO	COOH
CH ₂	0	644.6 ^a	1300.0 ^a	472.6 ^a	139.4 ^a
OH	328.2 ^a	0	28.73 ^a	67.07 ^a	-104.0 ^a
H ₂ O	342.4 ^a	-122.4 ^a	0	-171.8 ^a	-465.7 ^a
CH ₂ CO	66.56 ^a	216.0 ^a	634.8 ^a	0	1247.0 ^a
COOH	1744.0 ^a	118.4 ^a	652.3 ^a	-101.3 ^a	0
Na ⁺	3000.0	1417.5	752.5	3000.0	890.4
NH ₄ ⁺	834.5	N.A.	219.0	-269.7	99.14
Ca ²⁺	1667.1	-848.6	395.0	N.A.	873.7
Cl ⁻	1949.9	-585.3	-807.5	261.3	1077.5
NO ₃ ⁻	999.2	N.A.	-546.9	-424.9	372.3
SO ₄ ²⁻	1889.6	-994.7	658.4	-300.6	528.9

^a Group-group interaction parameters between solvent groups are fixed to those values optimized in the UNIFAC-LLE method presented by Magnussen *et al.* (1981).

^b N.A.: parameters are not available from the basis set (Table 3.2).

Table 3.4b. Group-group interaction parameters obtained by Ionic-UNIFAC.1 optimization using the basis set (Table 3.2).

	Na ⁺	NH ₄ ⁺	Ca ²⁺	Cl ⁻	NO ₃ ⁻	SO ₄ ²⁻
CH ₂	1270.6	610.5	593.9	653.9	549.4	1930.5
OH	496.7	N.A. ^b	-108.7	111.5	N.A.	410.6
H ₂ O	-913.8	371.0	-1025.0	-1272.6	2169.3	-2507.2
CH ₂ CO	-1185.6	-199.8	N.A.	25.56	-1010.8	-179.8
COOH	374.6	296.6	590.6	540.0	-480.1	892.0
Na ⁺	0	N.A.	N.A.	-11.68	-860.4	-381.8
NH ₄ ⁺	N.A.	0	N.A.	N.A.	N.A.	-26.85
Ca ²⁺	N.A.	N.A.	0	-14.48	N.A.	N.A.
Cl ⁻	15.67	N.A.	-34.21	0	N.A.	N.A.
NO ₃ ⁻	-9.937	N.A.	N.A.	N.A.	0	N.A.
SO ₄ ²⁻	-14.87	-354.6	N.A.	N.A.	N.A.	0

^a Group-group interaction parameters between solvent groups are fixed to those values optimized in the UNIFAC-LLE method presented by Magnussen *et al.* (1981).

^b N.A.: parameters are not available from the basis set (Table 3.2).

Table 3.5. Average standard errors of solvent compounds in the test set (Table 3.3).

Solvent compound	$\bar{\sigma}_n^a$
Water	0.02
1-Butanol	0.04
<i>t</i> -Butanol	0.19
3-Pentanol	0.01
2-Methyl-1-butanol	0.09
4-Methyl-2-pentanone	0.05
Propanoic acid	0.02
Butanoic acid	0.14

^a The average standard error $\bar{\sigma}_n$ of solvent compound n is calculated as the arithmetic average of the individual standard error values of that solvent.

Table 3.6a. Group-group interaction parameters obtained by Ionic-UNIFAC.1 optimization using the basis set (Table 3.2) and the test set (Table 3.3).

	CH ₂	OH	H ₂ O	CH ₂ CO	COOH
CH ₂	0	644.6 ^a	1300.0 ^a	472.6 ^a	139.4 ^a
OH	328.2 ^a	0	28.73 ^a	67.07 ^a	-104.0 ^a
H ₂ O	342.4 ^a	-122.4 ^a	0	-171.8 ^a	-465.7 ^a
CH ₂ CO	66.56 ^a	216.0 ^a	634.8 ^a	0	1247.0 ^a
COOH	1744.0 ^a	118.4 ^a	652.3 ^a	-101.3 ^a	0
Na ⁺	3000.0	1003.2	-216.0	168.3	1678.3
NH ₄ ⁺	2017.3	N.A.	-401.6	-311.5	-477.7
Ca ²⁺	2367.5	-908.8	394.1	N.A.	1419.7
Cl ⁻	2469.7	-363.3	-756.4	1567.9	1602.5
NO ₃ ⁻	2226.5	N.A.	-562.9	-510.3	-906.8
SO ₄ ²⁻	2635.0	-1113.4	283.5	1163.3	1364.1

^a Group-group interaction parameters between solvent groups are fixed to those values optimized in the UNIFAC-LLE method presented by Magnussen *et al.* (1981).

^b N.A.: parameters are not available from the basis set (Table 3.2) or the test set (Table 3.3).

Table 3.6b. Group-group interaction parameters obtained by Ionic-UNIFAC.1 optimization using the basis set (Table 3.2) and the test set (Table 3.3).

	Na ⁺	NH ₄ ⁺	Ca ²⁺	Cl ⁻	NO ₃ ⁻	SO ₄ ²⁻
CH ₂	1487.9	2019.0	887.6	750.7	1300.1	1448.7
OH	790.0	N.A. ^b	-214.4	-37.64	N.A.	619.6
H ₂ O	-905.5	2726.5	-1444.5	-1431.7	1952.4	-381.31
CH ₂ CO	-1218.8	-1698.0	N.A.	-43.82	-1585.9	-958.9
COOH	1533.9	1594.3	847.9	903.4	87.20	1138.6
Na ⁺	0	N.A.	N.A.	-48.42	-1493.7	-1520.1
NH ₄ ⁺	N.A.	0	N.A.	N.A.	N.A.	-123.9
Ca ²⁺	N.A.	N.A.	0	-26.34	N.A.	N.A.
Cl ⁻	-66.15	N.A.	-52.00	0	N.A.	N.A.
NO ₃ ⁻	49.01	N.A.	N.A.	N.A.	0	N.A.
SO ₄ ²⁻	-518.6	-2422.6	N.A.	N.A.	N.A.	0

^a Group-group interaction parameters between solvent groups are fixed to those values optimized in the UNIFAC-LLE method presented by Magnussen *et al.* (1981).

^b N.A.: parameters are not available from the basis set (Table 3.2) or the test set (Table 3.3).

Table 3.7. PM-phase activity coefficients of water and four α -pinene/O₃ oxidation products at RH = 50% and $T = 306$ K.

Compound	% of total mass	predicted ζ^a	
		no salt	$2\ m\ (\text{NH}_4)_2\text{SO}_4$
Water	9	1.66	0.50
norpinonic acid	15	1.28	0.97
pinonic acid	22	1.51	1.74
pinic acid	31	1.13	8.76
Hydroxy pinonic acid	23	0.67	0.22

^a Activity coefficients predicted with Ionic-UNIFAC.1 using the group-group interaction parameters in Table 3.6.

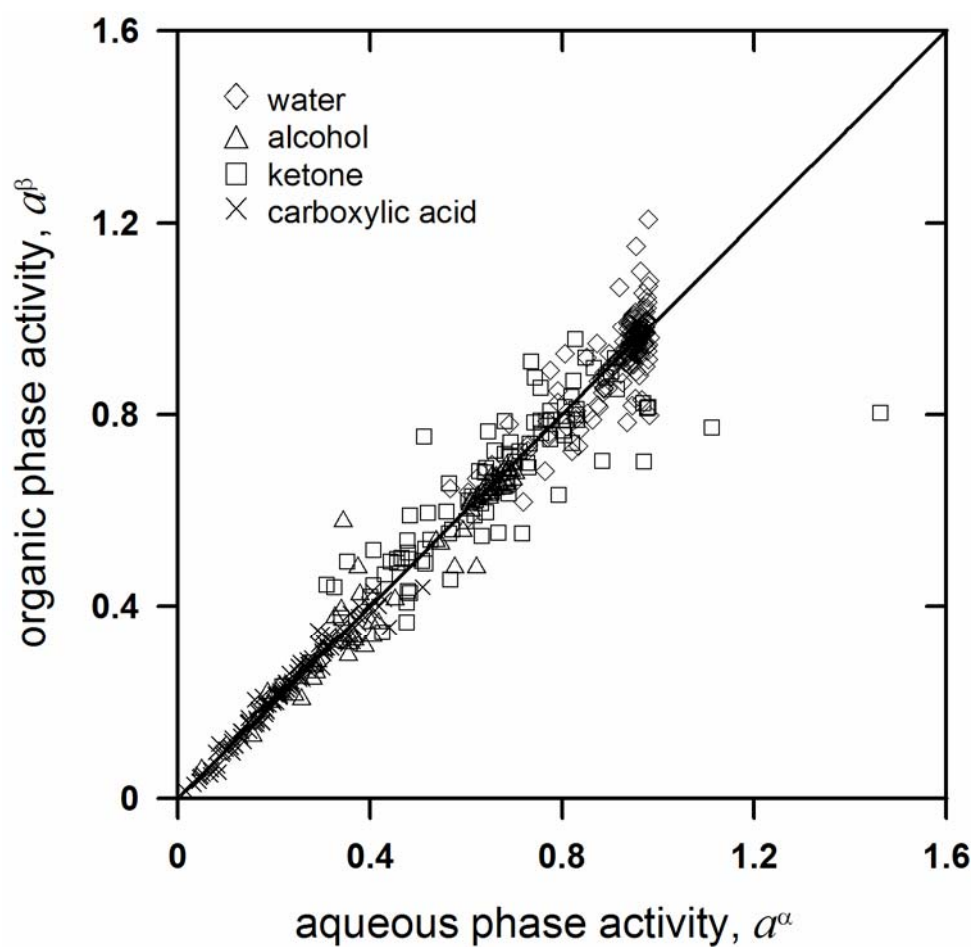


Figure 3.1. Comparison of back-calculated aqueous- and organic-phase activities of all solvent compounds in the basis and test set LLE systems listed in Tables 2 and 3. The solid line represents the 1:1 ratio between aqueous- and organic-phase activities (i.e., points with perfect agreement between solvent activities in the two phases of a given system will fall on the solid line).

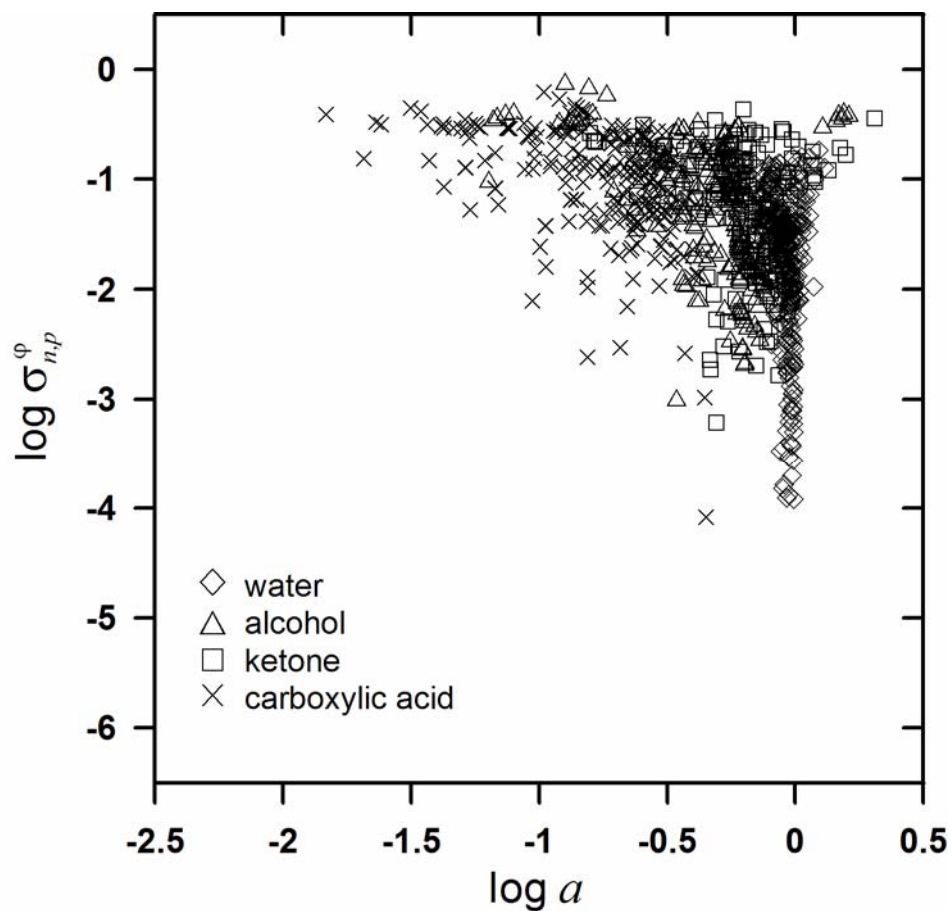


Figure 3.2. The logarithm of the standard error of each predicted activity coefficient $\zeta_{n,p}^{\phi,\text{pred}}$ of each solvent n in each phase ϕ of each system p in the basis set (Table 2). $\log \sigma_{n,p}^{\phi}$ is calculated according to Eq. (3.15) and plotted here as a function of $\log a$. The group-group interaction parameters used to predict values of $\zeta_{n,p}^{\phi,\text{pred}}$ are listed in Table 6.

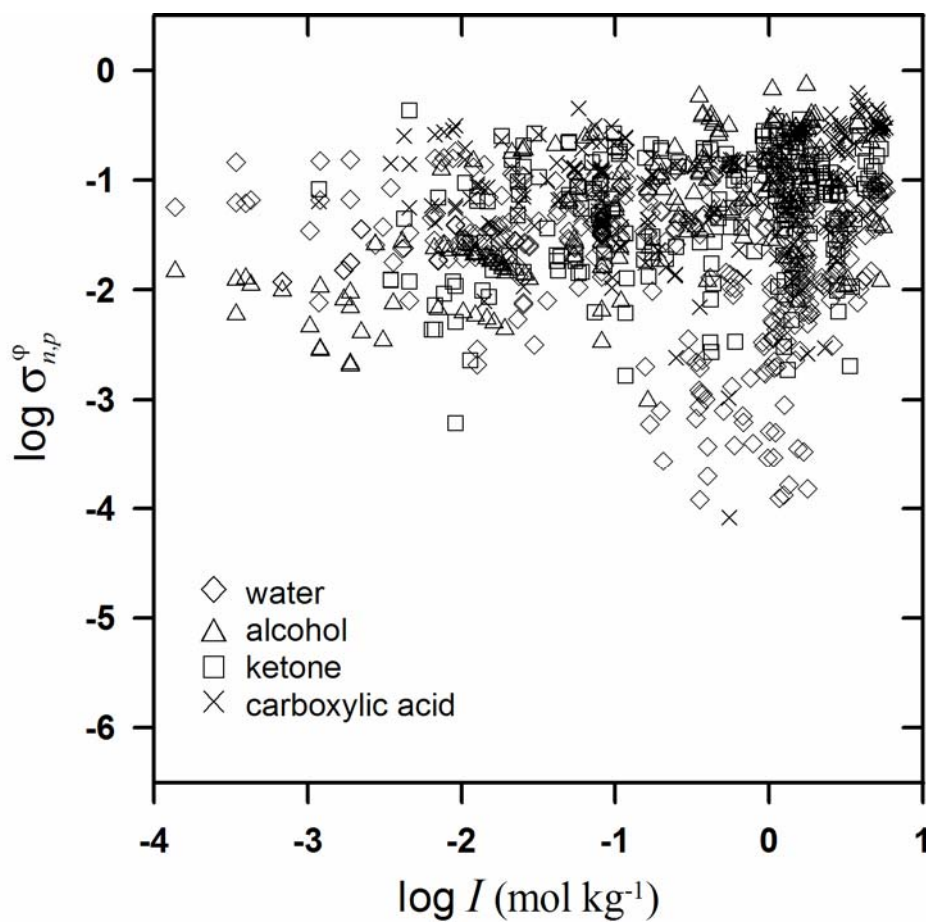


Figure 3.3. The logarithm of the standard error of each predicted activity coefficient $\zeta_{n,p}^{\phi,\text{pred}}$ of each solvent n in each phase ϕ of each system p in the basis set (Table 2).

$\log \sigma_{n,p}^{\phi}$ is calculated according to Eq. (3.15) and plotted here as a function of $\log I$. The group-group interaction parameters used to predict values of $\zeta_{n,p}^{\phi,\text{pred}}$ are listed in Table 6.

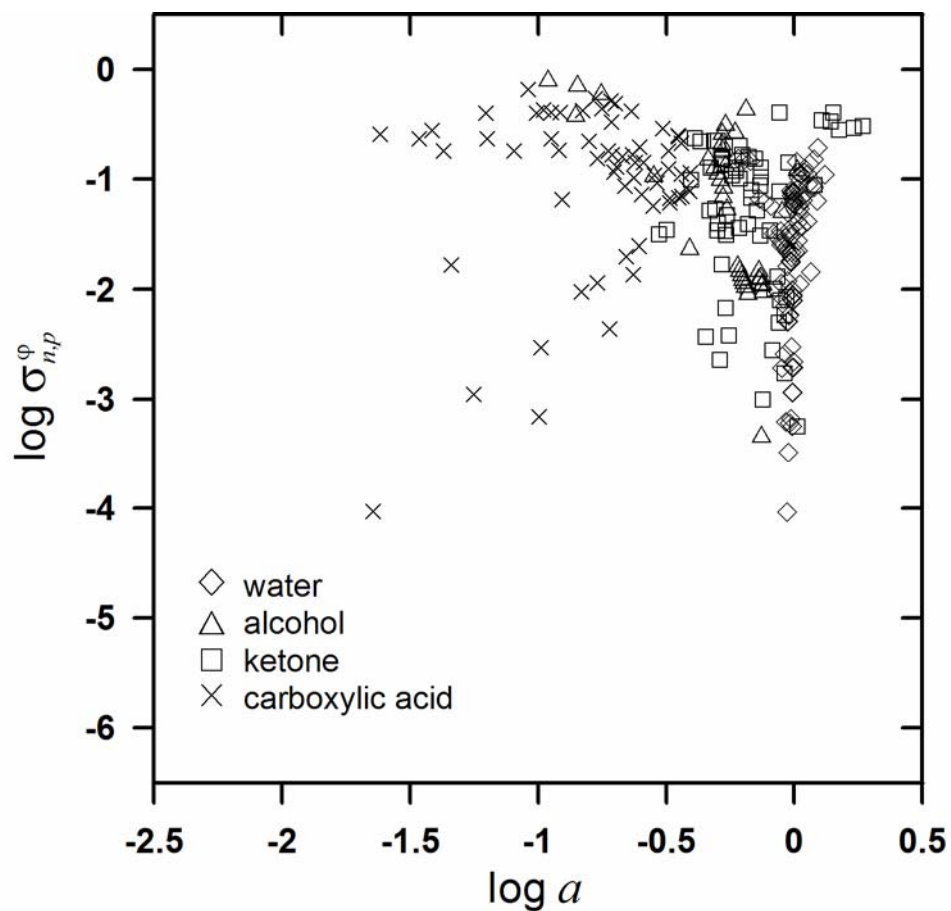


Figure 3.4. The logarithm of the standard error of each predicted activity coefficient $\zeta_{n,p}^{\phi,\text{pred}}$ of each solvent n in each phase ϕ of each system p in the test set (Table 3). $\log \sigma_{n,p}^{\phi}$ is calculated according to Eq. (3.15) and plotted here as a function of $\log a$. The group-group interaction parameters used to predict values of $\zeta_{n,p}^{\phi,\text{pred}}$ are listed in Table 6.

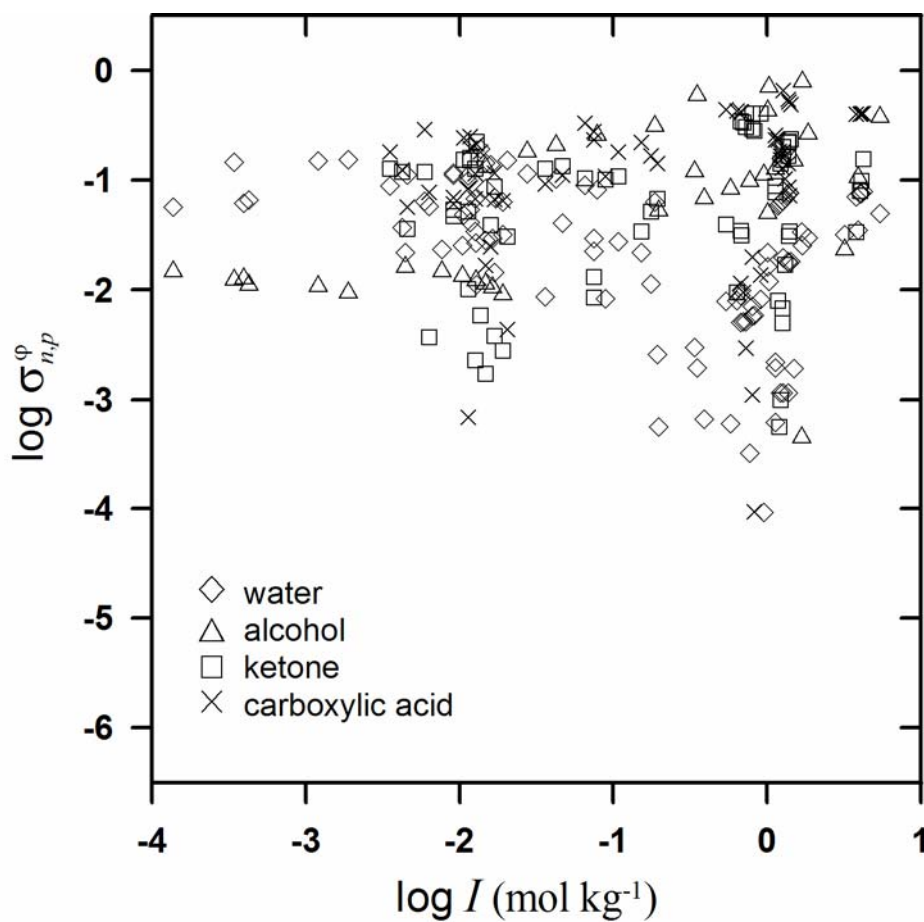


Figure 3.5. The logarithm of the standard error of each predicted activity coefficient $\zeta_{n,p}^{\phi,\text{pred}}$ of each solvent n in each phase ϕ of each system p in the test set (Table 3).

$\log \sigma_{n,p}^{\phi}$ is calculated according to Eq. (3.15) and plotted here as a function of the $\log I$.

The group-group interaction parameters used to predict values of $\zeta_{n,p}^{\phi,\text{pred}}$ are listed in Table 6.

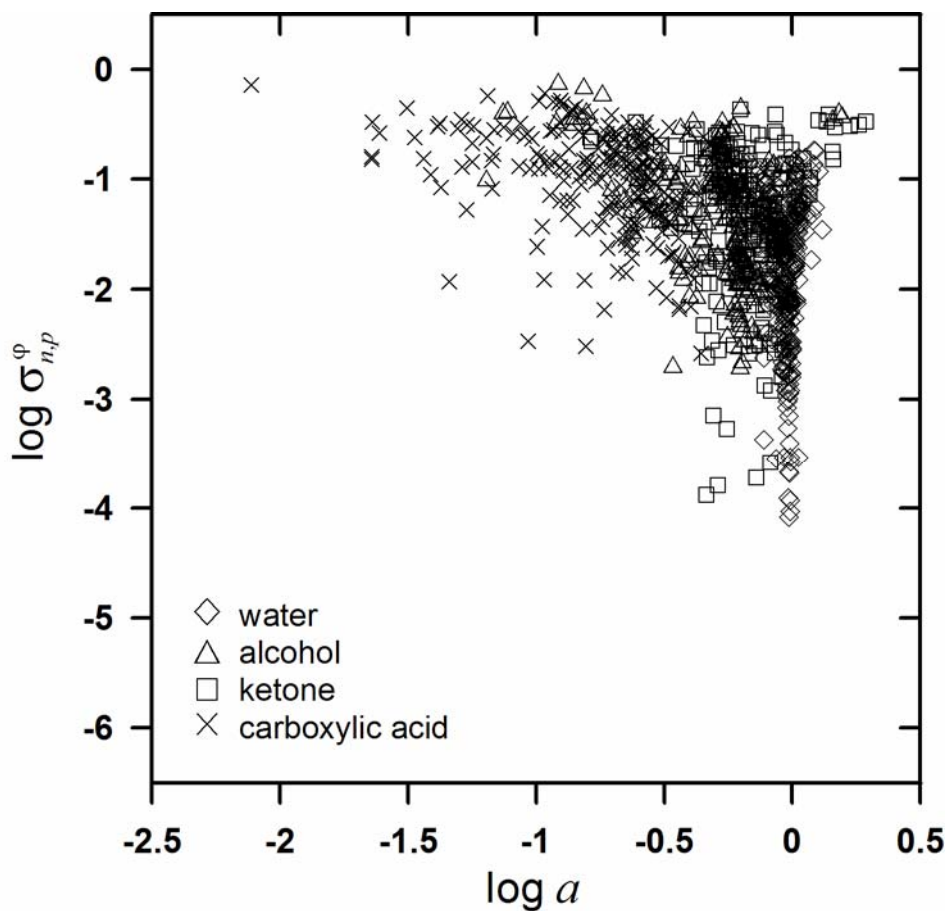


Figure 3.6. The logarithm of the standard error of each predicted activity coefficient $\zeta_{n,p}^{\phi,\text{pred}}$ of each solvent n in each phase ϕ of each system p in the basis and test sets (Tables 2 and 3). $\log \sigma_{n,p}^{\phi}$ is calculated according to Eq. (3.15) and plotted here as a function of the logarithm of the activity $a_{n,p}^{\phi}$ corresponding to each predicted $\zeta_{n,p}^{\phi,\text{pred}}$. The group-interaction parameters used to predict values of $\zeta_{n,p}^{\phi,\text{pred}}$ are listed in Table 6.

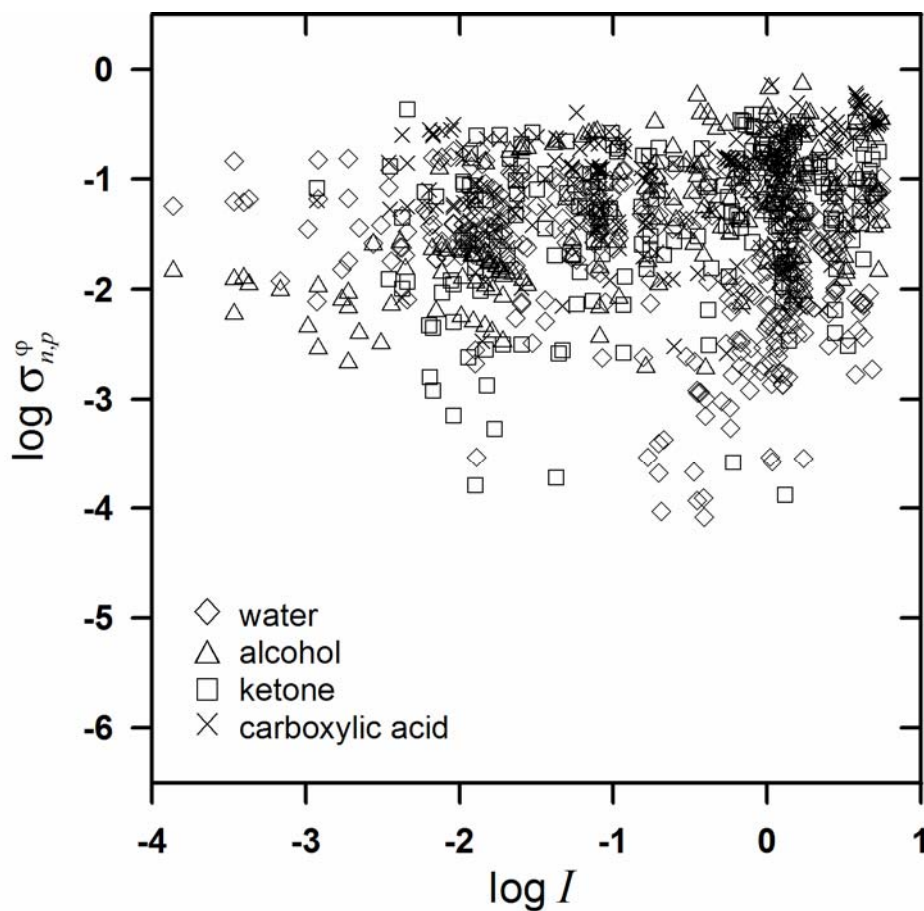


Figure 3.7. The logarithm of the standard error of each predicted activity coefficient $\zeta_{n,p}^{\phi,\text{pred}}$ of each solvent n in each phase ϕ of each system p in the basis and test sets (Tables 2 and 3). $\log \sigma_{n,p}^\phi$ is calculated according to Eq. (3.15) and plotted here as a function of the logarithm of the ionic strength I_p^ϕ of phase ϕ of system p . The group-interaction parameters used to predict values of $\zeta_{n,p}^{\phi,\text{pred}}$ are listed in Table 6.

CHAPTER 4

THE PREDICTED EFFECTS OF DISSOLVED INORGANIC SALTS ON THE FORMATION OF LIQUID PARTICULATE MATTER CONTAINING ORGANIC COMPOUNDS AND WATER

4.1 Abstract

Aerosol particulate matter (PM) in the ambient atmosphere may be comprised of a mixture of non-polar and relatively polar organic compounds, inorganic salts, and water. The overall composition of atmospheric PM influences the effects of PM on visibility, cloud formation, and human health. In this study, a thermodynamic model of the gas/particle (G/P) equilibrium of aerosols was implemented to predict the effects of dissolved inorganic salts on the formation of PM containing organic compounds and water over a range of relative humidity (RH) values. Results are presented for the effects of four individual salts (NaCl; $(\text{NH}_4)_2\text{SO}_4$; Na_2SO_4 ; and CaCl_2) on the α -pinene/ O_3 and cyclohexene/ O_3 aerosol systems. It was predicted that all salts result in a “salting out” effect in the α -pinene/ O_3 system, while a “salting in” effect is predicted for oxalic acid in the cyclohexene/ O_3 system. In the α -pinene/ O_3 system, the presence of dissolved inorganic salts tended to reduce the total PM (TPM) concentration: decreases up to 45% were predicted. In the cyclohexene/ O_3 system, dissolved inorganic salts tended to increase the TPM concentration: an average increase of 70% was predicted. The increases in TPM were largely due to significant predicted uptake of water. While predicted hygroscopic growth factors agree with measured values within about a factor of two, predicted aerosol yields agree on average with measured values to within ~20%.

4.2 Introduction

Aerosol particulate matter (PM) in the ambient atmosphere may be comprised of a mixture of organic and inorganic species (Seinfeld and Pandis, 1998). The formation of organic PM (OPM) and the effects of relative humidity (RH) thereon have been studied previously (Pankow et al., 2001; Seinfeld et al., 2001). That previous work satisfactorily reproduced measured organic aerosol yields and hygroscopic growth factors when OPM formed in the presence of dry inorganic salt seed aerosol: growth factors at 85% RH, $G(85\%)$, in the α -pinene/ O_3 aerosol system were predicted to be about 1.2, while values of 1.3 were measured. Predicted increases in organic aerosol yields were found to be attributable to the uptake of water at elevated RH and the corresponding decrease in the mean molecular weight of PM formed. Activity coefficient (ζ) values of individual oxidation products in the systems considered did not vary significantly from unity. The uptake of water in the cyclohexene/ O_3 system was predicted to be much greater than that in the α -pinene/ O_3 system. This difference was determined to be largely due to the relatively higher polarity of the major cyclohexene/ O_3 oxidation products.

In contrast to dry salt seed aerosol conditions as well as homogeneous nucleation conditions (at $\sim 0\%$ RH and elevated RH), reductions of organic aerosol yields have been observed in the α -pinene/ O_3 system when OPM forms in the presence of an aqueous salt seed ($41\% < RH < 62\%$) (Cocker et al., 2001). Furthermore, the hygroscopic growth of mixed organic/inorganic PM has been shown to vary from that of both purely inorganic PM and purely organic PM (Chan and Chan, 2003; Choi and Chan, 2002; Cocker et al., 2001; Cruz and Pandis, 2000; Ansari and Pandis, 2000; Lightstone et al., 2000; Saxena et al., 1995). Both Chan and Chan (2003) and Choi and Chan (2002) measured increases of the hygroscopic growth factors of OPM when individual organic species were mixed with either NaCl or $(NH_4)_2SO_4$. Cruz and Pandis (2000) measured decreases of the hygroscopic growth for inorganic PM when the inorganic salt was mixed with an organic species. These changes in hygroscopic growth are influenced by changes in the ζ values of each PM constituent from their pure phase values.

In the present work, condensation of secondary organic compounds is modeled using absorptive gas/particle (G/P) partitioning theory (Pankow, 1994a; Pankow, 1994b, Pankow, 2003), in the absence and presence of dissolved inorganic salt. The required ζ

values of all partitioning species are estimated with a group contribution method (GCM) recently developed by Erdakos et al. (submitted for publication, 2004). Effects of dissolved inorganic salts on the formation of OPM are predicted over a range of RH values (45-60%) in the α -pinene/O₃ and cyclohexene/O₃ aerosol systems. These two systems have been well-characterized and successfully modeled in the absence of dissolved salts (Pankow et al., 2001; Seinfeld et al., 2001; Erdakos and Pankow, 2004). Moreover, the α -pinene/O₃ system was investigated experimentally by Cocker et al. (2001) in the presence of dissolved inorganic salts. Effects are examined for four individual salts: NaCl; (NH₄)₂SO₄; Na₂SO₄; and CaCl₂. Specifically, changes in: 1) aerosol yields; 2) PM composition; and 3) individual oxidation product ζ values are quantified.

Following is a description of the systems studied, the modeling approach used, and modeling results, which are compared with experimental measurements.

4.3 Aerosol Systems Studied

The systems modeled are hypothetical systems derived from the α -pinene/O₃ and cyclohexene/O₃ aerosol systems discussed by Pankow et al. (2001) and Seinfeld et al. (2001) by adding dissolved inorganic salt. For the α -pinene/O₃ systems, $T = 306$ K; for the cyclohexene/O₃ system, $T = 298$ K. These are the same temperatures as those in the elevated RH cases for the two salt-free systems evaluated by Seinfeld et al. (2001). For each aerosol system, two cases are studied here in which $500 \mu\text{g m}^{-3}$ of parent hydrocarbon (HC) is reacted to produce stoichiometric amounts of oxidation products according to Eq. (4.7). Tables 4.2a and 4.2b list the individual oxidation products and their physico-chemical properties. The two cases considered differ by the amount of inorganic salt added to the system: 1 and 2 mol kg⁻¹ concentrations. The salt is assumed to be dissolved in a liquid phase comprised of the organic oxidation products and the water present due to RH. In addition to the assumption stated earlier, namely that dissolved salts remain in the condensed phase, it is also assumed that only a single liquid PM phase is present. Therefore, it is only necessary to calculate ζ values for the organic species and water.

Additional α -pinene/O₃ cases are studied in order to compare: 1) predicted yields with measured values from Cocker et al. (2001); and 2) hygroscopic growth factors with measured values from Cruz and Pandis (2000) and Choi and Chan (2002). These cases are characterized by the same α -pinene/O₃ oxidation products listed in Table 4.2a, however the amounts of reacted HC and T are varied to match the conditions of the experimental systems.

4.4 Thermodynamic Modeling Approach

4.4.1 Gas-particle partitioning numerics

When a parent HC is reacted to form OPM, the organic aerosol yield is

$$Y = \frac{M_o}{\Delta\text{HC}} \quad (4.1)$$

where ΔHC ($\mu\text{g m}^{-3}$) is the amount of parent hydrocarbon that has reacted and M_o ($\mu\text{g m}^{-3}$) is the mass concentration of OPM formed. Since OPM may absorb water, Seinfeld et al. (2001) gave the following definitions of aerosol yield:

$$Y_o = \frac{M_o}{\Delta\text{HC}} \quad (4.2)$$

$$Y_w = \frac{M_w}{\Delta\text{HC}} \quad (4.3)$$

$$Y_t = \frac{M_t}{\Delta\text{HC}} = Y_o + Y_w \quad (4.4)$$

where M_w ($\mu\text{g m}^{-3}$) is the water-only portion of aerosol mass concentration, and

$$M_t = M_o + M_w \quad (4.5)$$

is the total mass concentration ($\mu\text{g m}^{-3}$) of PM formed.

The partition constant that describes the G/P equilibrium in an aerosol system is

$$K_{p,i} = \frac{F_i / \text{TPM}}{A_i} \quad (4.6)$$

where F_i (ng m^{-3}) is the mass concentration of component i associated with the PM phase, TPM ($\mu\text{g m}^{-3}$) is the total suspended PM, and A_i (ng m^{-3}) is the gas-phase concentration of i . The total amount of compound i in the system is

$$T_i = F_i + A_i = 10^3 \alpha_i \Delta\text{HC} \quad (4.7)$$

where α_i is the mass stoichiometric factor of compound i . T_i is related to the partition constant by:

$$F_i = \frac{K_{p,i} \text{TPM}}{1 + K_{p,i} \text{TPM}} T_i \quad (4.8)$$

or in matrix form:

$$\begin{bmatrix} F_1 \\ F_2 \\ \cdot \\ \cdot \\ F_n \end{bmatrix} = \begin{bmatrix} \frac{K_{p,1} \text{TPM}}{1 + K_{p,1} \text{TPM}} & 0 & \cdot & \cdot \\ 0 & \frac{K_{p,2} \text{TPM}}{1 + K_{p,2} \text{TPM}} & \cdot & \cdot \\ \cdot & \cdot & \cdot & \cdot \\ \cdot & \cdot & \cdot & \frac{K_{p,n} \text{TPM}}{1 + K_{p,n} \text{TPM}} \end{bmatrix} \begin{bmatrix} T_1 \\ T_2 \\ \cdot \\ \cdot \\ T_n \end{bmatrix} \quad (4.9)$$

G/P equilibrium of all partitioning species is determined by solving Eq. (4.9). As discussed by Pankow et al. (2001), this is accomplished by: 1) assuming initial guesses for the value of TPM and the PM composition; then 2) iteratively computing the F_i values in Eq. (4.9) while updating the corresponding $K_{p,i}$ values until convergence is achieved. In the cases considered here, only the organic species and water are allowed to partition; the dissociated inorganic ions are assumed to remain entirely in the PM phase. Therefore, as described by Pankow (2003):

$$\text{TPM} = 10^{-3} \left(\sum_i F_i + F_{\text{non-vol}} \right) \quad (4.10)$$

where $F_{\text{non-vol}}$ (ng m^{-3}) is the mass concentration of the non-volatile component of TPM (i.e., dissociated ions), and the factor 10^{-3} is for conversion between ng m^{-3} and $\mu\text{g m}^{-3}$. Eq. (4.10) illustrates that the non-volatile component of TPM is decoupled from the individual F_i , although F_i is not decoupled from $F_{\text{non-vol}}$ (Pankow, 2003). Also note that $T_{\text{non-vol}} = F_{\text{non-vol}}$. Thus, we define here:

$$M_t = 10^{-3} \sum_i F_i \quad (4.11)$$

For a given amount of dissolved inorganic salt ($F_{\text{non-vol}}$) and an initial guess for M_t , the resulting vector $\hat{\mathbf{F}}$ of the iterative solution of Eq. (4.9) will not necessarily satisfy Eq. (4.11). Pankow et al. (2001) discuss how the equilibrium vector $\hat{\mathbf{F}}$ can be calculated by

iteratively solving Eq. (4.9) with successive guess values of M_t and minimization of the variable ε

$$\varepsilon = \left| \sum_{i=1}^n F_i - 1000 M_t (\text{guess}) \right| \quad (4.12)$$

to within some tolerance. In this work, $\varepsilon \leq 10^{-4}$.

In all of the cases considered here, the formation of PM is governed by absorptive G/P partitioning. The G/P partition constant in Eq. (4.6) for condensable species i can thus be written as (Pankow, 1994a;1994b)

$$K_{p,i} = \frac{760RT f}{10^6 MW_{\text{om}} \zeta_i p_{L,i}^{\circ}} \quad (4.13)$$

where R is the gas constant, T is temperature (K), f is the mass fraction of the absorbing phase in the TPM (including *all* the constituents in that phase), MW_{om} (g mol^{-1}) is the number average molecular weight of the absorbing phase, ζ_i is the mole fraction-scale activity coefficient of species i in the absorbing phase, and $p_{L,i}^{\circ}$ (Torr) is the pure liquid vapor pressure (sub-cooled if necessary) of species i . Pure liquid vapor pressure values are estimated with UNIFAC- p_L° (Asher and Pankow, in preparation) and SPARC (Hilal et al., 1994); ζ values are estimated with Ionic-UNIFAC.1 (Erdakos et al., submitted for publication, 2004).

4.4.2. Input p_L° values

The pure liquid compound vapor pressures (sub-cooled if necessary) of all HC oxidation products were initially estimated using the UNIFAC- p_L° method of Asher and Pankow (in preparation). After predicting the G/P equilibrium of products in the α -pinene/ O_3 system in the absence of aqueous salt seed, it was found that the distribution of species in the PM phase did not agree with experimental measurements of Yu et al. (1999). The distribution also did not agree with earlier model predictions (Pankow et al., 2001) in which an earlier version of UNIFAC- p_L° (Asher et al., 2002) was used to estimate vapor pressure values. The PM-phase mass concentrations of two major α -pinene/ O_3 products, pinonic acid and norpinonic acid, were significantly under-predicted

using the initial set of $p_{L,i}^{\circ}$ values. The initial estimates of the p_L° values for those two products were found to be much higher than estimates obtained from the SPARC method of Hilal et al. (1994). Table 4.1 shows a comparison of the p_L° values for these two products using the two different estimation methods. A final set of p_L° values obtained by using the SPARC estimates for pinonic and norpinonic acids in the initial set of p_L° values results in distribution of all oxidation products that agrees with both the experimental measurements of Yu et al. (1999) and the earlier predictions of Pankow et al. (2001). It was therefore determined that this final set of p_L° values be used for the current study.

The p_L° values of all cyclohexene/O₃ oxidation products used in this study were estimated using the UNIFAC- p_L° method of Asher and Pankow (in preparation).

4.4.3. Estimating ζ with Ionic-UNIFAC.1

Ionic-UNIFAC.1 expresses $\ln \zeta_n$ for a solvent compound n (i.e., an organic species or water) in a general liquid PM mixture as a sum of contributions due to long- and short-range interactions:

$$\ln \zeta_n = \ln \zeta_n^{\text{D-H}} + \ln \zeta_n^{\text{C}} + \ln \zeta_n^{\text{R}} \quad (4.14)$$

where $\ln \zeta_n^{\text{D-H}}$ is a Debye-Hückel term accounting for long-range electrostatic interactions, and $\ln \zeta_n^{\text{C}}$ and $\ln \zeta_n^{\text{R}}$ are the combinatorial (C) and residual (R) terms of the original UNIFAC equation accounting for short-range interactions (Fredenslund et al., 1975, 1977).

The Debye-Hückel term used in Eq. (4.14) is that derived by Macedo et al. (1990):

$$\ln \zeta_n^{\text{D-H}} = \frac{2AMW_n \rho_s}{b^3 \rho_n} \left[1 + b\sqrt{I} - \frac{1}{1+b} \sqrt{I} - 2 \ln(1 + b\sqrt{I}) \right] \quad (4.15)$$

where: $A = 1.327757 \times 10^5 \rho_s^{1/2} / (\epsilon_s T)^{3/2}$; $b = 6.359696 \rho_s^{1/2} / (\epsilon_s T)^{1/2}$; $I = \frac{1}{2} \sum_j m_j z_j^2$ is the ionic strength of the mixture of interest (mol kg⁻¹); MW_n is the molecular weight of solvent n (g mol⁻¹); ρ_n is the density of pure solvent n (kg m⁻³); ρ_s is the density of the

salt-free solution phase (kg m^{-3}); ϵ_s is the dielectric constant of the solution phase; m_j is the molality of ion j in the mixture of interest (mol kg^{-1}); and z_j is the charge number of ion j .

Pure compound density values are estimated using SPARC (Hilal et al., 1994). Except for water, the pure compound dielectric constants are each arbitrarily set equal to 10. This value is roughly the same as that of short-chained monofunctional carboxylic acid, aldehyde, and ketone organic compounds. The dielectric constant of water at temperature T is estimated using a parameterization presented by Wohlfarth (1995). Calculations showed that changing the dielectric constant value of the organic species by a factor of two (either larger or smaller) did not change the predicted value of M_t by more than a few percent. Methods used for calculating ρ_s and ϵ_s are described in detail by Erdakos et al. (submitted for publication, 2004).

The combinatorial term of the UNIFAC equation is given by Fredenslund *et al.* (1975):

$$\ln \zeta_n^C = \ln \frac{\Phi_n}{X_n} + 5q_n \frac{\theta_n}{\Phi_n} + l_n - \frac{\Phi_n}{X_n} \sum_i X_i l_i \quad (4.16)$$

where: $l_n = 5(r_n - q_n) - (r_n - 1)$; $\theta_n = \frac{q_n X_n}{\sum_i q_i X_i}$; $\Phi_n = \frac{r_n X_n}{\sum_i r_i X_i}$; and X_i is the mole

fraction of component i . Summations in these equations are taken over all components i in the mixture (including organic species, ions, and water). The parameters q and r represent the surface area and volume, respectively, of pure component i . They are calculated from the surface area (Q_k) and volume (R_k) parameters of the individual functional groups k that comprise i : $q_i = \sum_k v_k^i Q_k$ and $r_i = \sum_k v_k^i R_k$, where v_k^i is the number of groups of type k in mixture component i .

The residual term of the UNIFAC equation is given by Fredenslund *et al.* (1975):

$$\ln \zeta_n^R = \sum_k v_k^n [\ln Z_k - \ln Z_k^n] \quad (4.17)$$

where Z_k is the residual activity coefficient of functional group k and Z_k^n is the residual activity coefficient of group k in a reference solution containing only molecules of type n . Both Z_k and Z_k^n are expressed by

$$\ln Z_k = Q_k [1 - \ln(\sum_m \Theta_m \Psi_{mk}) - \sum_m (\Theta_m \Psi_{mk} / \sum_o \Theta_o \Psi_{om})] \quad (4.18)$$

where summations are taken over all functional groups m and o in the mixture of interest,

and $\Theta_m = \frac{Q_m X_m}{\sum_o Q_o X_o}$ is the area fraction of group m in the mixture. The interaction term

in Eq. (4.18) is

$$\Psi_{mo} = \exp\left[-\frac{U_{mo} - U_{oo}}{RT}\right] = \exp(-A_{mo}/T) \quad (4.19)$$

where U_{mo} (J mol^{-1}) = measure of the energy of interaction between groups m and o in the mixture, R ($\text{J mol}^{-1} \text{K}^{-1}$) = the ideal gas constant, A_{mo} (K^{-1}) = group-group interaction parameter, and $A_{mm} \equiv 0$, since the standard state chosen for i is pure component in which $\zeta \equiv 1$. There are two interaction parameters for each pair of functional groups, where $A_{mo} \neq A_{om}$.

The interaction parameters for the group pair NH_4^+ -CHO are not available for Ionic-UNIFAC.1. That pair is, however, necessary to represent the aldehyde oxidation products in the α -pinene/ O_3 system containing aqueous $(\text{NH}_4)_2\text{SO}_4$ seed. It is assumed here that interactions parameters for the pair NH_4^+ - CH_2CO can be used for the pair NH_4^+ -CHO. This substitution should not be problematic, since the aldehyde compounds in the α -pinene/ O_3 system are minor constituents of the PM phase (<0.5% of the total PM concentration).

4.5 Modeling Results

4.5.1 Total aerosol yields

Predicted total PM mass concentrations M_t with and without dissolved inorganic salt over the range of RH values (45-60%) are shown in Figures. 4.1 and 4.2 for the α -pinene/ O_3 and cyclohexene/ O_3 systems, respectively. The results shown are for the 2 m salt concentration cases. Results for the individual salts at 0, 1 and 2 m salt concentrations are shown in Figures 4.3 and 4.4 for the two systems. M_t is predicted to decrease in the α -pinene/ O_3 system when 2:1 and 1:2 electrolytes are present, but predicted to increase in the presence of NaCl. In the cyclohexene/ O_3 system, M_t is

predicted to increase in the presence of all salts considered except $(\text{NH}_4)_2\text{SO}_4$. The percent changes in M_t averaged over the range of RH values for each system and each salt are summarized in Table 4.3. Compared to the α -pinene/ O_3 system, increases in M_t in the presence of aqueous NaCl are predicted to be significantly larger in the cyclohexene/ O_3 system. This is likely due to the relatively higher polarity of cyclohexene/ O_3 oxidation products and the subsequent larger uptake of water.

4.5.2. Concentrations of organic species and water

In the α -pinene/ O_3 system, “salting out” behavior is predicted in the presence of each dissolved inorganic salt (Figure 4.5). The “salting out” of organic constituents is more pronounced in the presence of CaCl_2 than in the presence of $(\text{NH}_4)_2\text{SO}_4$. The increase in water mass concentration is significantly higher in the presence of CaCl_2 than in the presence of $(\text{NH}_4)_2\text{SO}_4$ (Figure 4.6). In the cyclohexene/ O_3 system, “salting out” of organic species is predicted except for oxalic acid, where ζ is lowered by the presence of salt. The effects of each salt on total organic and water concentrations in the cyclohexene/ O_3 system are shown in Figures 4.7 and 4.8. The mass concentration of water in the cyclohexene/ O_3 system is much greater than that in the α -pinene/ O_3 system, both with and without dissolved inorganic salt present. Moreover, a significant increase in the mass concentration of water is predicted when dissolved CaCl_2 is present in the cyclohexene/ O_3 system.

The changes in mass concentrations of organic species and water are a result of the changes in the molecular weight of the PM phase from uptake of water and changes in ζ values of each component. As discussed by Seinfeld et al. (2001), uptake of water reduces the molecular weight of the PM phase, which in turn increases the value of $K_{p,i}$ (see Eq. (4.13)). According to Eq. (4.13), decreasing ζ_i will also increase $K_{p,i}$, thereby increasing the mass concentration of i in the PM phase. In both systems and for all salt cases considered, the presence of dissolved inorganic salts lowers the ζ of water. This is illustrated for the $(\text{NH}_4)_2\text{SO}_4$ and CaCl_2 cases in Figures 4.9 and 4.10 for the α -pinene/ O_3 and cyclohexene/ O_3 systems, respectively. In these figures, only the major PM-phase constituents (i.e., $M_i > 1 \mu\text{g m}^{-3}$) are included. Except for oxalic acid in the $(\text{NH}_4)_2\text{SO}_4$

case in the cyclohexene/O₃ system, the ζ values of organic species are predicted to increase in the presence of aqueous salt seed aerosol. However, the total concentration of organic species in that system is predicted to increase as a result of the large uptake of water.

4.5.3 Comparison between model predictions and experimental measurements

The accuracy of these model predictions can be evaluated by a comparison to experimental observations. Predicted changes in M_t values are compared to changes in aerosol yields measured by Cocker et al. (2001) in Tables 4.4 and 4.5. Table 4.4 compares the predicted percent changes in M_t at RH = 50% with the percent changes calculated from the yield curves presented by Cocker et al. (2001). Excellent agreement is obtained for both the aqueous (NH₄)₂SO₄ and CaCl₂ seed cases. Table 4.5 compares predicted and measured aerosol yields. The measured yields were calculated from the yield curve fits of Cocker et al. (2001); the predicted values were obtained by changing the value of ΔHC at $T = 301$ K until the desired value of M_t was obtained. 10-30% differences between predicted and measured yields are calculated for the values in Table 4.5. This amount of error is within the expected uncertainty of Ionic-UNIFAC.1-estimated activity coefficients (Erdakos et al., submitted for publication, 2004).

Hygroscopic growth factors were calculated from predicted mass concentrations according to:

$$M_t / M_o = G_f^3 \quad (4.20)$$

Where M_o is the organic mass concentration at RH = 0%, and M_t is the total mass concentration at elevated RH. Results for several mixed organic/inorganic-salt particles are compared to the experimental results of Choi and Chan (2002) and Cruz and Pandis (2000) in Table 4.6. Prediction errors average a factor of three for the results of Choi and Chan, where the growth factor of mixed (NH₄)₂SO₄-malonic acid PM exhibits the highest error. Indeed, the quality of UNIFAC-based ζ -estimates decreases as structural effects become more important. For the results of Cruz and Pandis, the model predictions are a factor of two larger than measured values for particles with 50% total organic mass, and only 20% larger than measured values for particles with 80% organic mass fraction. These results are not surprising, since Ionic-UNIFAC.1 was developed for PM phases

with salt concentrations $\leq 2 \text{ mol kg}^{-1}$. As short-chained diacids are among the major PM-phase constituents in the cyclohexene/ O_3 system, these results are indicative of the quality of the TPM predictions presented earlier for that system.

4.6 Conclusions

Mass concentrations of PM in the absence and presence of dissolved inorganic salt are predicted in the α -pinene/ O_3 and cyclohexene/ O_3 systems by modeling the G/P equilibrium of partitioning organic species and water. Relative to homogeneous nucleation and dry salt seed cases, decreases in aerosol yield are predicted in the α -pinene/ O_3 system in the presence of dissolved $(\text{NH}_4)_2\text{SO}_4$, Na_2SO_4 , and CaCl_2 , while increases are predicted in the presence of dissolved NaCl . In the cyclohexene/ O_3 system, increases in aerosol yield are predicted for all salts except $(\text{NH}_4)_2\text{SO}_4$. The ζ -estimation method used here (Ionic-UNIFAC.1) was developed for PM phases in which the salt concentrations are relatively low ($\leq 2 \text{ mol kg}^{-1}$). Average errors in predicted aerosol yields and hygroscopic growth factors in such systems are $\sim 20\%$, which is within the expected range of error for Ionic-UNIFAC.1. Excellent agreement is obtained between predicted and measured decreases in aerosol yield in the α -pinene/ O_3 system at $\text{RH} = 50\%$ with aqueous $(\text{NH}_4)_2\text{SO}_4$ and CaCl_2 seed: 45% vs. 44%, and 21% vs. 24%, respectively.

4.7 Acknowledgement

This work was supported by the Electric Power Research Institute (EPRI) research grant EP-P4650/C2267, Thermodynamics of Atmospheric Organic Aerosols.

4.8 References

- Ansari, A.S., Pandis, S.N., 2000. Water absorption by secondary organic aerosol and its effect on inorganic aerosol behavior. *Environmental Science & Technology* 34, 71-77.
- Asher, W.E., Pankow, J.F., 2004. Estimating Vapor Pressures of Unsaturated Oxygen-Containing Organic Compounds Using Group Contribution Methods. In preparation.

- Chan, M.N., Chan, C.K., 2003. Hygroscopic properties of two model humic-like substances and their mixtures with inorganics of atmospheric importance. *Environmental Science & Technology* 37, 5109-5115.
- Choi, M.Y., Chan, C.K., 2002. The effects of organic species on the hygroscopic behaviors of inorganic aerosols. *Environmental Science & Technology* 36, 2422-2428.
- Cocker, D. R. III; Clegg, S. L.; Flagan, R. C.; Seinfeld, J. H., 2001. The effect of water on gas-particle partitioning of secondary organic aerosol. Part I: α -pinene/ozone system. *Atmospheric Environment* 35, 6049-6072.
- Cruz, C.N., Pandis, S.N., 2000. Deliquescence and hygroscopic growth of mixed inorganic-organic atmospheric aerosol. *Environmental Science & Technology* 34, 4313-4319.
- Erdakos, G.B., Asher, W.E., Seinfeld, J.H., Pankow, J.F., 2004. Gas/Particle Partitioning of Neutral and Ionizing Compounds to Single- and Multi-Phase Aerosol Particles. 3. Ionic-UNIFAC.1: A Method for Predicting Activity Coefficients of Neutral Compounds in Liquid Particulate Matter Containing Organic Compounds, Inorganic Salts, and Water. Submitted to *Atmospheric Environment*.
- Erdakos, G.B., Pankow, J.F., 2003. Gas/Particle Partitioning of Neutral and Ionizing Compounds to Single- and Multi-Phase Aerosol Particles. 2. Phase Separation in Liquid Particulate Matter Containing Both Polar and Low-Polarity Organic Compounds. *Atmospheric Environment* 38, 1005-1013.
- Fredenslund, A., Jones, R.L., Prausnitz, J.M., 1975. Group-contribution estimation of activity coefficients in nonideal liquid mixtures. *American Institute of Chemical Engineers Journal* 21, 1086-1099.
- Fredenslund, A., Gmehling, J., Rasmussen, P., 1977. *Vapor-Liquid Equilibria Using UNIFAC: A Group-Contribution Method*, Elsevier Scientific Publishing, New York.
- Hilal, S.H., Carreira, L.A., Karickhoff, S.W., 1994. *Estimation of chemical reactivity parameters and physical properties of organic molecules using SPARC*. In: Murray, P.P.a.J.S. (Ed.), *Quantitative Treatments of Solute/Solvent Interactions*. Elsevier, Amsterdam.
- Lightstone, J.M., Onasch, T.B., Imre, D., Oatis, S., 2000. Deliquescence, efflorescence, and water activity in ammonium nitrate and mixed ammonium nitrate/succinic acid microparticles. *Journal of Physical Chemistry A* 104, 9337-9346.

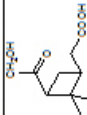
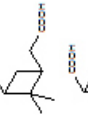
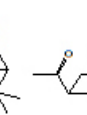
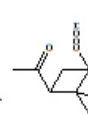
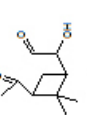
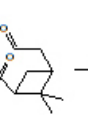
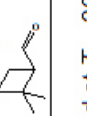
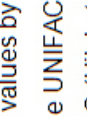
- Macedo, E.A., Skovborg, P., Rasmussen, P., 1990. Calculation of phase equilibria for solutions of strong electrolytes in solvent-water mixtures. *Chemical Engineering Science* 45, 875-882.
- Pankow, J.F., 1994a. An absorption model of gas/particle partitioning of organic compounds in the atmosphere. *Atmospheric Environment* 28, 185-188.
- Pankow, J.F., 1994b. An absorption model of the gas/aerosol partitioning involved in the formation of secondary organic aerosol. *Atmospheric Environment* 28, 189-193.
- Pankow, J.F., 2003. Gas/particle partitioning of neutral and ionizing compounds to single and multi-phase particles. 1. Unified modeling framework. *Atmospheric Environment* 37, 3323-3333.
- Pankow, J.F., Seinfeld, J.H., Asher, W.E., Erdakos, G.B., 2001. Modeling the formation of secondary organic aerosol: 1. The application of theoretical principles to measurements obtained in the α -pinene-, β -pinene-, sabinene-, Δ^3 -carene-, and cyclohexene-ozone systems. *Environmental Science and Technology* 35, 1164-1172.
- Peng, C., Chan, M.N., Chan, C.K., 2001. The hygroscopic properties of dicarboxylic and multifunctional acids: Measurements and UNIFAC predictions. *Environmental Science & Technology* 35, 4495-4501.
- Saxena, P., Hildemann, L.M., McMurry, P.H., Seinfeld, J.H., 1995. Organics alter hygroscopic behavior of atmospheric particles. *Journal of Geophysical Research* 100, 18755-18770.
- Seinfeld, J.H., Pandis, S.N., 1998. *Atmospheric Chemistry and Physics: from air pollution to climate change*, John Wiley & Sons, New York.
- Seinfeld, J.H., Erdakos, G.B., Asher, W.E., Pankow, J.F., 2001. Modeling the formation of secondary organic aerosols: 2. The predicted effects of relative humidity on aerosol formation in the α -pinene-, β -pinene-, sabinene-, Δ^3 -carene-, and cyclohexene-ozone systems. *Environmental Science and Technology* 35, 1806-1817.
- Wohlfarth, C., 1995. *Temperature Dependence of the Permittivity (Dielectric Constant) of Liquids*. In: Lide, D.R. (Editor-in-Chief), *CRC Handbook of Chemistry and Physics*. CRC Press, Boca Raton.

Table 4.1. Comparison of estimated sub-cooled p_L° values of pinonic acid and norpinonic acid at $T = 308\text{K}$ using the UNIFAC- p_L° and SPARC methods.^a

Compound	sub-cooled p_L° (Torr)	
	UNIFAC- p_L°	SPARC
pinonic acid	1.61×10^{-3}	9.38×10^{-6}
norpinonic acid	2.48×10^{-3}	5.28×10^{-5}

^a UNIFAC- p_L° : Asher and Pankow (in preparation); SPARC: Hilal et al. (1994).

Table 4.2a. Products of the ozone oxidation of α -pinene and their physico-chemical properties.^a

Parent HC	Oxidation product	Structure	MW (g mol ⁻¹)	$\alpha_{\text{product}}^b$	P_L^o (Torr) ^c	ρ (g L ⁻¹) ^d
α -pinene	Hydroxy pinonic acid		200	0.0397	8.36×10^{-7}	1118
	Pinic acid		186	0.0661	1.14×10^{-6}	1127
	Norpinic acid		172	0.0012	6.16×10^{-6}	1128
	Pinonic acid		184	0.0568	2.74×10^{-5}	1019
	Norpinonic acid		170	0.1129	8.36×10^{-5}	1039
	Hydroxy pinonaldehyde		184	0.0762	5.85×10^{-4}	1020
	Pinonaldehyde		168	0.1458	2.81×10^{-2}	936
	Norpinonaldehyde		154	0.0208	1.22×10^{-1}	938

^a The properties for the α -pinene/O₃ system are calculated at $T = 306$ K.

^b Mass stoichiometric factors were calculated as average values by Pankow et al. (2001).

^c Pure compound vapor pressures are estimated using the UNIFAC- P_L^o method (Asher and Pankow, in preparation), except norpinonic acid pinonic acid vapor pressures which are estimated using SPARC (Hilal et al., 1994).

^d Densities are estimated using SPARC (Hilal et al., 1994).

Table 4.2b. Products of the ozone oxidation of cyclohexene and their physico-chemical properties.^a

Parent HC	Oxidation product	Structure	MW (g mol ⁻¹)	$\alpha_{\text{product}}^b$	P_L^o (Torr) ^c	ρ (g L ⁻¹) ^d
Cyclohexene	2-Hydroxy-adipic acid		162	0.0187	3.02×10^{-3}	1087
	2-Hydroxy-glutaric acid		148	0.0331	7.21×10^{-3}	1079
	Adipic acid		146	0.0406	9.14×10^{-3}	1218
	Glutaric acid		132	0.1064	2.49×10^{-3}	1258
	Succinic acid		118	0.0096	6.21×10^{-5}	1309
	Malonic acid		104	0.0969	1.35×10^{-4}	1378
	Oxalic acid		90	0.0703	2.28×10^{-4}	1371
	2-Hydroxy-pentanoic acid		118	0.0158	8.20×10^{-4}	1010
	6-Oxo-hexanoic acid		130	0.0714	1.78×10^{-3}	982
	5-Oxo-pentanoic acid		116	0.0688	5.00×10^{-3}	1165
	4-Oxo-butanoic acid		102	0.0963	1.28×10^{-2}	1399
	4-Hydroxy-butanal		88	0.0303	2.08×10^{-1}	1026
	1,6-hexanedial		114	0.0262	2.50×10^{-1}	948
	1,5-pentanedial		100	0.0060	7.12×10^{-1}	1131
1,4-butanedial		86	0.0061	1.85×10^0	1333	

^a The properties for the cyclohexene/O₃ system are calculated at $T = 298$ K.

^b Mass stoichiometric factors were calculated as average values by Pankow et al. (2001).

^c Pure compound vapor pressures are estimated using the UNIFAC- P_L^o method (Asher and Pankow, in preparation).

^d Densities are estimated using SPARC (Hilal et al., 1994).

Table 4.3. Average percent changes in predicted total mass concentrations M_t from conditions of wet homogeneous nucleation to aqueous salt seed in the α -pinene/ O_3 and cyclohexene/ O_3 systems.

System ^a	Salt molality	avg. % change in M_t^b			
		$(NH_4)_2SO_4$	Na_2SO_4	NaCl	$CaCl_2$
α -pinene/ O_3	1	-22	-31	5	-2
	2	-45	-36	7	-21
cyclohexene/ O_3	1	-13	3	30	94
	2	-12	27	67	327

^a The α -pinene/ O_3 system is at $T = 306$ K; the cyclohexene/ O_3 system is at $T = 298$ K.

^b Averages are taken over the range of RH (45-60%).

Table 4.4. Measured and predicted change in aerosol yield Y from conditions of wet nucleation to aqueous salt seed at $RH = 50\%$ and $T = 301\text{ K}$.

Salt	Change in Y (%)	
	Meas. ^a	Pred.
$(\text{NH}_4)_2\text{SO}_4$	-44	-45
CaCl_2	-24	-21

^a Measured values are calculated from the yield curve fittings of Cocker et al. (2001). For $(\text{NH}_4)_2\text{SO}_4$, $45.2\% < RH < 55.2\%$; for CaCl_2 , $41.5\% < RH < 57.5\%$.

Table 4.5. Measured and predicted aerosol yields with aqueous salt seed at RH = 50% and $T = 301$ K.

Salt	M_{o+w} ($\mu\text{g m}^{-3}$)	Aerosol yield	
		Meas. ^a	Pred.
(NH ₄) ₂ SO ₄	50	0.11	0.08
	100	0.15	0.12
	150	0.17	0.14
	200	0.19	0.16
	250	0.20	0.17
CaCl ₂	50	0.15	0.10
	100	0.19	0.14
	150	0.21	0.17
	200	0.22	0.19
	250	0.24	0.21

^a Measured values are calculated from the yield curve fittings of Cocker et al. (2001). For (NH₄)₂SO₄, 45.2% < RH < 55.2%; for CaCl₂, 41.5% < RH < 57.5%.

Table 4.6. Measured and predicted growth factors for mixed $(\text{NH}_4)_2\text{SO}_4$ -organic aerosol PM at RH = 85%

Composition	Meas. G(85%)	Pred. G(85%)
50% malonic acid ^a	1.45	7.30
50% succinic acid ^a	1.43	3.90
50% glutaric acid ^a	1.38	3.69
50% pinonic acid ^b	1.39 ± 0.04	2.21
80% pinonic acid ^b	1.35 ± 0.03	1.11
50% glutaric acid ^b	1.35 ± 0.03	3.60
80% glutaric acid ^b	1.20 ± 0.06	1.44

^a Composition given on a mole fraction basis. Measured data taken from Choi and Chan (2002).

^b Composition given on a mass fraction basis. Measured data taken from Cruz and Pandis (2000).

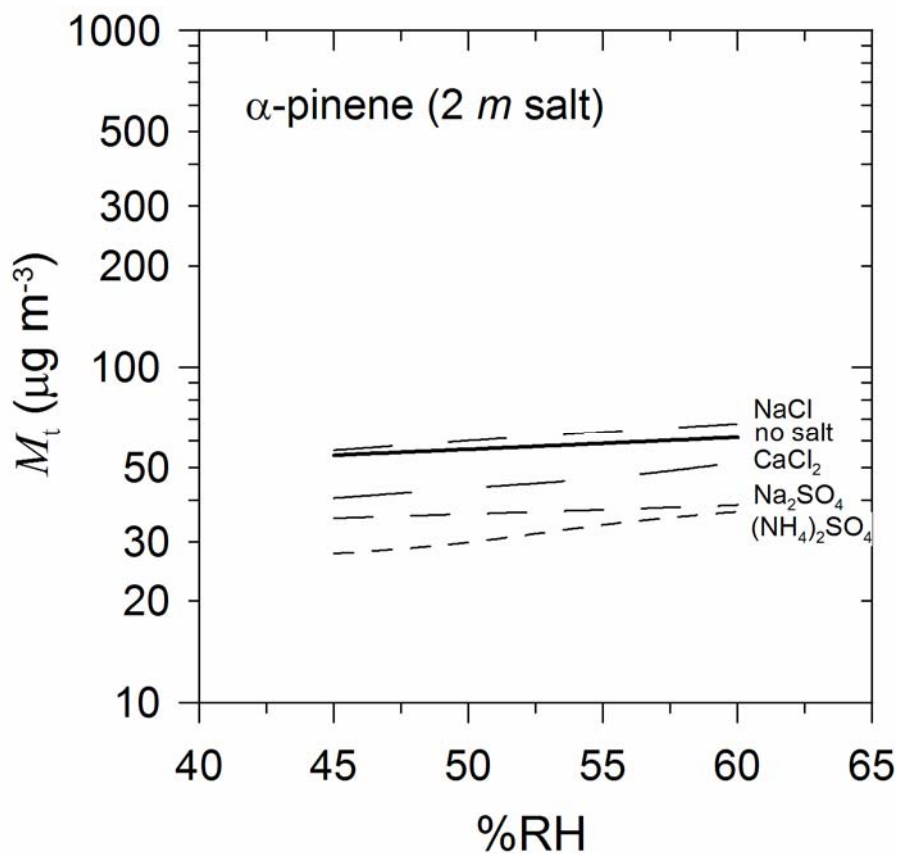


Figure 4.1. Predicted total mass concentrations M_t , including organic species and water, at $T = 306$ K in the α -pinene/ O_3 system with and without 2 mol kg^{-1} dissolved inorganic salt from $\text{RH} = 45\%$ to $\text{RH} = 60\%$. Solid line: no salt present (i.e., homogeneous nucleation); shortest dashed line: dissolved $(\text{NH}_4)_2\text{SO}_4$ is present; short dashed line: dissolved Na_2SO_4 is present; long dashed line: dissolved NaCl is present; and longest dashed line: dissolved CaCl_2 present.

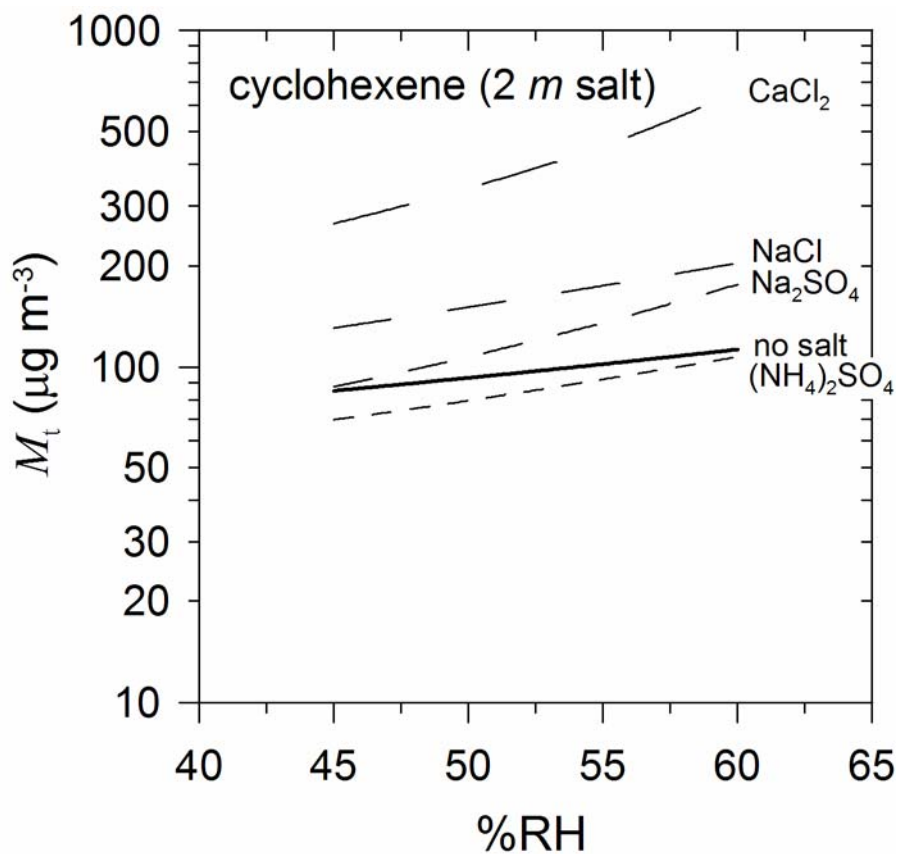


Figure 4.2. Predicted total mass concentrations M_t , including organic species and water, at $T = 298$ K in the cyclohexene/ O_3 system with and without 2 mol kg^{-1} dissolved inorganic salt from $\text{RH} = 45\%$ to $\text{RH} = 60\%$. Solid line: no salt present (i.e., homogeneous nucleation); shortest dashed line: dissolved $(\text{NH}_4)_2\text{SO}_4$ is present; short dashed line: dissolved Na_2SO_4 is present; long dashed line: dissolved NaCl is present; and longest dashed line: dissolved CaCl_2 present.

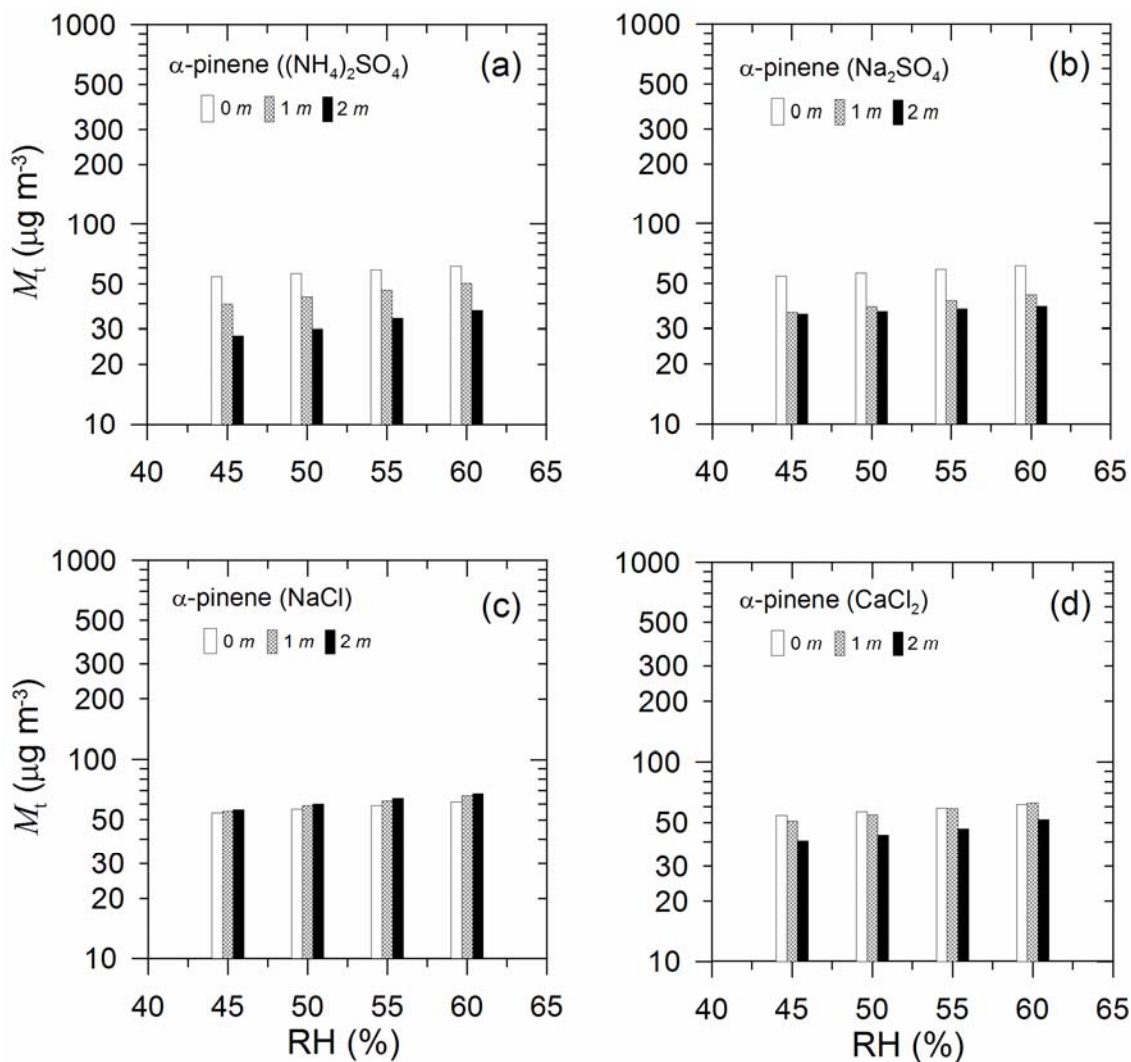


Figure 4.3. Predicted total mass concentrations M_t , including organic species and water, at $T = 306$ K in the α -pinene/ O_3 system with 0, 1, or 2 mol kg^{-1} dissolved inorganic salt. Panel (a) shows M_t when dissolved $(\text{NH}_4)_2\text{SO}_4$ is present; panel (b) shows M_t when dissolved Na_2SO_4 is present; panel (c) shows M_t when dissolved NaCl is present; and panel (d) shows M_t when dissolved CaCl_2 is present. The white bar is the result for homogeneous nucleation (i.e., 0 mol kg^{-1} dissolved salt); the shaded bar is for 1 mol kg^{-1} dissolved salt present; and the solid bar is for 2 mol kg^{-1} dissolved salt present.

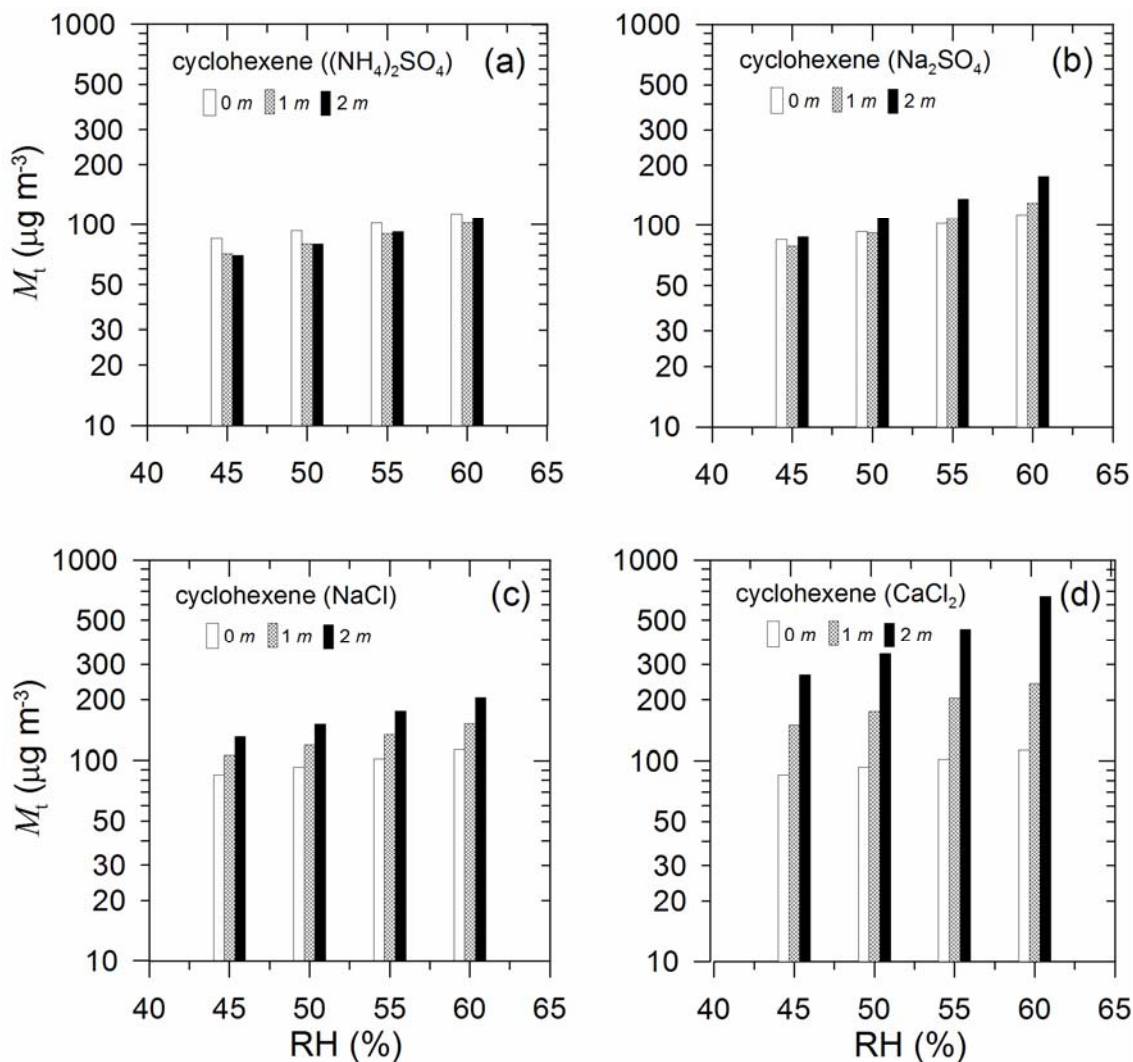


Figure 4.4. Predicted total mass concentrations M_t , including organic species and water, at $T = 298$ K in the cyclohexene/ O_3 system with 0, 1, or 2 mol kg^{-1} dissolved inorganic salt. Panel (a) shows M_t when dissolved $(\text{NH}_4)_2\text{SO}_4$ is present; panel (b) shows M_t when dissolved Na_2SO_4 is present; panel (c) shows M_t when dissolved NaCl is present; and panel (d) shows M_t when dissolved CaCl_2 is present. The white bar is the result for homogeneous nucleation (i.e., 0 mol kg^{-1} dissolved salt); the shaded bar is for 1 mol kg^{-1} dissolved salt present; and the solid bar is for 2 mol kg^{-1} dissolved salt present.

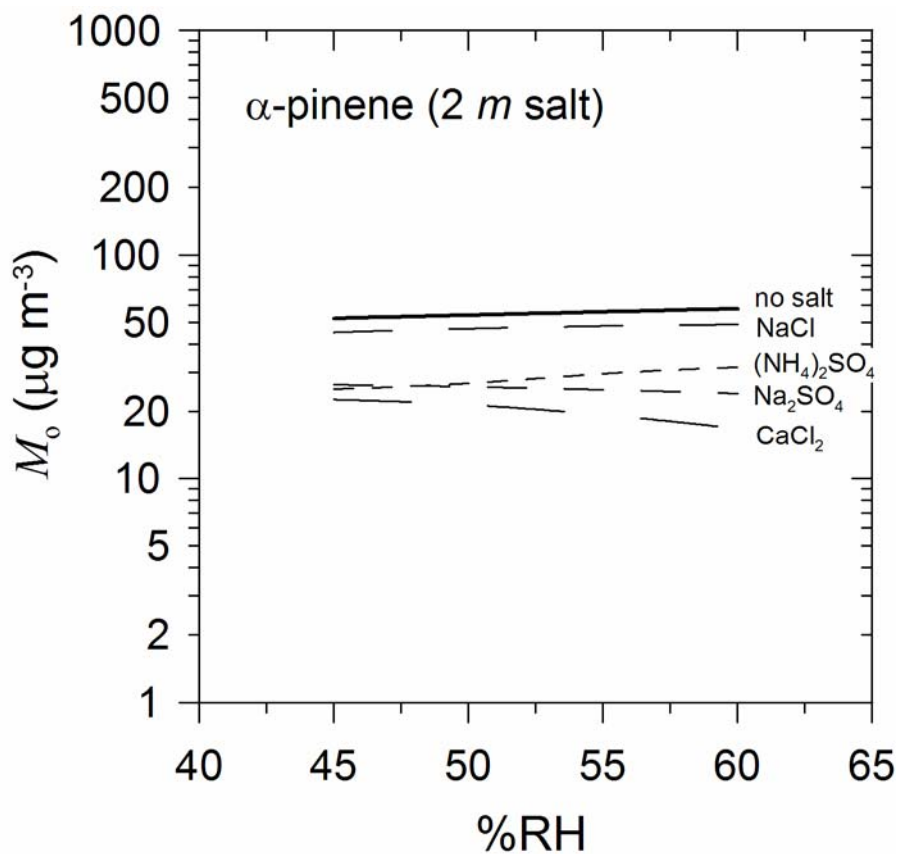


Figure 4.5. Predicted mass concentrations of organic species at $T = 306$ K in the α -pinene/ O_3 system with and without 2 mol kg^{-1} dissolved inorganic salt. Solid line: no salt present (i.e., homogeneous nucleation); shortest dashed line: dissolved $(\text{NH}_4)_2\text{SO}_4$ is present; short dashed line: dissolved Na_2SO_4 is present; long dashed line: dissolved NaCl is present; and longest dashed line: dissolved CaCl_2 present.

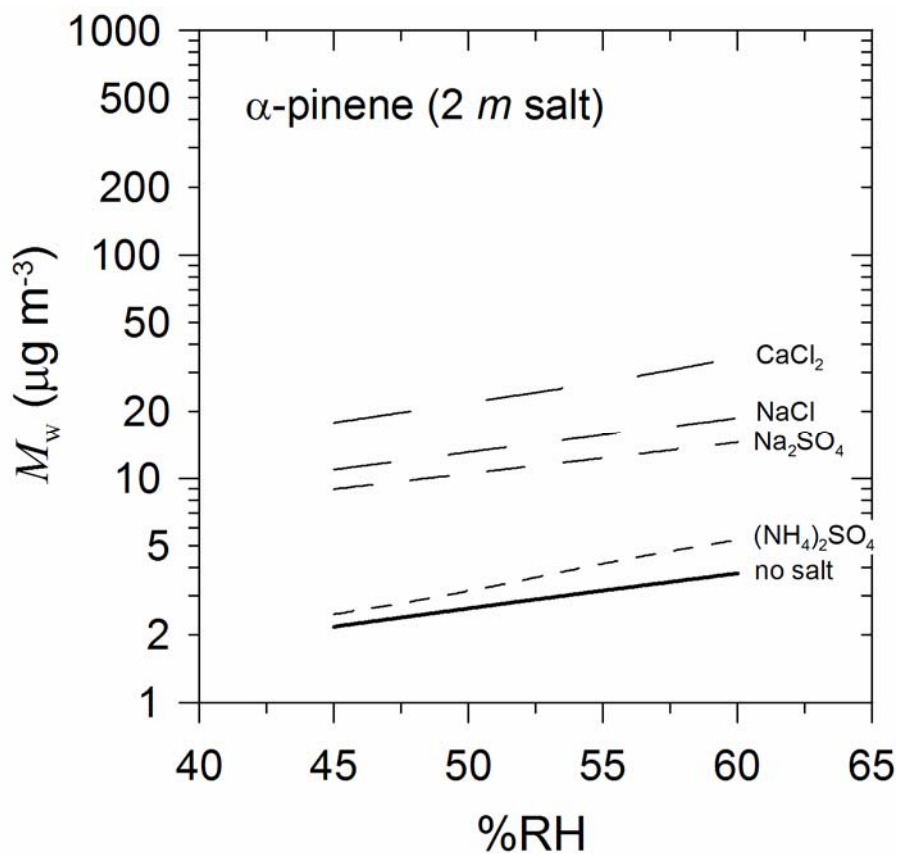


Figure 4.6. Predicted mass concentrations of water at $T = 306$ K in the α -pinene/ O_3 system with and without 2 mol kg^{-1} dissolved inorganic salt. Solid line: no salt present (i.e., homogeneous nucleation); shortest dashed line: dissolved $(\text{NH}_4)_2\text{SO}_4$ is present; short dashed line: dissolved Na_2SO_4 is present; long dashed line: dissolved NaCl is present; and longest dashed line: dissolved CaCl_2 present.

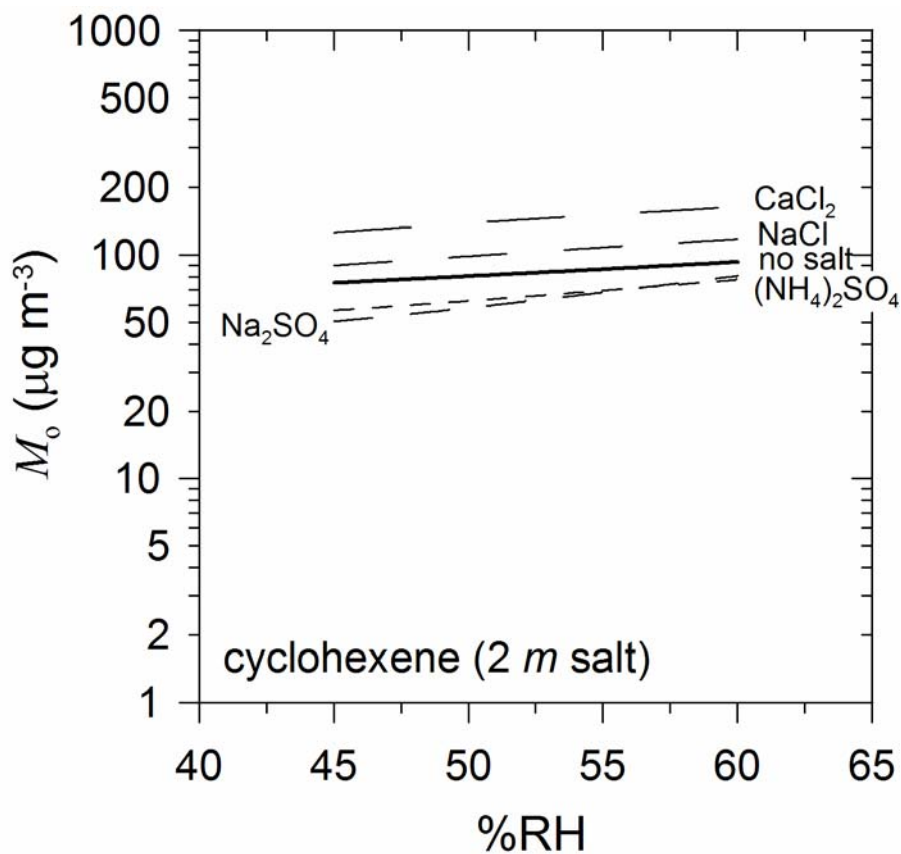


Figure 4.7. Predicted mass concentrations of organic species at $T = 298$ K in the cyclohexene/ O_3 system with and without 2 mol kg^{-1} dissolved inorganic salt. Solid line: no salt present (i.e., homogeneous nucleation); shortest dashed line: dissolved $(\text{NH}_4)_2\text{SO}_4$ is present; short dashed line: dissolved Na_2SO_4 is present; long dashed line: dissolved NaCl is present; and longest dashed line: dissolved CaCl_2 present.

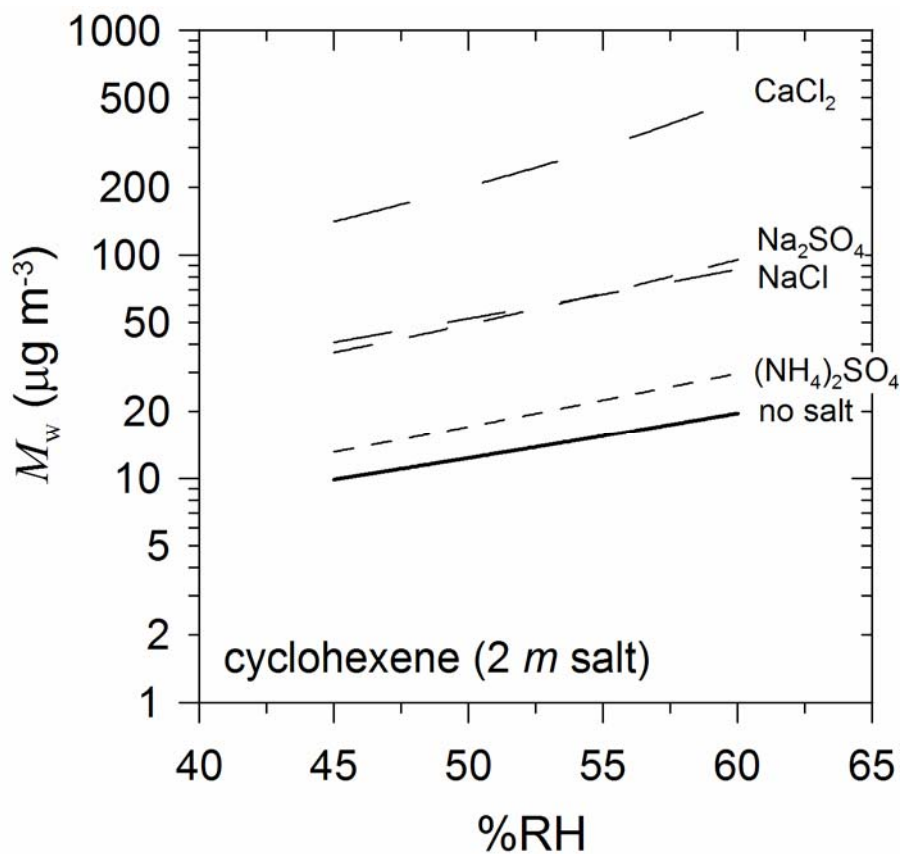


Figure 4.8. Predicted mass concentrations of water at $T = 298$ K in the cyclohexene/ O_3 system with and without 2 mol kg^{-1} dissolved inorganic salt. Solid line: no salt present (i.e., homogeneous nucleation); shortest dashed line: dissolved $(\text{NH}_4)_2\text{SO}_4$ is present; short dashed line: dissolved Na_2SO_4 is present; long dashed line: dissolved NaCl is present; and longest dashed line: dissolved CaCl_2 present.

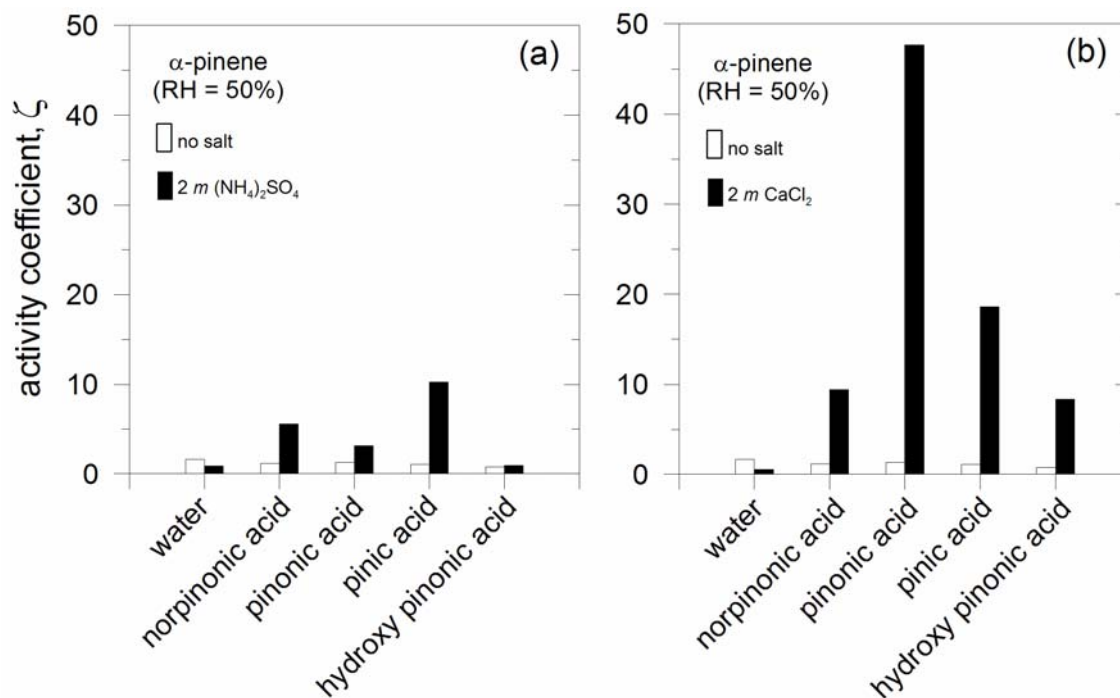


Figure 4.9. Predicted activity coefficients of the major oxidation products in the α -pinene/ O_3 system at $T = 306$ K with and without 2 mol kg^{-1} dissolved inorganic salt. Panel (a) shows results for dissolved $(NH_4)_2SO_4$; panel (b) shows results for dissolved $CaCl_2$. The white bar is the result for homogeneous nucleation, and the solid bar is for 2 mol kg^{-1} dissolved salt present.

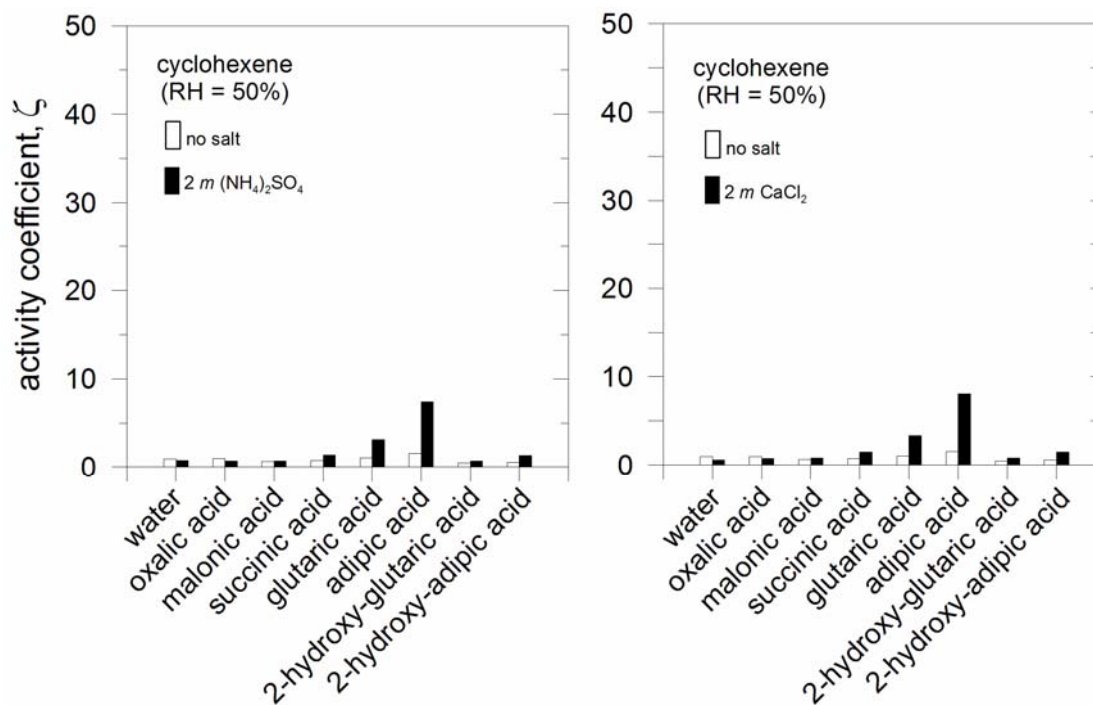


Figure 4.10. Predicted activity coefficients of the major oxidation products in the cyclohexene/ O_3 system at $T = 298$ K with and without 2 mol kg^{-1} dissolved inorganic salt. Panel (a) shows results for dissolved $(NH_4)_2SO_4$; panel (b) shows results for dissolved $CaCl_2$. The white bar is the result for homogeneous nucleation, and the solid bar is for 2 mol kg^{-1} dissolved salt present.

CHAPTER 5

SUMMARY

5.1 General

In Chapter 2 of this dissertation, a method for testing the stability of multiple phases in aerosol particulate matter (PM) was presented. Implementation of the method showed that the combined presence of low-polarity compounds together with higher polarity compounds from the oxidation of parent volatile organic compounds (VOCs) in aerosol PM can lead to phase separation to two liquid phases. This can occur even in the absence of water in the PM. The assumption of a single PM phase when in fact the PM is more stable as two phases will lead to errors in the predicted total PM (TPM) value; the examples considered gave errors in the range -3.9% to -21.8%. It was also concluded that, all other factors remaining equal, the error in the predicted TPM value will tend to maximize as the fractional mass contribution from higher polarity compounds and low polarity compounds become similar.

In Chapter 3 of this dissertation, a method (Ionic-UNIFAC.1) for calculating activity coefficients (ζ) of neutral compounds in liquid PM comprised of a mixture of organic compounds, inorganic salts, and water with total salt concentrations as much as 2 mol kg⁻¹ was presented. Preliminary applications of Ionic-UNIFAC.1 to hypothetical liquid PM compositions provided estimates of the significant thermodynamic errors that can result when neglecting the effects of such levels of dissolved salts on organic-compound ζ values. The relative error in ζ values predicted with this method was shown to be independent of the ionic strength (I). On average, the relative error tended to decrease with increasing activity (a) over the range $-2 < \log a < 0.5$, and did not exceed 20% for the data fitted. The basis set used to fit Ionic-UNIFAC.1 pertains to ambient temperatures and involves salts and organic compound groups typically found in atmospheric PM.

In Chapter 4 of this dissertation, a study of the effects of dissolved inorganic salts on the formation of organic/water PM phases was presented. Ionic-UNIFAC.1 was used in that study within a gas/particle (G/P) equilibrium model to predict concentrations and organic/water compositions of aerosol PM. Predictions showed that relative to homogeneous nucleation and dry salt seed cases, aerosol yields were decreased in the α -pinene/O₃ system in the presence of dissolved (NH₄)₂SO₄, Na₂SO₄, and CaCl₂, while yields increased in the presence of dissolved NaCl. In the cyclohexene/O₃ system, increases in aerosol yield were predicted for all salts considered except (NH₄)₂SO₄. Average errors in predicted aerosol yields and hygroscopic growth factors in systems containing low amounts of dissolved salt ($\leq 2 \text{ mol kg}^{-1}$) were $\sim 20\%$, which is within the expected range of error for Ionic-UNIFAC.1. Excellent agreement was obtained between predicted and measured decreases in aerosol yield in the α -pinene/O₃ system at RH = 50% with dissolved (NH₄)₂SO₄ and CaCl₂: 45% vs. 44%, and 21% vs. 24%, respectively.

5.2 Implications

The research results presented in this dissertation have various implications for regional air-shed modeling and management of air quality. Failing to account for multiple liquid PM phases in G/P equilibrium models will result in predicted TPM errors. Assuming a single liquid PM phase when in fact two phases are present will result in an under-prediction of the TPM value. Therefore, such predictions could falsely indicate that PM concentrations for a given aerosol system would meet regulatory standards. The presence of multiple liquid PM phases will also affect the light-scattering properties of aerosol particles. Assuming a single liquid PM phase when in fact multiple phases are present could, therefore, result in errors of predicted visibility effects due to PM.

Neglecting effects of dissolved inorganic salts on PM concentrations of organic species and water will also lead to errors in predicted TPM values. In this case, PM concentrations may be under- or over-predicted depending on the characteristics of the partitioning species in the system of interest. In the research presented here, dissolved inorganic salts tended to decrease PM concentrations in an aerosol system containing the ozone-oxidation products of a biogenic VOC, while they tended to increase PM

concentrations in a system containing the ozone-oxidation products of an anthropogenic VOC.

Dissolved inorganic salts such as $(\text{NH}_4)_2\text{SO}_4$ and Na_2SO_4 are derived from anthropogenic sources. While these salts result in a reduction of PM mass concentration in the α -pinene/ O_3 aerosol system, it is anthropogenic emission sources that lead to the oxidation of α -pinene and thus PM formation. It would therefore be foolish to conclude that the presence of these dissolved inorganic salts is a benefit to air quality. Furthermore, biogenic dissolved inorganic salts either decrease TPM concentrations in α -pinene/ O_3 system to a much lesser extent than the anthropogenic salts or actually increase the TPM concentrations. Moreover, an air quality manager must consider the anthropogenic sources of PM in the atmosphere as those which can be controlled or regulated.

The effect of dissolved inorganic salts on the concentrations of PM are more dramatic in the cyclohexene/ O_3 system than in the α -pinene/ O_3 system, and dissolved inorganic salts tend to increase PM concentrations in the cyclohexene/ O_3 system. The effect is most significant for biogenic salts. As cyclohexene is an anthropogenic VOC, this further demonstrates that anthropogenic sources of PM need to be regulated.

In conclusion, the research results presented here are important to the understanding of atmospheric and other aerosols and the formation of aerosol PM. The methods developed in this work can be implemented as stand-alone applications, as well as within overall G/P equilibrium models or regional air-shed models. They are necessary tools for the proper management of air quality.

APPENDIX 1

VOLUME-CONCENTRATIONS OF PM-PHASE COMPONENTS

Values of c used to determine Δc were calculated as follows. For each component i and phase k (*i.e.*, α or β)

$$c_i^k = n_i^k MW_i / v^k \quad (\text{A1.1})$$

where: n_i^k is the number of mols of i in phase k ; MW_i (g mol^{-1}) is the molecular weight of i ; and v^k (cm^3) is the volume of phase k . If $n_T^k = \sum_i n_i^k$ is the total number of mols in phase k , then $X_i^k = n_i^k / n_T^k$, and Eq. (A1.1) becomes

$$c_i^k = X_i^k n_T^k MW_i / v^k = X_i^k MW_i / \bar{v}^k \quad (\text{A1.2})$$

where \bar{v}^k is the molar volume of phase k . All values of $c_{i,\text{bulk}}^\alpha$, $c_{i,\text{bulk}}^\beta$, $c_{i,\text{int}}^\alpha$, and $c_{i,\text{int}}^\beta$ were calculated using Eq. (A1.2). When used to calculate $c_{i,\text{int}}^\alpha$ and $c_{i,\text{int}}^\beta$, it was necessary to assume that the molar volume of the interfacial region was the same as that of the bulk region. As each numerical simulation converged, that approximation became increasingly accurate. It was also assumed that volume is always conserved upon mixing of constituents so that for each phase $v^k = \sum_i n_i^k MW_i / \rho_i$, where ρ_i is the density (g cm^{-3}) of i as a pure liquid. When not available in the literature, values of ρ_i were estimated using SPARC (scalable processor architecture performs automated reasoning in chemistry; Hilal *et al.*, [1994, Quantitative Treatments of Solute/Solvent Interactions, Murray, P.P.a.J.S. (Ed.), Elsevier, Amsterdam]).

APPENDIX 2

FREE-ENERGY CHANGES DURING PHASE SEPARATION

For a PM composition that is more stable as two phases than as one phase, the free energy of the two-phase PM will be lower than that of the corresponding single-phase PM. The free energy of the system during the execution of the pseudo-diffusion method can be tracked. The total free energy of the PM is

$$G = \sum_i n_i^\alpha (\mu_i^\circ + RT \ln a_i^\alpha) + \sum_i n_i^\beta (\mu_i^\circ + RT \ln a_i^\beta) \quad (\text{A2.1})$$

$$= \sum_i (n_i^\alpha + n_i^\beta) \mu_i^\circ + RT \left(\sum_i n_i^\alpha \ln a_i^\alpha + \sum_i n_i^\beta \ln a_i^\beta \right) \quad (\text{A2.2})$$

where the summations are taken over all compounds, μ_i° is the standard chemical potential of compound i , and R is the ideal gas constant. Since the first summation in Eq. (A2.2) is a constant, any change in the free energy as the PM moves toward (or away from) equilibrium can be monitored by the change in the last term. The last term in Eq. (A2.2) was calculated during the phase stability tests for all of the cases considered here; when the PM was more stable as two phases, its value always decreased to a minimum constant value over the course of the iterations. Figure A2.1 provides the results of such calculations for the PM composition considered in Figure 2.2.

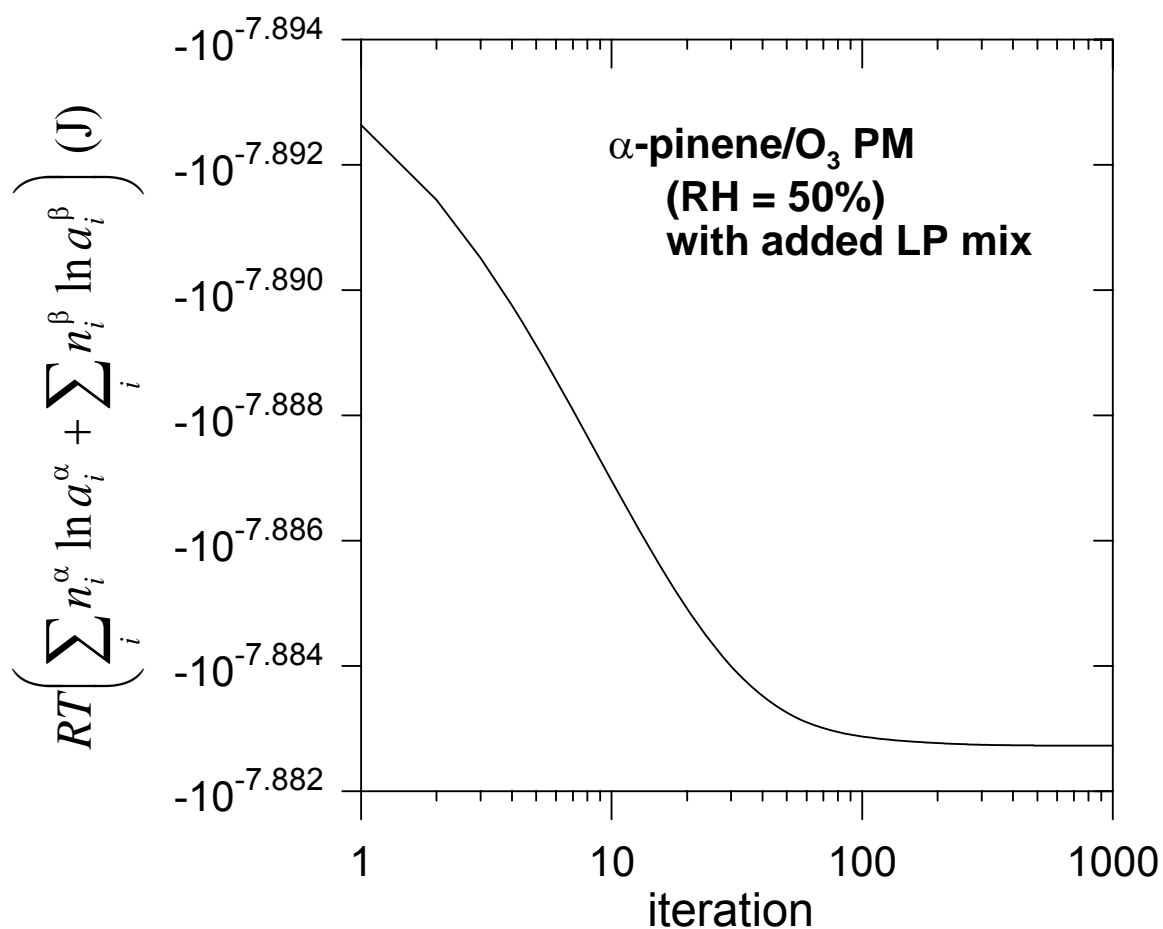


Figure A2.1. Calculated change in free energy of two-phase PM as a function of iteration number during the pseudo-diffusion phase stability test for the PM formed by amending the PM composition (Table 2.2) for the α -pinene/O₃ case so that 10% of the total organic carbon (OC) in the resulting PM was from the low-polarity (LP) mix (Table 2.1).

APPENDIX 3

DENSITIES OF PURE SOLVENTS AND SOLVENT MIXTURES

The density of pure solvent n is calculated at the temperature of interest using the modified form of the Rackett equation (Yaws, 1999):

$$\rho_n \text{ (g mL}^{-1}\text{)} = A_\rho B_\rho^{-(1-T/T_c)^{n_\rho}} \quad (\text{A3.1})$$

where A_ρ , B_ρ , and n_ρ are correlation coefficients and T_c is the critical temperature of solvent n . (Note that the symbol n_ρ is not related to the solvent compound symbol n .) Values of these parameters are listed in Table A3.1 for each of the solvents that appear in the mixtures of the basis set (Table 3.2) and test set (Table 3.3).

The density of a solvent mixture is calculated according to

$$\rho_s = \frac{\text{MW}_s}{\sum_n X'_n \text{MW}_n / \rho_n} \quad (\text{A2})$$

where: X'_n is the salt-free mole fraction of solvent n (i.e., the mole fraction of solvent n assuming no salt is present in the mixture); and $\text{MW}_s = \sum X'_n \text{MW}_n$ is the molecular weight of the solvent mixture (g mol^{-1}).

Table A3.1. Correlation coefficients used to calculate densities of the solvent compounds comprising the experimental liquid-liquid equilibrium (LLE) systems listed in Tables 3.2 and 3.3.

Solvent compound	Formula	Density (ρ_n) coefficients ^a			
		A_ρ	B_ρ	n_ρ	T_c (K)
Water	H ₂ O	0.34710	0.27400	0.28571	647.13
<i>Alcohols</i>					
1-Butanol	C ₄ H ₁₀ O	0.26891	0.26674	0.24570	562.93
<i>t</i> -Butanol	C ₄ H ₁₀ O	0.26921	0.25650	0.27370	506.20
<i>Ketones</i>					
4-Methyl-2-pentanone	C ₆ H ₁₂ O	0.26654	0.25887	0.28571	571.40
<i>Carboxylic acids</i>					
Acetic acid	C ₂ H ₄ O ₂	0.35182	0.26954	0.26843	592.71
Propanoic acid	C ₃ H ₆ O ₂	0.32283	0.25916	0.27644	604.00
Butanoic acid	C ₄ H ₈ O ₂	0.31132	0.26192	0.27997	628.00

^a Density coefficients are from Yaws (1999).

APPENDIX 4

DIELECTRIC CONSTANTS OF PURE SOLVENTS AND SOLVENT MIXTURES

The dielectric constant of pure solvent n is calculated at the temperature of interest according to (Wohlfarth, 1995):

$$\varepsilon_n = a_\varepsilon + b_\varepsilon T + c_\varepsilon T^2 + d_\varepsilon T^3 \quad (\text{A4.1})$$

where a_ε , b_ε , c_ε , and d_ε are correlation coefficients. Values of these parameters are listed in Table A4.1 for each of the solvents that appear in the mixtures of the basis set (Table 3.2) and test set (Table 3.3).

When a solvent mixture is binary, wherein one component is water ($n = 1$) and the other is a polar organic solvent ($n = 2$), Oster's empirical mixing rule is used to estimate the dielectric constant of the solvent mixture (Hasted, 1973). This rule gives the dielectric constant of the solvent mixture as

$$\varepsilon_s = \varepsilon_1 + [(\varepsilon_2 - 1)(2\varepsilon_2 + 1) / 2\varepsilon_2 - (\varepsilon_1 - 1)] X_2' V_2 / V \quad (\text{A4.2})$$

where: V_n is the molar volume of pure solvent n ($\text{m}^3 \text{mol}^{-1}$); and $V = \sum X_n' V_n$ is the molar volume of the solvent mixture ($\text{m}^3 \text{mol}^{-1}$). No simple methods exist for calculating dielectric constants of solvent mixtures that contain water and more than one organic solvent. In this work, the dielectric constant of such mixtures was calculated three ways:

$$\varepsilon_s = \sum_n X_n' \varepsilon_n \quad (\text{A4.3})$$

$$\varepsilon_s = \frac{\sum_n X_n' \varepsilon_n}{2} \quad (\text{A4.4})$$

$$\varepsilon_s = 2 \sum_n X_n' \varepsilon_n \quad (\text{A4.5})$$

The model was optimized using each of these methods. The goodness of fit, determined

by the standard error of the fit, was identical in each case. However, Eq. (A4.4) yielded the lowest value of the objective function (Eq. (3.12)): $F_{\text{MIN}} = 69.8$, compared to $F_{\text{MIN}} = 71.5$ with Eq. (A4.3) and $F_{\text{MIN}} = 72.7$ with Eq. (A4.5). The presence of relatively non-polar organic compounds in these solvent mixtures will disrupt the dipole correlation of water molecules (Hasted, 1973). It is therefore not surprising that Eq. (A4.4) yields a lower objective value than either Eqs. (A4.3) or (A4.5). Based on this numerical test, Eq. (A4.4) was used to calculate the dielectric constant of ternary solvent mixtures.

Table A4.1. Correlation coefficients used to calculate dielectric constants of the solvent compounds comprising the experimental liquid-liquid equilibrium (LLE) systems listed in Tables 3.2 and 3.3.

Solvent compound	Formula	Dielectric constant (ϵ_n) coefficients ^a			
		a_ϵ	b_ϵ	c_ϵ	d_ϵ
Water	H ₂ O	2.4921×10^2	-7.9069×10^{-1}	7.2997×10^{-4}	0
<i>Alcohols</i>					
1-Butanol	C ₄ H ₁₀ O	1.0578×10^2	-5.0587×10^{-1}	8.4733×10^{-4}	-4.8841×10^{-7}
<i>t</i> -Butanol	C ₄ H ₁₀ O	2.2541×10^2	-1.4990×10^0	3.4050×10^{-3}	-2.5968×10^{-6}
<i>Ketones</i>					
4-Methyl-2-pentanone	C ₆ H ₁₂ O	3.6341×10^1	-9.7119×10^{-2}	6.1896×10^{-5}	0
<i>Carboxylic acids</i>					
Acetic acid	C ₂ H ₄ O ₂	-1.5731×10^1	1.2662×10^{-1}	-1.7738×10^{-4}	0
Propanoic acid	C ₃ H ₆ O ₂	1.8793×10^0	4.6841×10^{-3}	1.9983×10^{-6}	0
Butanoic acid	C ₄ H ₈ O ₂	1.5010×10^0	5.0046×10^{-3}	0	0

^a Dielectric constant coefficients are from Wohlfarth (1995).

BIOGRAPHICAL SKETCH

Garnet Erdakos was born in Oak Lawn, IL on the south-side of Chicago. She spent much of her K-12 years performing in theatrical plays and earning Girl Scout badges. She enjoys playing the piano and guitar, hiking, biking, and playing with her dog, Roxi.

Garnet earned her Bachelor of Science degree in Physics from Illinois State University in 1997 and her Master of Science degree in Environmental Science & Engineering from the Oregon Graduate Institute of Science & Technology in 1998. She has participated in many activities to encourage girls to become involved in science, mathematics, and engineering. She has also participated in leadership roles as a Student Council member during both her undergraduate and graduate education. Garnet also earned awards for her achievements as a student at both her undergraduate and graduate schools. Her list of publications includes:

Erdakos, G.B., Pankow, J.F., 2003. Gas/Particle Partitioning of Neutral and Ionizing Compounds to Single- and Multi-Phase Aerosol Particles. 2. Phase Separation in Liquid Particulate Matter Containing Both Polar and Low-Polarity Organic Compounds. *Atmospheric Environment* 38, 1005-1013.

Asher, W.E., Pankow, J.F., Erdakos, G.B., Seinfeld, J.H., 2002. Estimating the Vapor Pressures of Multi-Functional Oxygen-Containing Organic Compounds Using Group Contribution Methods. *Atmospheric Environment* 36, 1483-1498.

Pankow, J.F., Seinfeld, J.H., Asher, W.E., Erdakos, G.B., 2001. Modeling the Formation of Secondary Organic Aerosol. 1. Application of Theoretical Principles to Measurements Obtained in the α -Pinene/, β -Pinene/, Sabinene/, Δ^3 -Carene/, and Cyclohexene/Ozone Systems. *Environmental Science & Technology* 35, 1164-1172.

Seinfeld, J.H., Erdakos, G.B., Asher, W.E., Pankow, J.F., 2001. Modeling the Formation of Secondary Organic Aerosol (SOA). 2. The Predicted Effects of Relative Humidity on Aerosol Formation in the α -Pinene-, β -Pinene-, Sabinene-, Δ^3 -Carene-, and Cyclohexene-Ozone Systems. *Environmental Science & Technology* 35, 1806-1817.

Walsh, T.J., Caruthers, C.G., Heinitz, A.C., Myers, E.P., Baptista, A.M., Erdakos, G.B., Kamphaus, R. A., October 2000. Tsunami Hazard Map of the Southern Washington Coast: Modeled Cascadia Subduction Zone Earthquake. Washington Division of Geology and Earth Resources, Geologic Map GM-49.

Erdakos, G. B., Ren, Shang-Fen. 1998. Poisson's Ratios in Diamond/Zincblende Crystals. *Journal of the Physics & Chemistry of Solids* 59, 21-26.